FEDERAL SERVICE OF RUSSIA FOR HYDROMETEOROLOGY AND ENVIRONMENTAL MONITORING

Federal State Budgetary Institution "Arctic and Antarctic Research Institute"
Russian Antarctic Expedition

QUARTERLY BULLETIN

№3 (64)
July - September 2013

STATE OF ANTARCTIC ENVIRONMENT

Operational data of Russian Antarctic stations

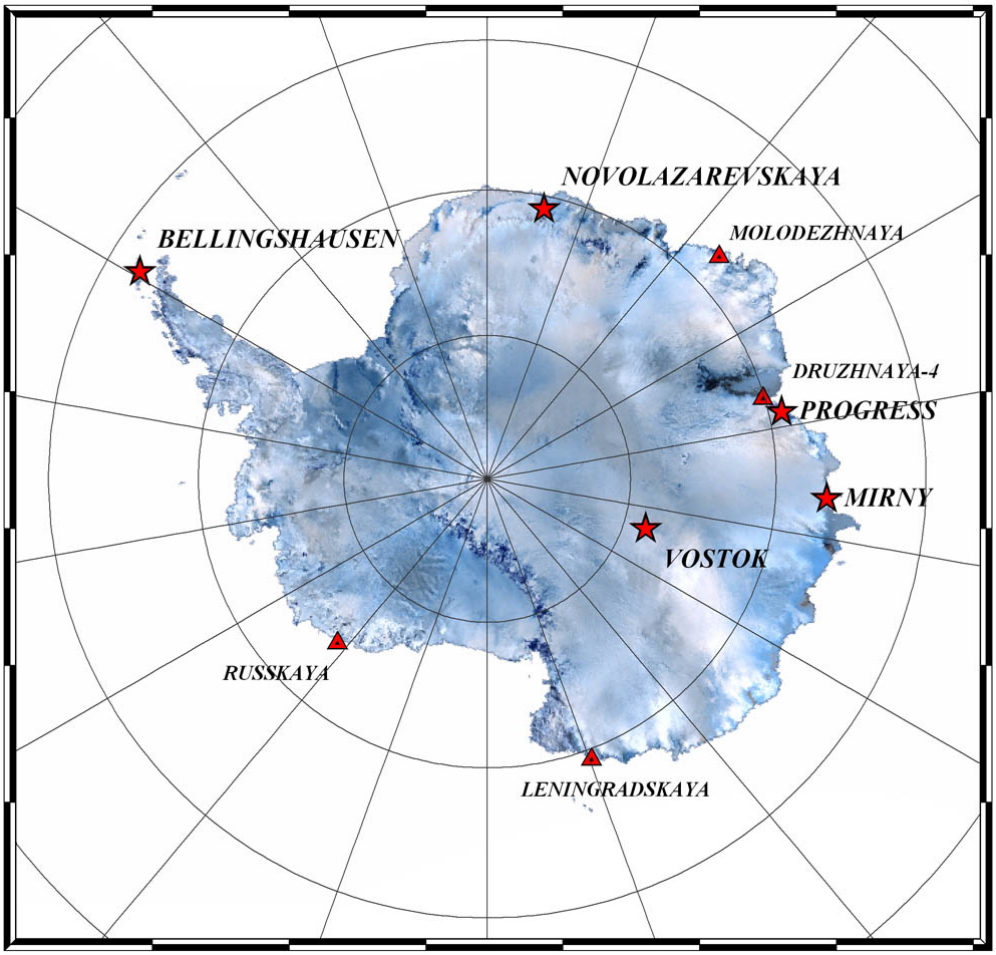

St. Petersburg

2013

FEDERAL SERVICE OF RUSSIA FOR HYDROMETEOROLOGY AND ENVIRONMENTAL MONITORING

Federal State Budgetary Institution "Arctic and Antarctic Research Institute"
Russian Antarctic Expedition

QUARTERLY BULLETIN

№3 (64)
July – September 2013

STATE OF ANTARCTIC ENVIRONMENT

Operational data of Russian Antarctic stations

Edited by V.V. Lukin

St. Petersburg
2013

Editor-in-Chief - M.O. Krichak (Russian Antarctic Expedition – RAE)

Authors and contributors
Section 1 M. O. Krichak (RAE),
Section 2 Ye .I. Aleksandrov (Department of Sea – Air Interaction),
Section 3 G. Ye. Rybkov (Department of Ice Regime and Forecasting),
Section 4 A. I. Korotkov (Department of Ice Regime and Forecasting),
Section 5 Ye. Ye. Sibir (Department of Sea – Air Interaction),
Section 6 I. V. Moskvin, Yu.G. Turbin (Department of Geophysics),
Section 7 V. I. Zaitsev, A. A. Kalinkin, S. G. Poigina (GS RAS),
Section 8 V. L. Martyanov (RAE),

Translated by I.I. Solovieva

http://www.aari.aq/, Antarctica/ Quarterly Bulletin/

Acknowledgements:
Russian Antarctic Expedition is grateful to all AARI staff for participation and help in preparing this Bulletin.

For more information about the contents of this publication, please, contact
Arctic and Antarctic Research Institute of Roshydromet
Russian Antarctic Expedition
Bering St., 38, St. Petersburg 199397 Russia
Phone: (812) 352 15 41; 337 31 04
Fax: (812) 337 31 86
E-mail: lukin@aari.aq

CONTENTS

PREFACE 1

1. DATA OF AEROMETEOROLOGICAL OBSERVATIONS AT THE RUSSIAN ANTARCTIC STATIONS 3
2. METEOROLOGICAL CONDITIONS IN JULY - SEPTEMBER 2013 42
3. REVIEW OF THE ATMOSPHERIC PROCESSES OVER THE ANTARCTIC IN JULY – SEPTEMBER 2013 48
4. BRIEF REVIEW OF ICE PROCESSES IN THE SOUTHERN OCEAN FROM DATA OF SATELLITE AND COASTAL OBSERVATIONS AT THE RUSSIAN ANTARCTIC STATIONS IN JULY – SEPTEMBER 2013 50
5. RESULTS OF TOTAL OZONE MEASUREMENTS AT THE RUSSIAN ANTARCTIC STATIONS IN THE THIRD QUARTER OF 2013 53
6. GEOPHYSICAL OBSERVATIONS AT THE RUSSIAN ANTARCTIC STATIONS IN JULY – SEPTEMBER 2013 55
7. SEISMIC OBSERVATION IN ANTARCTICA IN 2012 67
8. MAIN RAE EVENTS IN THE THIRD QUARTER OF 2013 74

PREFACE

The activity of the Russian Antarctic Expedition in the third quarter of 2013 was carried out at five permanent year-round Antarctic stations - Mirny, Novolazarevskaya, Bellingshausen, Progress and Vostok and at the field bases Molodezhnaya, Leningradskaya, Russkaya and Druzhnaya-4. The work was carried out by the wintering team of the 58th RAE over a full complex of the Antarctic environmental monitoring programs.

At the field bases, Molodezhnaya, Lenigradskaya, Russkaya and Druzhnaya-4, the automatic weather stations AWS of the model MAWS-110 and automatic geodetic complexes FAGS were in operation. The information of Molodezhnaya and Druzhnaya-4 stations is not transmitted temporarily via the satellite communication system due to technical failure, being stored at the stations until the time of the information readout during their visit.

Section I of the Bulletin contains monthly averages and extreme data of standard meteorological and solar radiation observations carried out at permanent operating stations during July-September 2013 and data of upper-air sounding carried out at two stations Mirny and Novolazarevskaya once a day at 00.00 h Universal Time Coordinated (UTC). In accordance with the International Geophysical Calendar, more frequent sounding during the periods of the International Geophysical Interval is conducted in 2013 during 11-24 February, 06–19 May, 12 - 15 August and 04 - 17 November at 00 h and 12 h UTC.

In the meteorological tables, the atmospheric pressure for the coastal stations is referenced to the sea level. The atmospheric pressure at Vostok station is not referenced to the sea level and is presented at the level of the meteorological site. Along with the monthly averages of meteorological parameters, the tables in Section 1 contain their deviations from multiyear averages (anomalies) and deviations in σ_f fractions (normalized anomalies $(f-f_{avg})/\sigma_f$). For the monthly totals of precipitation and total radiation, relative anomalies (f/f_{avg}) are also presented. The statistical characteristics necessary for the calculation of anomalies were derived at the AARI Department of Meteorology for the period 1961-1990 as recommended by the World Meteorological Organization. For Progress station, the anomalies are not calculated due to a short observation series.

The Bulletin contains brief overviews with an assessment of the state of the Antarctic environment based on the actual data for the quarter under consideration. Sections 2 and 3 are devoted to the meteorological and synoptic conditions. A review of synoptic conditions (section 3) is prepared on the basis of the analysis of current aero-synoptic information, which is performed by RAE forecaster at Progress station and also on the basis of more complete data of the Southern Hemisphere contained in the Internet.

The analysis of ice conditions in the Southern Ocean (section 4) is based on satellite data received at Bellingshausen, Novolazarevskaya, Mirny and Progress stations and on the observations conducted at the coastal Bellingshausen, Mirny and Progress stations. The anomalous character of ice conditions is evaluated against the multiyear averages of the drifting ice edge location and the mean multiyear dates of the onset of different ice phases in the coastal areas of the Southern Ocean adjoining the Antarctic stations. As the average and extreme values of ice edge location, the updated data are used which are received at the AARI for each month based on the results of processing the entire available historical archive of predominantly national information on the Antarctic for the period 1971 to 2005.

Section 5 presents an overview of the total ozone (TO) on the basis of measurements at the Russian Antarctic stations during the given quarter. The measurements are interrupted in the wintertime at the Sun's height of less than 5^o.

Data of geophysical observations published in Section 6 present the results of geomagnetic measurements and measurements of space radio-emission at Mirny, Novolazarevskaya, Vostok and Progress stations.

Section 7 of this issue publishes the results of seismic observations in Antarctica in 2012, which are carried out in the stationary mode at the RAS Geophysical Service (GS) stations Mirny and Novolazarevskaya.

Section 8 is devoted to the main events of RAE logistical activities during the quarter under consideration.

RUSSIAN ANTARCTIC STATIONS AND FIELD BASES

MIRNY STATION

STATION SYNOPTIC INDEX	**89592**
METEOROLOGICAL SITE HEIGHT ABOVE SEA LEVEL	**39.9 m**
GEOGRAPHICAL COORDINATES	**φ = 66°33′ S; λ = 93°01′ E**
GEOMAGNETIC COORDINATES	**Φ = -76.8°; Δ = 151.1°**
BEGINNING AND END OF POLAR DAY	**December 7 – January 5**
BEGINNING AND END OF POLAR NIGHT	**No**

NOVOLAZAREVSKAYA STATION

STATION SYNOPTIC INDEX	**89512**
METEOROLOGICAL SITE HEIGHT ABOVE SEA LEVEL	**119 m**
GEOGRAPHICAL COORDINATES	**φ = 70°46′ S; λ = 11°50′ E**
GEOMAGNETIC COORDINATES	**Φ = -62.6°; Δ = 51.0°**
BEGINNING AND END OF POLAR DAY	**November 15 – January 28**
BEGINNING AND END OF POLAR NIGHT	**May 21 – July 23**

BELLINGSHAUSEN STATION

STATION SYNOPTIC INDEX	**89050**
METEOROLOGICAL SITE HEIGHT ABOVE SEA LEVEL	**15.4 m**
GEOGRAPHICAL COORDINATES	**φ = 62°12′ S; λ = 58°56′ W**
BEGINNING AND END OF POLAR DAY	**No**
BEGINNING AND END OF POLAR NIGHT	**No**

Progress Station

STATION SYNOPTIC INDEX	**89574**
METEOROLOGICAL SITE HEIGHT ABOVE SEA LEVEL	**14,6 m**
GEOGRAPHICAL COORDINATES	**φ = 69°23′ S; λ = 76°23′ E**
BEGINNING AND END OF POLAR DAY	**November 21 – January 22**
BEGINNING AND END OF POLAR NIGHT	**May 28 – July 16**

VOSTOK STATION

STATION SYNOPTIC INDEX	**89606**
METEOROLOGICAL SITE HEIGHT ABOVE SEA LEVEL	**3488 m**
GEOGRAPHICAL COORDINATES	**φ = 78°28′ S; λ = 106°48′ E**
GEOMAGNETIC COORDINATES	**Φ = -89.3°; Δ = 139.5°**
BEGINNING AND END OF POLAR DAY	**October 21 – February 21**
BEGINNING AND END OF POLAR NIGHT	**April 23 – August 21**

FIELD BASE MOLODEZHNAYA

STATION SYNOPTIC INDEX	**89542**
HEIGHT OF AWS ABOVE SEA LEVEL	**40 m**
GEOGRAPHICAL COORDINATES	**φ = 67°40′ S; λ = 46°08′ E**
BEGINNING AND END OF POLAR DAY	**November 29 – January 13**
BEGINNING AND END OF POLAR NIGHT	**June 11 – July 2**

FIELD BASE LENINGRADSKAYA

STATION SYNOPTIC INDEX	**89657**
HEIGHT OF AWS ABOVE SEA LEVEL	**291 m**
GEOGRAPHICAL COORDINATES	**φ = 69°30,1′ S; λ = 159°23,2′ E**

FIELD BASE RUSSKAYA

STATION SYNOPTIC INDEX	**89132**
HEIGHT OF AWS ABOVE SEA LEVEL	**140 m**
GEOGRAPHICAL COORDINATES	**φ = 76°46′ S; λ = 136°47,9′ E**

FIELD BASE DRUZHNAYA-4

HEIGHT OF ABOVE SEA LEVEL	**50 m**
GEOGRAPHICAL COORDINATES	**φ = 69°44′ S; λ = 73°42′ E**

FIELD BASE SOYUZ

HEIGHT OF ABOVE SEA LEVEL	**50 m**
GEOGRAPHICAL COORDINATES	**φ = 70°34′ S; λ = 68°47′ E**

1. DATA OF AEROMETEOROLOGICAL OBSERVATIONS AT THE RUSSIAN ANTARCTIC STATIONS

JULY 2013

MIRNY STATION

Table 1.1

Monthly averages of meteorological parameters (f) and their deviations from the multiyear averages (f_{avg})

Mirny, July 2013

Parameter	f	f_{max}	f_{min}	Anomaly $f-f_{avg}$	Normalized anomaly $(f-f_{avg})/\sigma_f$	Relative anomaly f/f_{avg}
Sea level air pressure, hPa	987.7	1012.0	945.6	1.7	0.3	
Air temperature, °C	-17.0	-6.5	-26.8	-0.3	-0.1	
Relative humidity, %	72			-2.2	-0.4	
Total cloudiness (sky coverage), tenths	7.8			1.1	1.0	
Lower cloudiness(sky coverage),tenths	3.3			0.3	0.2	
Precipitation, mm	60.4			-9.7	-0.2	0.9
Wind speed, m/s	14.0	29.0		1.3	0.9	
Maximum wind gust, m/s		39.0				
Prevailing wind direction, deg	90					
Total radiation, MJ/m^2	9.2			0.2	0.1	1.0
Total ozone content (TO), DU	-	-	-			

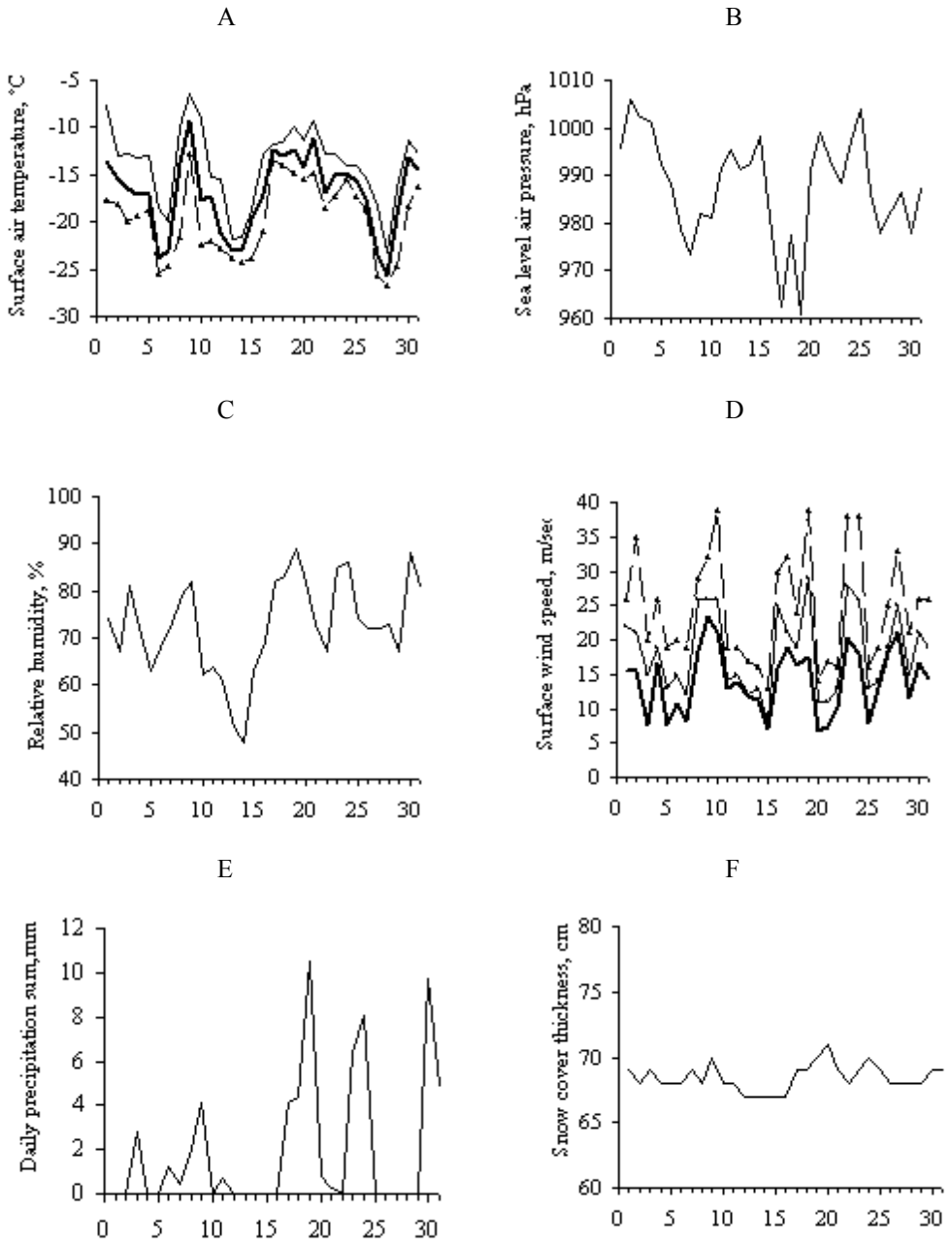

Fig. 1.1. Variations of daily mean values of surface temperature (A, bold line), maximum (A, thin line), minimum (A, dashed line) air temperature, sea level air pressure (B), relative humidity (C), mean (D, thick line), maximum (D, thin line) values of surface wind speed, maximum wind gust (D, dashed line), precipitation (E) and snow cover thickness (F).

Mirny station. July 2013.

Table 1.2

Results of aerological atmospheric sounding (from CLIMAT-TEMP messages)

Mirny, July 2013

Isobaric surface, P hPa	Isobaric surface height, H m	Temperature, T °C	Dew point deficit, D °C	Resultant wind direction, deg	Resultant wind speed, m/s	Wind stability parameter,%	Number of days without temperature data	Number of days without wind data
984	39	-16.7	3.5					
925	499	-16.7	3.8	93	15	98	2	3
850	1130	-19.0	4.4	90	13	90	2	3
700	2570	-21.3	5.6	72	1	8	2	2
500	4975	-37.1	5.4	292	5	36	2	2
400	6477	-48.5	4.8	282	9	56	2	2
300	8308	-61.4	4.7	279	13	67	2	2
200	10755	-69.7	4.8	270	15	78	2	2
150	12460	-71.4	4.9	271	19	86	2	2
100	14839	-75.5	5.2	267	23	89	4	4
70	16870	-79.0	5.4	270	30	93	5	5
50	18765	-81.6	5.4	272	36	95	5	5
30	21594	-83.2	5.4	272	44	95	8	8
20	23844	-83.5	5.8	271	50	96	11	≥9
10	27711	-78.6	5.8	271	58	98	17	≥9

Table 1.3

Anomalies of standard isobaric surface height and temperature

Mirny, July 2013

P hPa	$H-H_{avg}$, m	$(H-H_{avg})/\sigma_H$	$T-T_{avg}$, °C	$(T-T_{avg})/\sigma_T$
850	19	0.4	0.2	0.1
700	21	0.4	1.9	1.1
500	35	0.5	0.6	0.3
400	30	0.4	-0.6	-0.4
300	14	0.2	-1.5	-1.2
200	-8	-0.1	-1.4	-1.0
150	-22	-0.2	-1.8	-1.2
100	-40	-0.4	-2.4	-1.4
70	-76	-0.6	-2.9	-1.4
50	-135	-1.0	-3.7	-1.5
30	-248	-1.7	-4.1	-1.3
20	-340	-2.0	-5.0	-1.4
10	-453	-1.7	-3.9	-1.2

NOVOLAZAREVSKAYA STATION

Table 1.4

Monthly averages of meteorological parameters (f) and their deviations from the multiyear averages (f_{avg})

Novolazarevskaya, July 2013

Parameter	f	f_{max}	f_{min}	Anomaly $f-f_{avg}$	Normalized anomaly $(f-f_{avg})/\sigma_f$	Relative anomaly f/f_{avg}
Sea level air pressure, hPa	985.7	1002.0	955.9	-1.9	-0.3	
Air temperature, °C	-16.8	-5.1	-33.3	0.5	0.2	
Relative humidity, %	39			-11.4	-1.6	
Total cloudiness (sky coverage), tenths	6.9			1.4	1.0	
Lower cloudiness(sky coverage),tenths	1.4			0.3	0.3	
Precipitation, mm	28.3			-10.0	-0.2	0.7
Wind speed, m/s	11.9	32.0		1.3	0.6	
Maximum wind gust, m/s		42.0				
Prevailing wind direction, deg	135					
Total radiation, MJ/m^2	0.8			-1.2	-0.5	0.4
Total ozone content (TO), DU	-	-	-			

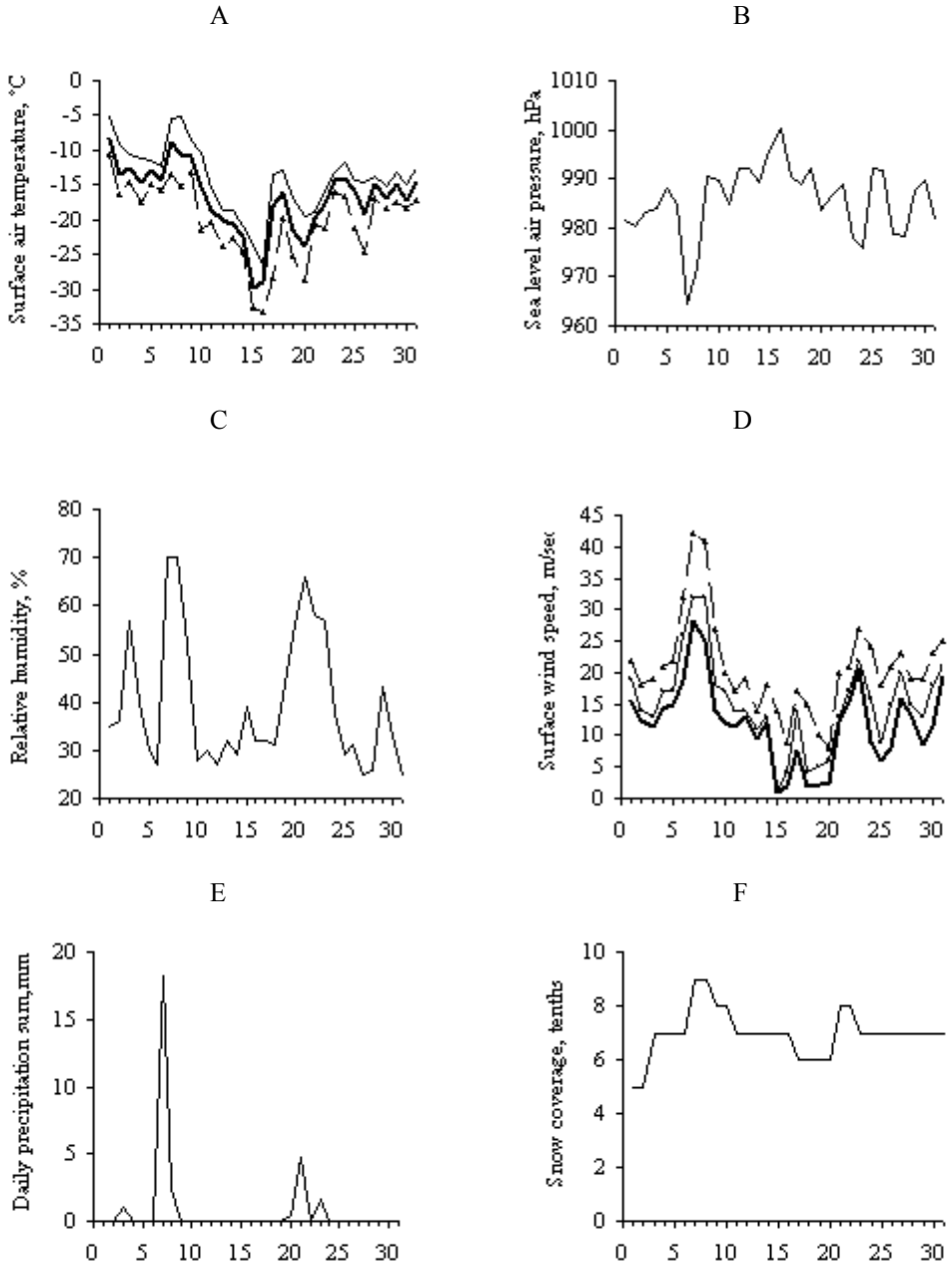

Fig. 1.2. Variations of daily mean values of surface temperature (A, bold line), maximum (A, thin line), minimum (A, dashed line) air temperature, sea level air pressure (B), relative humidity (C), mean (D, thick line), maximum (D, thin line) values of surface wind speed, maximum wind gust (D, dashed line), precipitation (E) and snow coverage (F). Novolazarevskaya station, July 2013.

Table 1.5

Results of aerological atmospheric sounding (from CLIMAT-TEMP messages)

Novolazarevskaya, July 2013

Isobaric surface, P hPa	Isobaric surface height, H m	Temperature, T °C	Dew point deficit, D °C	Resultant wind direction, deg	Resultant wind speed, m/s	Wind stability parameter,%	Number of days without temperature data	Number of days without wind data
970	122	-16.6	10.5					
925	475	-16.6	7.9	113	14	95	0	0
850	1104	-21.1	7.6	99	14	98	0	0
700	2515	-27.2	3.8	95	7	63	0	1
500	4869	-41.1	5.3	149	2	15	0	0
400	6350	-51.2	6.4	229	3	21	0	0
300	8170	-62.1	6.3	243	5	38	0	0
200	10616	-69.9	6.2	250	8	71	0	0
150	12317	-72.2	6.4	260	11	75	0	0
100	14676	-76.3	6.5	258	16	90	1	1
70	16709	-79.3	6.5	262	21	91	1	2
50	18601	-81.6	6.6	264	26	95	4	4
30	21418	-83.4	6.6	266	32	96	6	6
20	23666	-83.0	-	267	37	96	7	7

Table 1.6

Anomalies of standard isobaric surface heights and temperature

Novolazarevskaya, July 2013

P hPa	$H-H_{avg}$, m	$(H-H_{avg})/\sigma_H$	$T-T_{avg}$, °C	$(T-T_{avg})/\sigma_T$
850	-25	-0.6	-0.1	-0.1
700	-32	-0.7	0.1	0.0
500	-41	-0.7	-0.9	-0.5
400	-48	-0.7	-0.8	-0.5
300	-55	-0.8	0.1	0.1
200	-47	-0.6	1.6	1.0
150	-36	-0.5	1.3	0.9
100	-24	-0.3	1.5	1.1
70	-7	-0.1	2.2	1.5
50	-17	-0.2	2.3	1.3
30	-15	-0.1	2.0	1.2
20	53	0.4	2.3	1.2

BELLINGSHAUSEN STATION

Table 1.7

Monthly averages of meteorological parameters (f) and their deviations from the multiyear averages (f_{avg})

Bellingshausen, July 2013

Parameter	f	f_{max}	f_{min}	Anomaly $f-f_{avg}$	Normalized anomaly $(f-f_{avg})/\sigma_f$	Relative anomaly f/f_{avg}
Sea level air pressure, hPa	986.2	1024.9	950.7	-7.7	-1.3	
Air temperature, °C	-6.3	0.0	-18.9	0.3	0.1	
Relative humidity, %	89			0.6	0.2	
Total cloudiness (sky coverage), tenths	9.0			0.6	1.0	
Lower cloudiness (sky coverage),tenths	8.8			1.7	1.5	
Precipitation, mm	48.6			-4.4	-0.2	0.9
Wind speed, m/s	7.8	22.0		0.4	0.3	
Maximum wind gust, m/s		30.0				
Prevailing wind direction, deg	158					
Total radiation, MJ/m^2	21.0			-3.0	-0.9	0.9

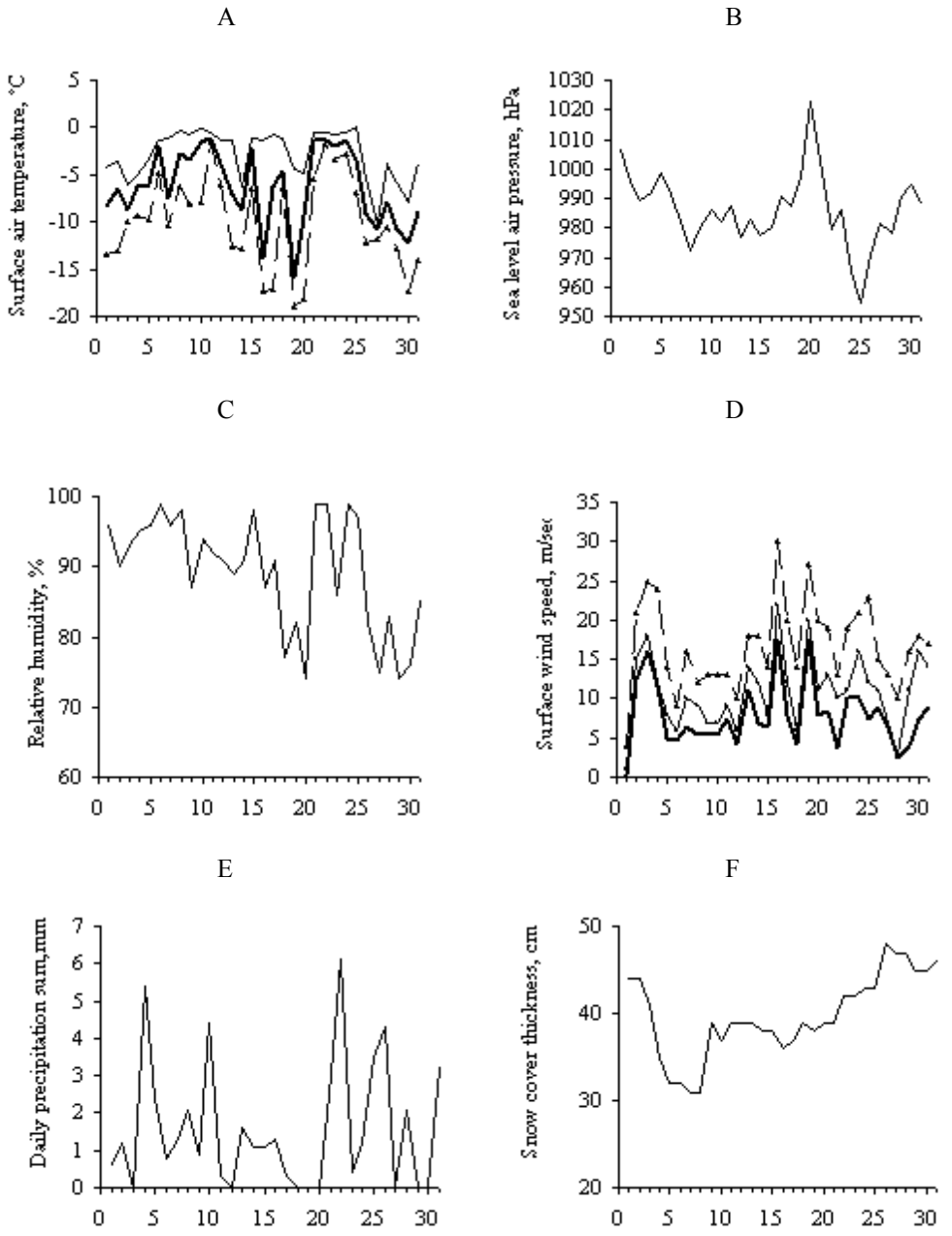

Fig. 1.3. Variations of daily mean values of surface temperature (A, bold line), maximum (A, thin line), minimum (A, dashed line) air temperature, sea level air pressure (B), relative humidity (C), mean (D, thick line), maximum (D, thin line) values of surface wind speed, maximum wind gust (D, dashed line), precipitation (E) and snow cover thickness (F).
.

Bellingshausen station. July 2013.

PROGRESS STATION

Table 1.8

Monthly averages of meteorological parameters (f)

Progress, July 2013

Parameter	f	f_{max}	f_{min}
Sea level air pressure, hPa	987.6	1009.0	955.7
Air temperature, ^{0}C	-14.9	-5.3	-33.3
Relative humidity, %	68		
Total cloudiness (sky coverage), tenths	8.4		
Lower cloudiness(sky coverage),tenths	4.3		
Precipitation, mm	50.4		
Wind speed, m/s	7.2	25.0	
Maximum wind gust, m/s		34.0	
Prevailing wind direction, deg	90		
Total radiation, MJ/m^2	3.3		

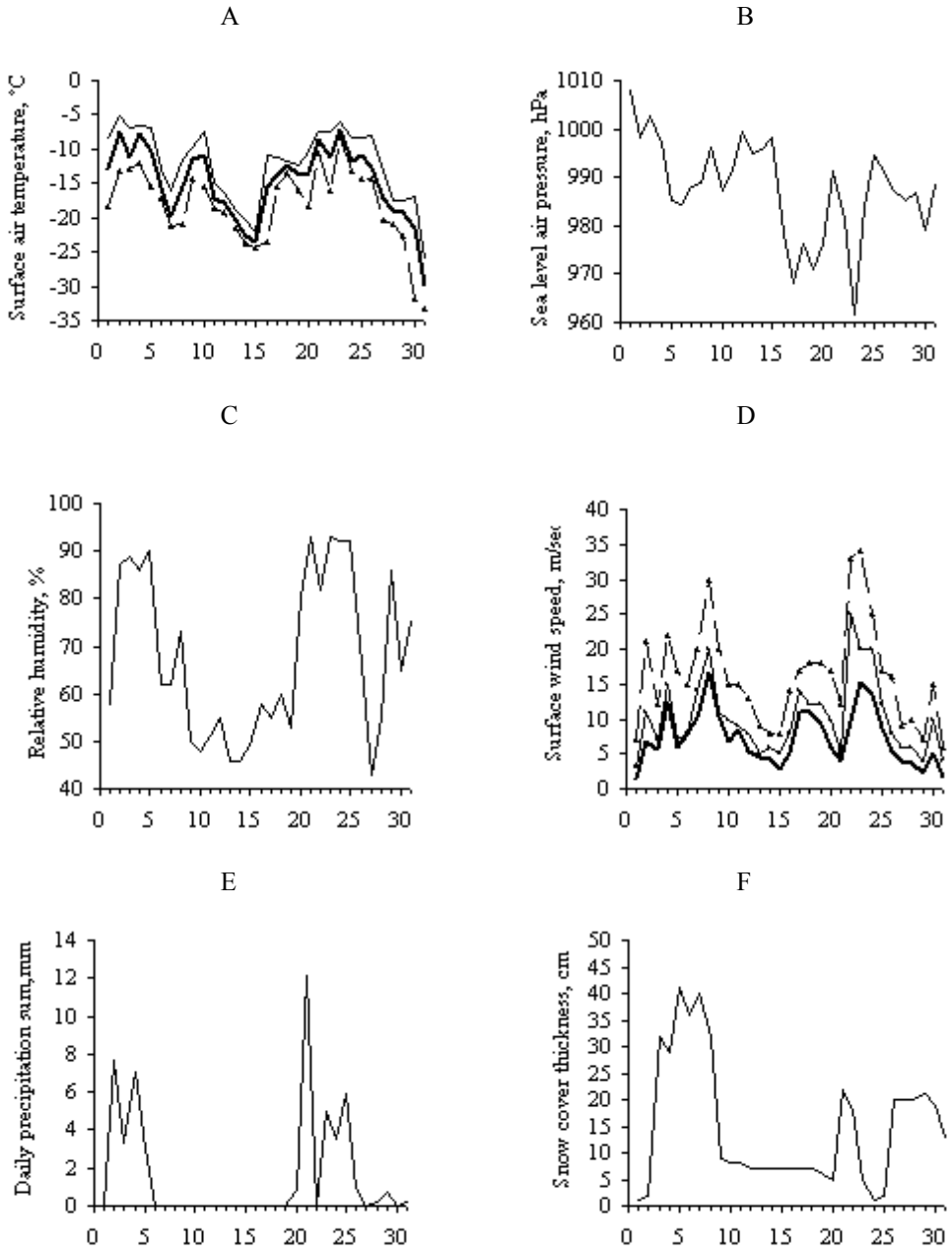

Fig. 1.4. Variations of daily mean values of surface temperature (A, bold line), maximum (A, thin line), minimum (A, dashed line) air temperature, sea level air pressure (B), relative humidity (C), mean (D, thick line), maximum (D, thin line) values of surface wind speed, maximum wind gust (D, dashed line), precipitation (E) and snow cover thickness (F). Progress station. April 2013.

VOSTOK STATION

Table 1.9

Monthly averages of meteorological parameters (f) and their deviations from the multiyear averages (f_{avg})

Vostok, July 2013

Parameter	f	f_{max}	f_{min}	Anomaly $f-f_{avg}$	Normalized anomaly $(f-f_{avg})/\sigma_f$	Relative anomaly f/f_{avg}
Station surface level air pressure, hPa	617.2	631.5	602.6	-3.9	-0.6	
Air temperature, °C	-65.9	-45.2	-79.2	1.2	0.4	
Relative humidity, %	56			-12.6	-2.9	
Total cloudiness (sky coverage), tenths	3.0				0.2	
Lower cloudiness(sky coverage),tenths	0.0			0.0	0.0	
Precipitation, mm	2.2			-1.0	-0.4	0.7
Wind speed, m/s	4.4	15.0		-1.3	-1.4	
Maximum wind gust, m/s		18.0				
Prevailing wind direction, deg	292					
Total radiation, MJ/m^2	0.0					
Total ozone content (TO), DU	-	-	-			

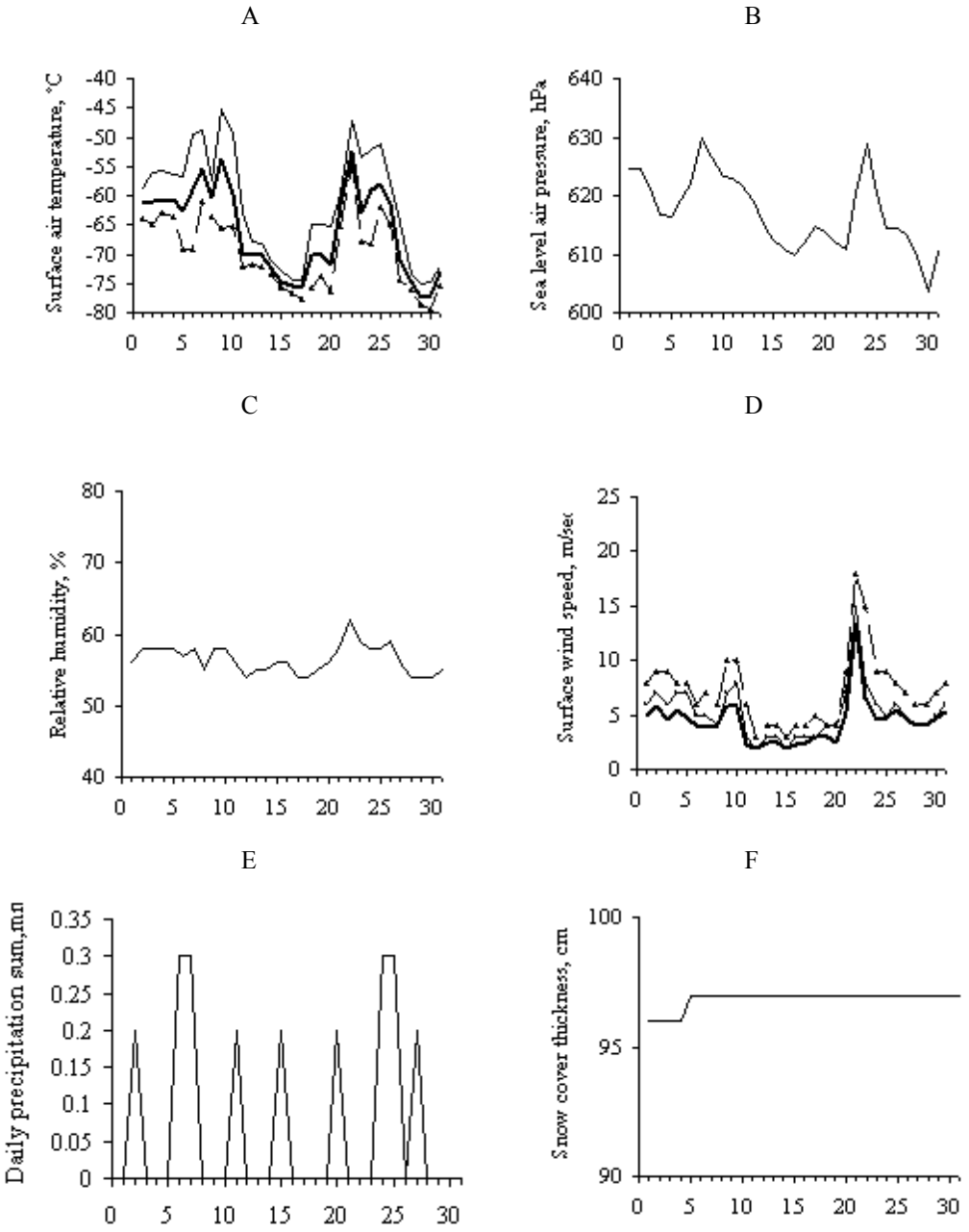

Fig. 1.5. Variations of daily mean values of surface temperature (A, bold line), maximum (A, thin line), minimum (A, dashed line) air temperature, ground level air pressure (B), relative humidity (C), mean (D, thick line), maximum (D, thin line) values of surface wind speed, maximum wind gust (D, dashed line, precipitation (E) and snow cover thickness (F).

Vostok station. July 2013.

July 2013

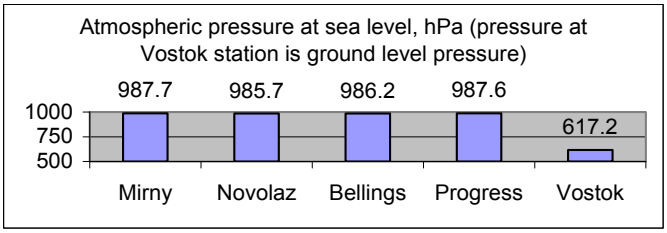

$(f-favg)/\sigma_f$	0.3	-0.3	-1.3	-0.6

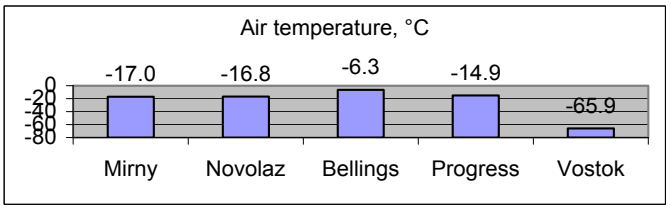

$(f-favg)/\sigma_f$	-0.1	0.2	0.1	0.4

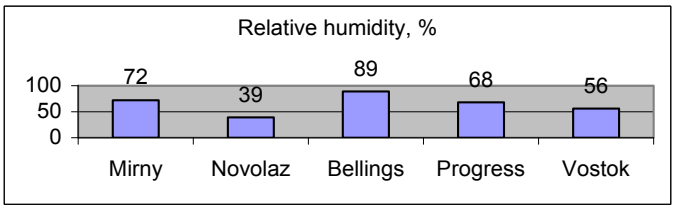

$(f-favg)/\sigma_f$	-0.4	-1.6	0.2	-2.9

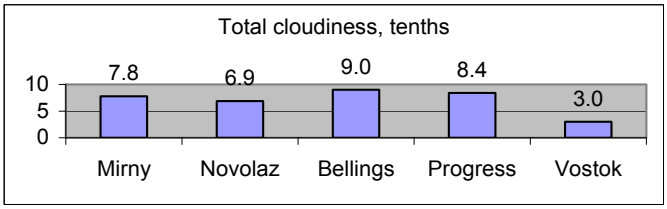

$(f-favg)/\sigma_f$	1.0	1.0	1.0	0.2

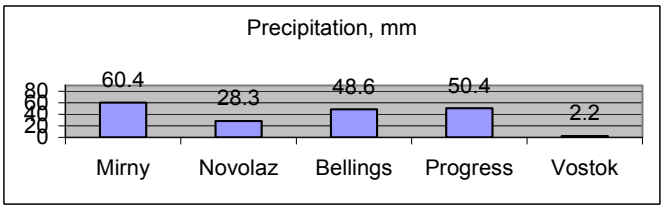

f/favg	0.9	0.7	0.9	0.7

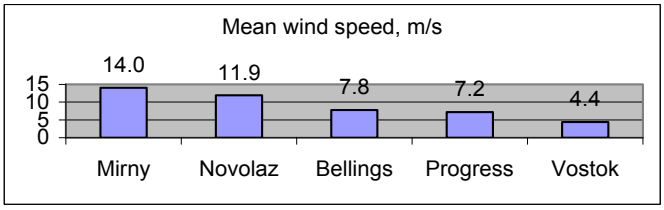

$(f-favg)/\sigma_f$	0.9	0.6	0.3	-1.4

Fig.1.6. Comparison of monthly averages of meteorological parameters at the stations. July 2013.

AUGUST 2013

MIRNY STATION

Table 1.10

Monthly averages of meteorological parameters (f) and their deviations from the multiyear averages (f_{avg})

Mirny, August 2013

Parameter	f	f_{max}	f_{min}	Anomaly $f-f_{avg}$	Normalized anomaly $(f-f_{avg})/\sigma_f$	Relative anomaly f/f_{avg}
Sea level air pressure, hPa	992.4	1009.8	964.8	8.0	1.4	
Air temperature, ^{0}C	-17.1	-3.1	-36.1	0.1	0.0	
Relative humidity, %	69			-4.0	-0.9	
Total cloudiness (sky coverage), tenths	7.1			0.4	0.4	
Lower cloudiness(sky coverage),tenths	2.5			-0.3	-0.2	
Precipitation, mm	32.6			-34.8	-0.7	0.5
Wind speed, m/s	12.0	24.0		-0.9	-0.6	
Maximum wind gust, m/s		36.0				
Prevailing wind direction, deg	135					
Total radiation, MJ/m^2	71.9			5.9	0.9	1.1
Total ozone content (TO), DU	277	386	216			

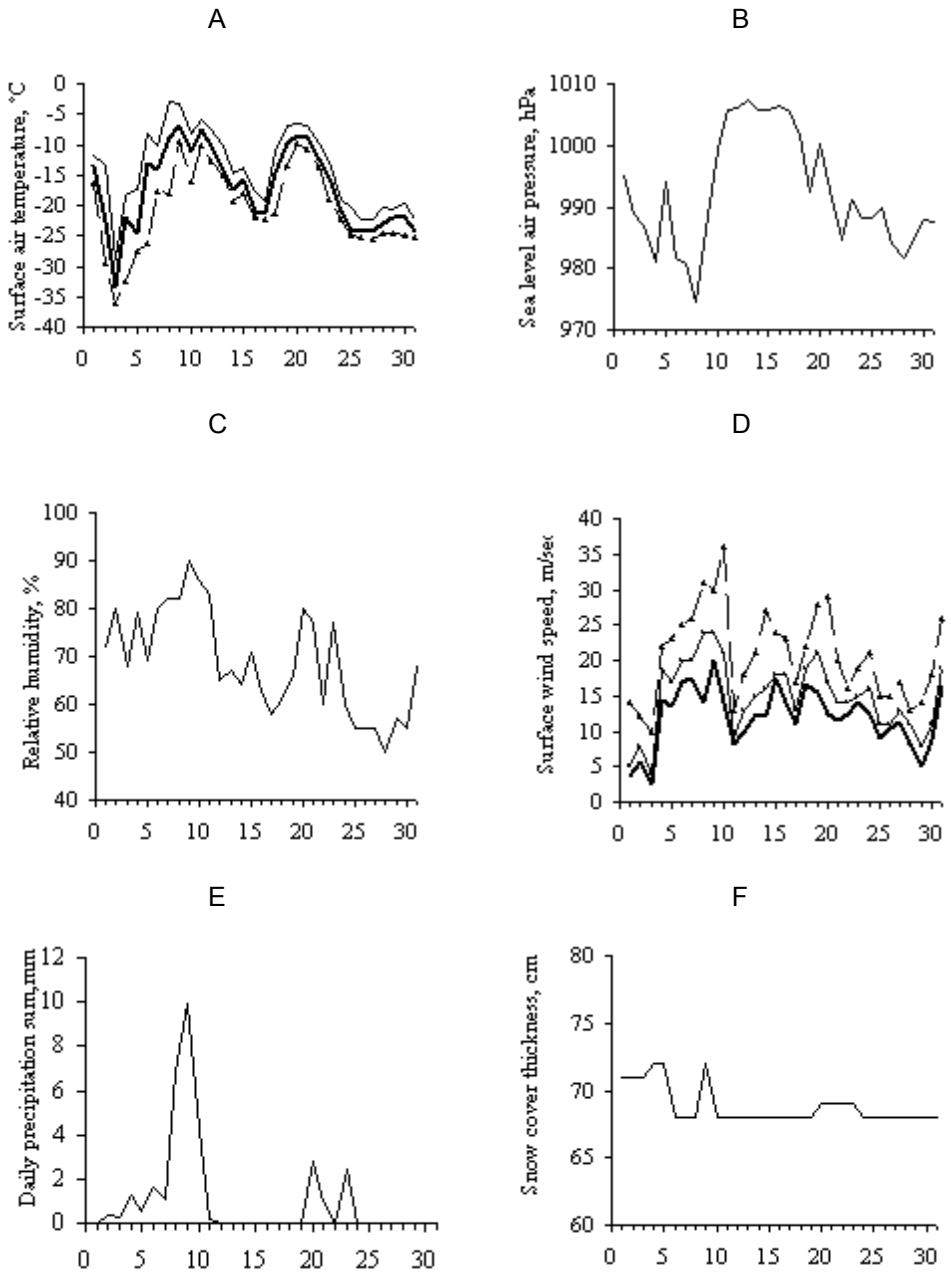

Fig. 1.13. Variations of daily mean values of surface temperature (A, bold line), maximum (A, thin line), minimum (A, dashed line) air temperature, sea level air pressure (B), relative humidity (C), mean (D, thick line), maximum (D, thin line) values of surface wind speed, maximum wind gust (D, dashed line), precipitation (E) and snow cover thickness (F). Mirny station. August 2013.

Table 1.11

Results of aerological atmospheric sounding (from CLIMAT-TEMP messages)

Mirny, August 2013

Isobaric surface, P hPa	Isobaric surface height, H m	Temperature, T ^{0}C	Dew point deficit, D ^{0}C	Resultant wind direction, deg	Resultant wind speed, m/s	Wind stability parameter,%	Number of days without temperature data	Number of days without wind data
990	39	-16.7	3.8					
925	549	-17.3	4.5	91	13	95	0	0
850	1177	-20.4	4.3	91	12	92	0	0
700	2602	-24.2	5.8	88	7	62	0	0
500	4986	-37.7	6.6	84	5	32	0	0
400	6491	-47.3	6.2	76	3	15	0	0
300	8337	-59.8	6.0	280	1	6	0	0
200	10792	-69.8	5.9	263	7	42	0	0
150	12488	-72.5	5.9	262	12	65	0	0
100	14849	-75.4	5.9	263	21	87	1	1
70	16899	-77.0	6.1	266	29	93	1	1
50	18824	-77.6	6.3	266	37	95	2	2
30	21757	-72.5	6.3	269	49	97	3	3
20	24128	-73.2	6.8	270	59	97	5	5
10	28006	-66.3	6.9	270	59	97	13	≥9

Table 1.12

Anomalies of standard isobaric surface heights and temperature

Mirny, August 2013

P hPa	$H-H_{avg}$, m	$(H-H_{avg})/\sigma_H$	$T-T_{avg}$, °C	$(T-T_{avg})/\sigma_T$
850	82	1.9	-0.6	-0.3
700	68	1.2	-0.6	-0.3
500	62	0.8	0.3	0.2
400	58	0.7	0.9	0.5
300	67	0.7	0.7	0.5
200	59	0.5	0.6	0.3
150	60	0.6	0.0	0.0
100	61	0.5	-0.3	-0.1
70	56	0.4	-0.2	-0.1
50	18	0.1	-0.5	-0.1
30	0	0.0	3.6	0.6
20	-13	0.0	0.1	0.0
10	-429	-0.6	-5.4	-0.4

NOVOLAZAREVSKAYA STATION

Table 1.13

Monthly averages of meteorological parameters (f) and their deviations from the multiyear averages (f_{avg})

Novolazarevskaya, August 2013

Parameter	f	f_{max}	f_{min}	Anomaly $f-f_{avg}$	Normalized anomaly $(f-f_{avg})/\sigma_f$	Relative anomaly f/f_{avg}
Sea level air pressure, hPa	992.8	1017.1	960.2	6.3	1.2	
Air temperature, ^{0}C	-16.6	-8.0	-32.7	1.7	0.7	
Relative humidity, %	44			-6.7	-0.9	
Total cloudiness (sky coverage), tenths	6.1			0.7	0.5	
Lower cloudiness(sky coverage),tenths	1.9			1.0	1.3	
Precipitation, mm	61.9			19.5	0.4	1.5
Wind speed, m/s	12.6	40.0		2.0	1.0	
Maximum wind gust, m/s		47.0				
Prevailing wind direction, deg	135					
Total radiation, MJ/m^2	32.1			-1.9	-0.4	0.9
Total ozone content (TO), DU	219	241	198			

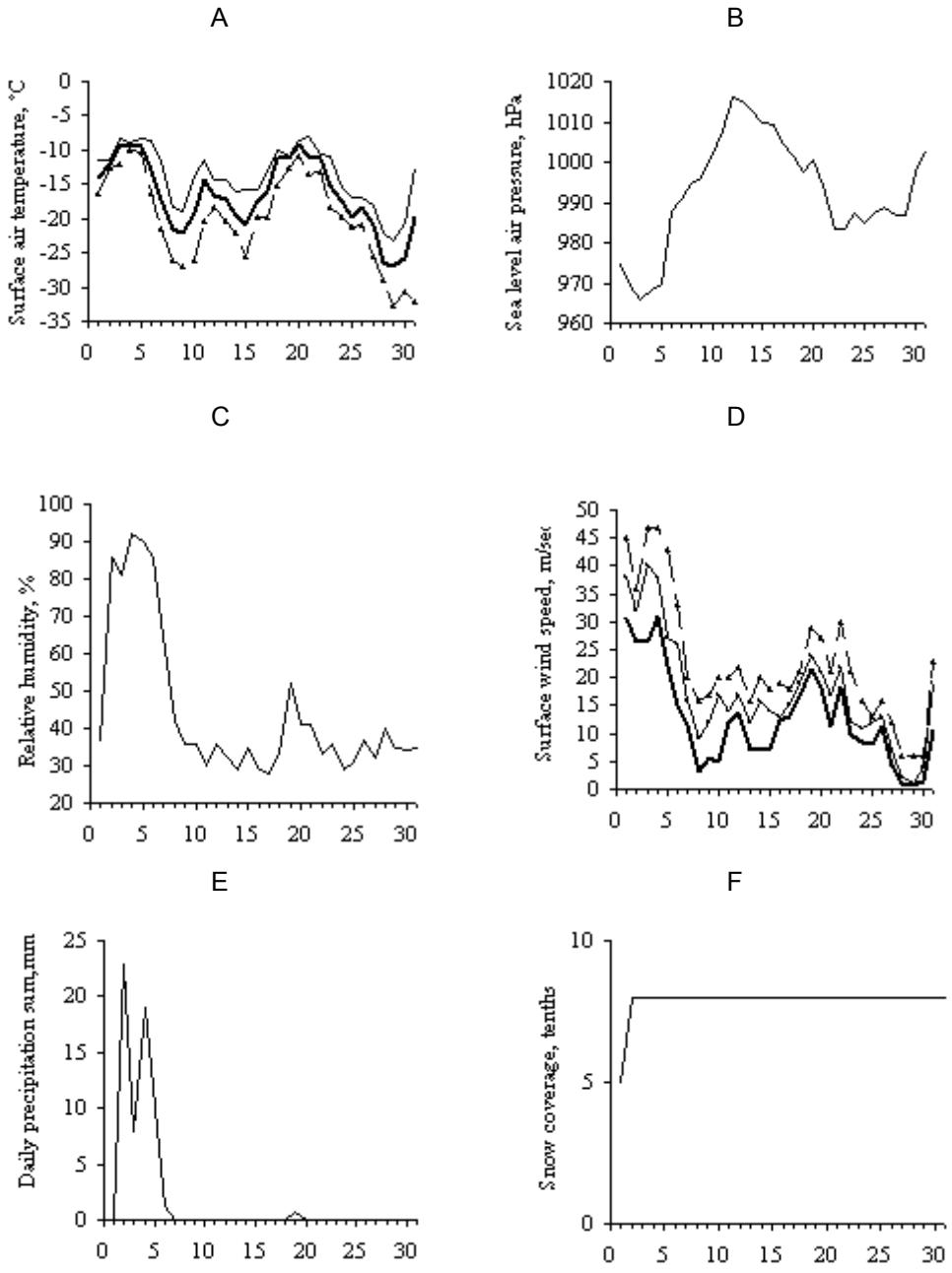

Fig. 1.14. Variations of daily mean values of surface temperature (A, bold line), maximum (A, thin line), minimum (A, dashed line) air temperature, sea level air pressure (B), relative humidity (C), mean (D, thick line), maximum (D, thin line) values of surface wind speed, maximum wind gust (D, dashed line), precipitation (E) and snow coverage (F). Novolazarevskaya station, August 2013.

Table 1.14

Results of aerological atmospheric sounding (from CLIMAT-TEMP messages)

Novolazarevskaya, August 2013

Isobaric surface, P hPa	Isobaric surface height, H m	Temperature, T ^{0}C	Dew point deficit, D ^{0}C	Resultant wind direction, deg	Resultant wind speed, m/s	Wind stability parameter,%	Number of days without temperature data	Number of days without wind data
980	122	-16.3	10.3					
925	555	-16.4	8.9	107	15	99	2	2
850	1184	-20.7	8.4	97	15	95	2	2
700	2596	-27.5	6.1	88	8	74	2	2
500	4949	-41.1	7.2	101	3	30	2	2
400	6428	-51.6	7.5	136	1	5	2	2
300	8241	-63.4	7.2	257	3	17	2	2
200	10665	-72.5	6.9	254	5	39	2	2
150	12340	-75.0	7.0	260	7	55	2	2
100	14668	-78.4	6.8	262	11	76	3	3
70	16679	-80.3	6.8	270	15	85	3	3
50	18567	-81.4	6.7	273	21	92	4	5
30	21423	-81.1	6.8	279	28	94	4	4
20	23697	-78.8	6.5	281	35	97	10	≥9

Table 1.15

Anomalies of standard isobaric surface heights and temperature

Novolazarevskaya, August 2013

P hPa	$H-H_{avg}$, m	$(H-H_{avg})/\sigma_H$	$T-T_{avg}$, °C	$(T-T_{avg})/\sigma_T$
850	71	1.4	1.2	0.6
700	71	1.2	0.3	0.2
500	67	0.9	-0.3	-0.2
400	61	0.8	-0.6	-0.5
300	53	0.6	-0.8	-0.8
200	44	0.5	0.0	0.0
150	40	0.4	0.5	0.4
100	40	0.4	0.8	0.5
70	18	0.2	1.4	0.8
50	-2	0.0	1.6	0.7
30	-12	-0.1	1.7	0.6
20	-10	0.0	1.8	0.5

BELLINGSHAUSEN STATION

Table 1.16

Monthly averages of meteorological parameters (f) and their deviations from the multiyear averages (f_{avg})

Bellingshausen, August 2013

Parameter	f	f_{max}	f_{min}	Anomaly $f-f_{avg}$	Normalized anomaly $(f-f_{avg})/\sigma_f$	Relative anomaly f/f_{avg}
Sea level air pressure, hPa	991.9	1031.4	966.2	-0.1	0.0	
Air temperature, ^{0}C	-8.1	0.0	-20.4	-1.4	-0.6	
Relative humidity, %	87			-0.9	-0.3	
Total cloudiness (sky coverage), tenths	8.9			0.4	0.8	
Lower cloudiness(sky coverage),tenths	8.4			1.2	1.2	
Precipitation, mm	94.6			26.4	0.7	1.4
Wind speed, m/s	9.1	30.0		1.3	1.4	
Maximum wind gust, m/s		39.0				
Prevailing wind direction, deg	112					
Total radiation, MJ/m^2	88.8			2.8	0.4	1.0

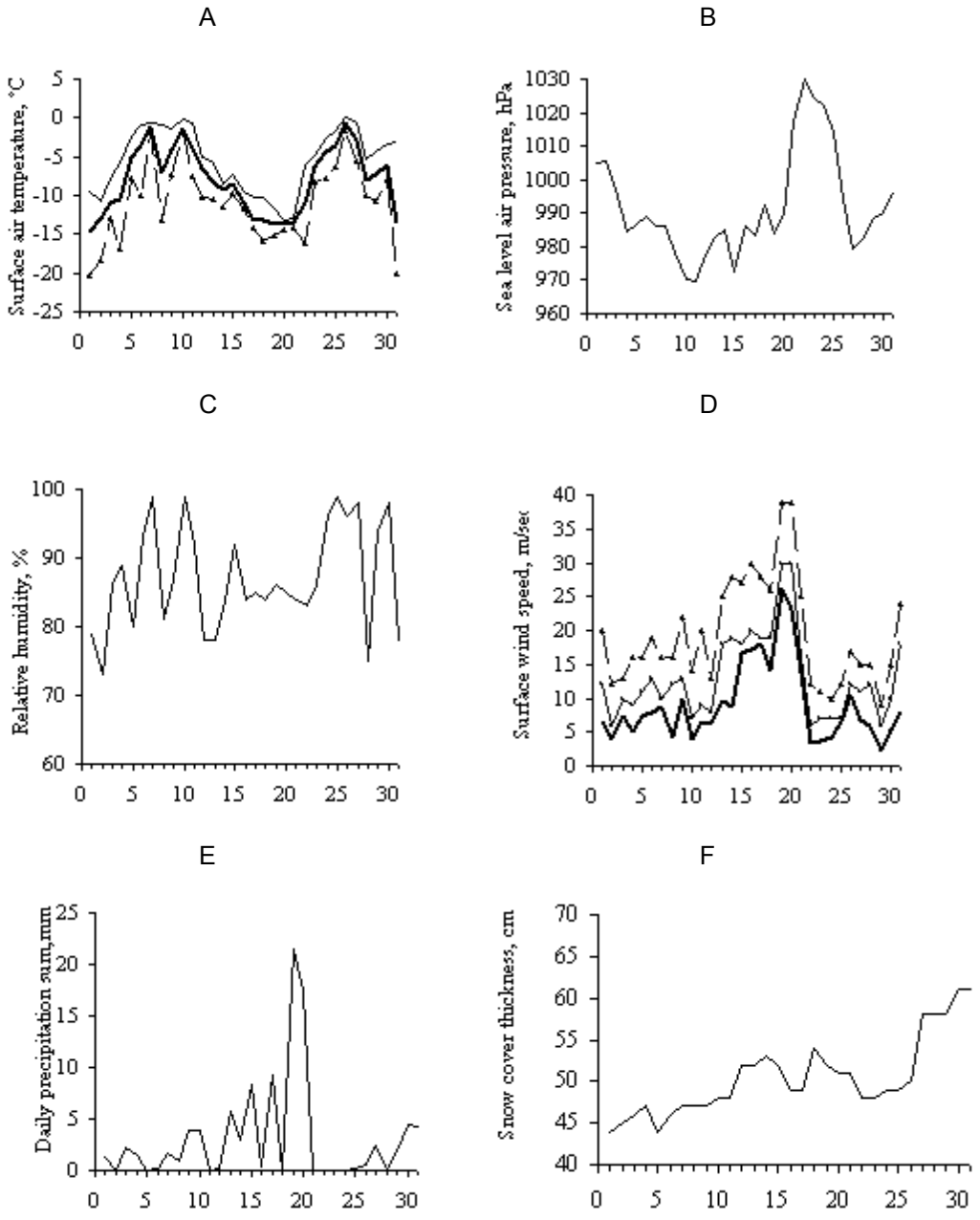

Fig. 1.15. Variations of daily mean values of surface temperature (A, bold line), maximum (A, thin line), minimum (A, dashed line) air temperature, sea level air pressure (B), relative humidity (C), mean (D, thick line), maximum (D, thin line) values of surface wind speed, maximum wind gust (D, dashed line), precipitation (E) and snow cover thickness (F). Bellingshausen station. August 2013.

PROGRESS STATION

Table 1.17

Monthly averages of meteorological parameters (f)

Progress, August 2012

Parameter	f	f_{max}	f_{min}
Sea level air pressure, hPa	997.4	1018.5	978.1
Air temperature, ^{0}C	-17.5	-3.9	-45.3
Relative humidity, %	58		
Total cloudiness (sky coverage), tenths	7.3		
Lower cloudiness(sky coverage),tenths	3.1		
Precipitation, mm	8.0		
Wind speed, m/s	6.1	15.0	
Maximum wind gust, m/s		26.0	
Prevailing wind direction, deg	90		
Total radiation, MJ/m^2	41.5		

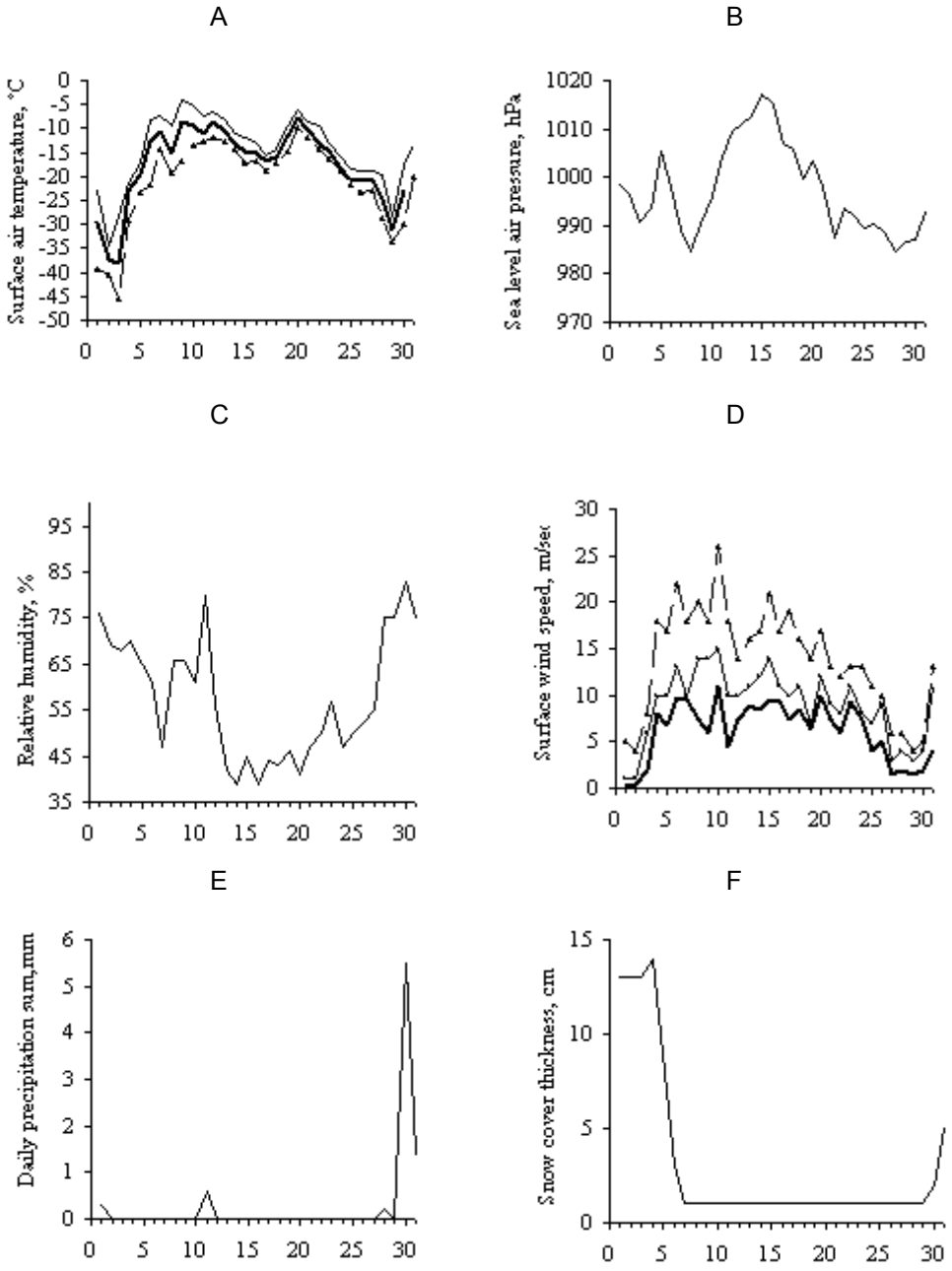

Fig. 1.16. Variations of daily mean values of surface temperature (A, bold line), maximum (A, thin line), minimum (A, dashed line) air temperature, sea level air pressure (B), relative humidity (C), mean (D, thick line), maximum (D, thin line) values of surface wind speed, maximum wind gust (D, dashed line), precipitation (E) and snow cover thickness (F).

Progress station. August 2013.

VOSTOK STATION

Table 1.18

Monthly averages of meteorological parameters (f) and their deviations from the multiyear averages (f_{avg})

Vostok, August 2013

Parameter	f	f_{max}	f_{min}	Anomaly $f-f_{avg}$	Normalized anomaly $(f-f_{avg})/\sigma_f$	Relative anomaly f/f_{avg}
Station surface level air pressure, hPa	629.2	651.4	600.7	9.6	1.3	
Air temperature, °C	-62.9	-34.8	-77.6	5.1	1.3	
Relative humidity, %	56			-12.6	-3.0	
Total cloudiness (sky coverage), tenths	2.1				-1.2	
Lower cloudiness(sky coverage),tenths	0.0			0.0	0.0	
Precipitation, mm	3.5			0.4	0.1	1.1
Wind speed, m/s	3.7	9.0		-1.9	-2.4	
Maximum wind gust, m/s		15.0				
Prevailing wind direction, deg	315					
Total radiation, MJ/m^2	0.0					
Total ozone content (TO), DU	-	-	-			

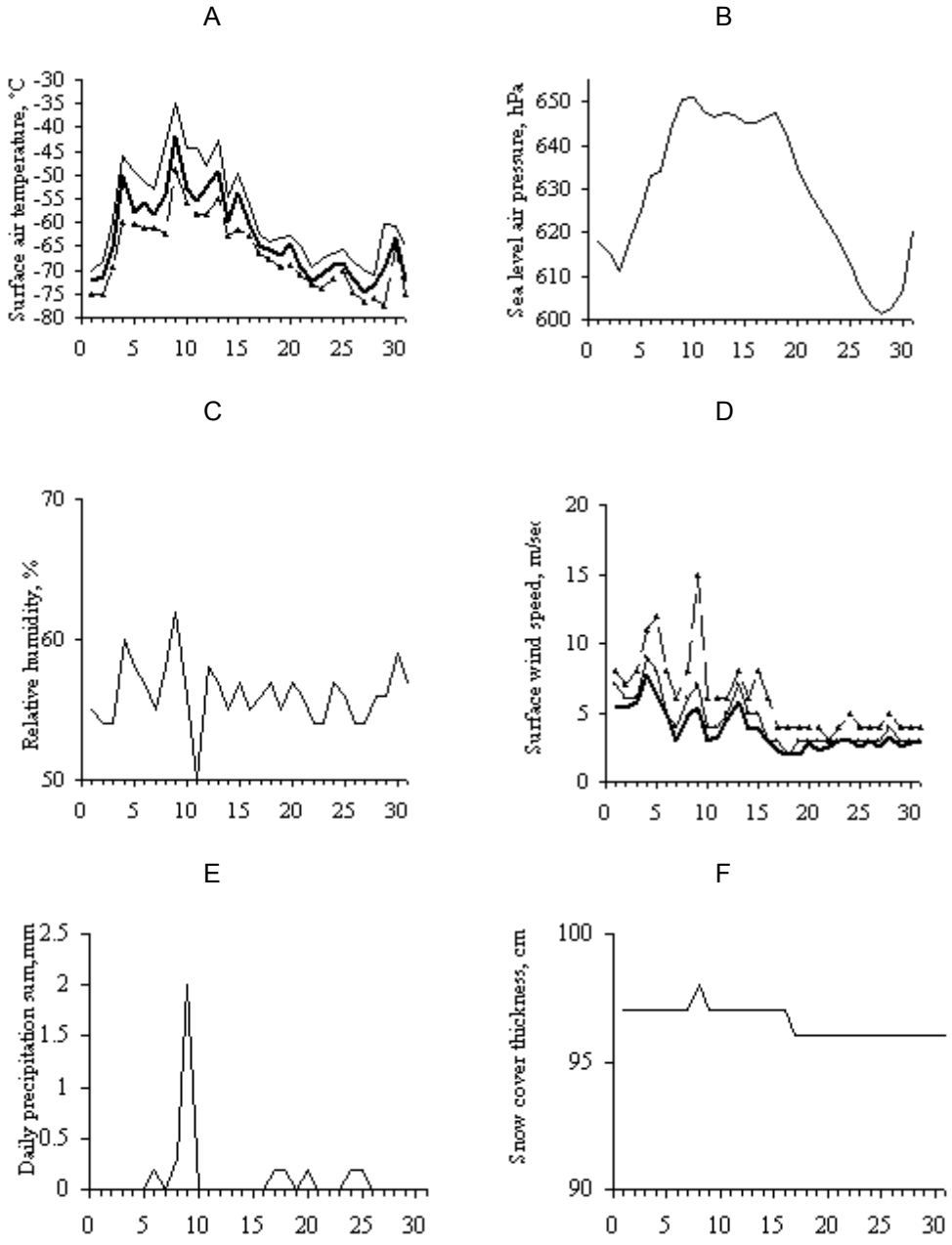

Fig. 1.17. Variations of daily mean values of surface temperature (A, bold line), maximum (A, thin line), minimum (A, dashed line) air temperature, ground level air pressure (B), relative humidity (C), mean (D, thick line), maximum (D, thin line) values of surface wind speed, maximum wind gust (D, dashed line), precipitation (E) and snow cover thickness (F).

Vostok station. August 2013.

A u g u s t 2 0 1 3

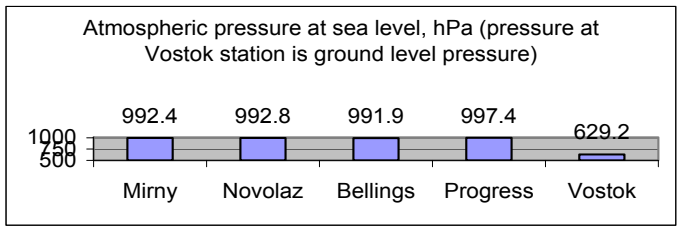

(f-favg)/σ_f	1.4	1.2	0.0		1.3

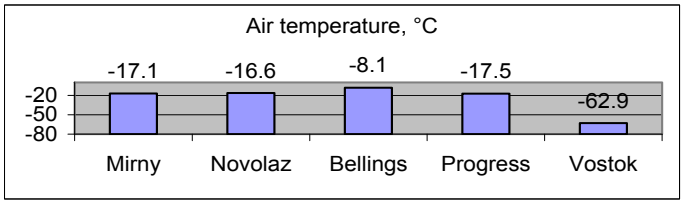

(f-favg)/σ_f	0.0	0.7	-0.6		1.3

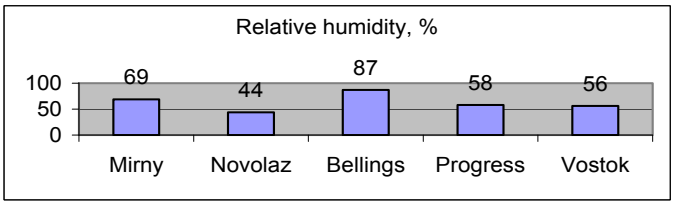

(f-favg)/σ_f	-0.9	-0.9	-0.3		-3.0

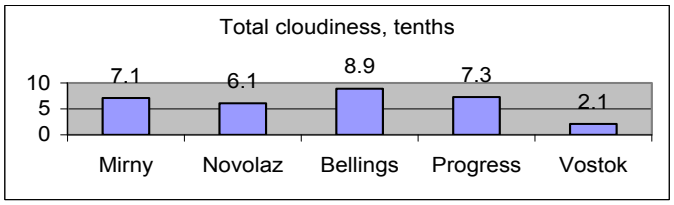

(f-favg)/σ_f	0.4	0.5	0.8		-1.2

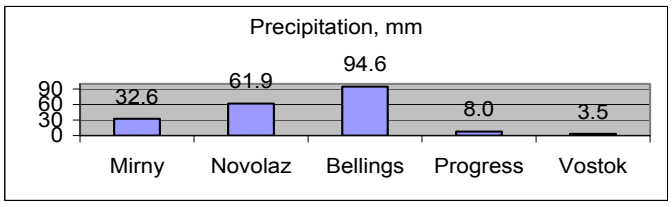

f/favg	0.5	1.5	1.4		1.1

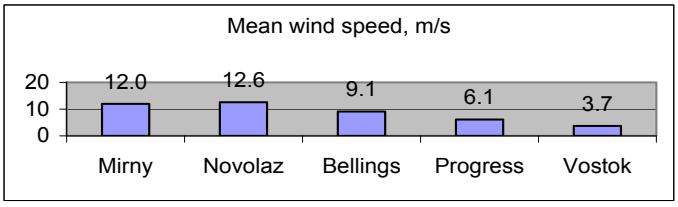

(f-favg)/σ_f	-0.6	1.0	1.4		-2.4

Fig. 1.18. Comparison of monthly averages of meteorological parameters at the stations. August 2013.

SEPTEMBER 2013

MIRNY STATION

Table 1.19

Monthly averages of meteorological parameters (f) and their deviations from the multiyear averages (f_{avg})

Mirny, September 2013

Parameter	f	f_{max}	f_{min}	Anomaly $f-f_{avg}$	Normalized anomaly $(f-f_{avg})/\sigma_f$	Relative anomaly f/f_{avg}
Sea level air pressure, hPa	987.8	1013.5	957.4	5.7	1.2	
Air temperature, ^{0}C	-10.5	-0.1	-33.8	6.2	2.4	
Relative humidity, %	74			2.6	0.6	
Total cloudiness (sky coverage), tenths	8.0			1.5	1.4	
Lower cloudiness(sky coverage),tenths	4.4			1.6	1.3	
Precipitation, mm	33.2			-27.7	-0.5	0.5
Wind speed, m/s	12.3	28.0		0.2	0.1	
Maximum wind gust, m/s		37.0				
Prevailing wind direction, deg	90					
Total radiation, MJ/m^2	199.4			-23.6	-1.5	0.9
Total ozone content (TO), DU	372	455	235			

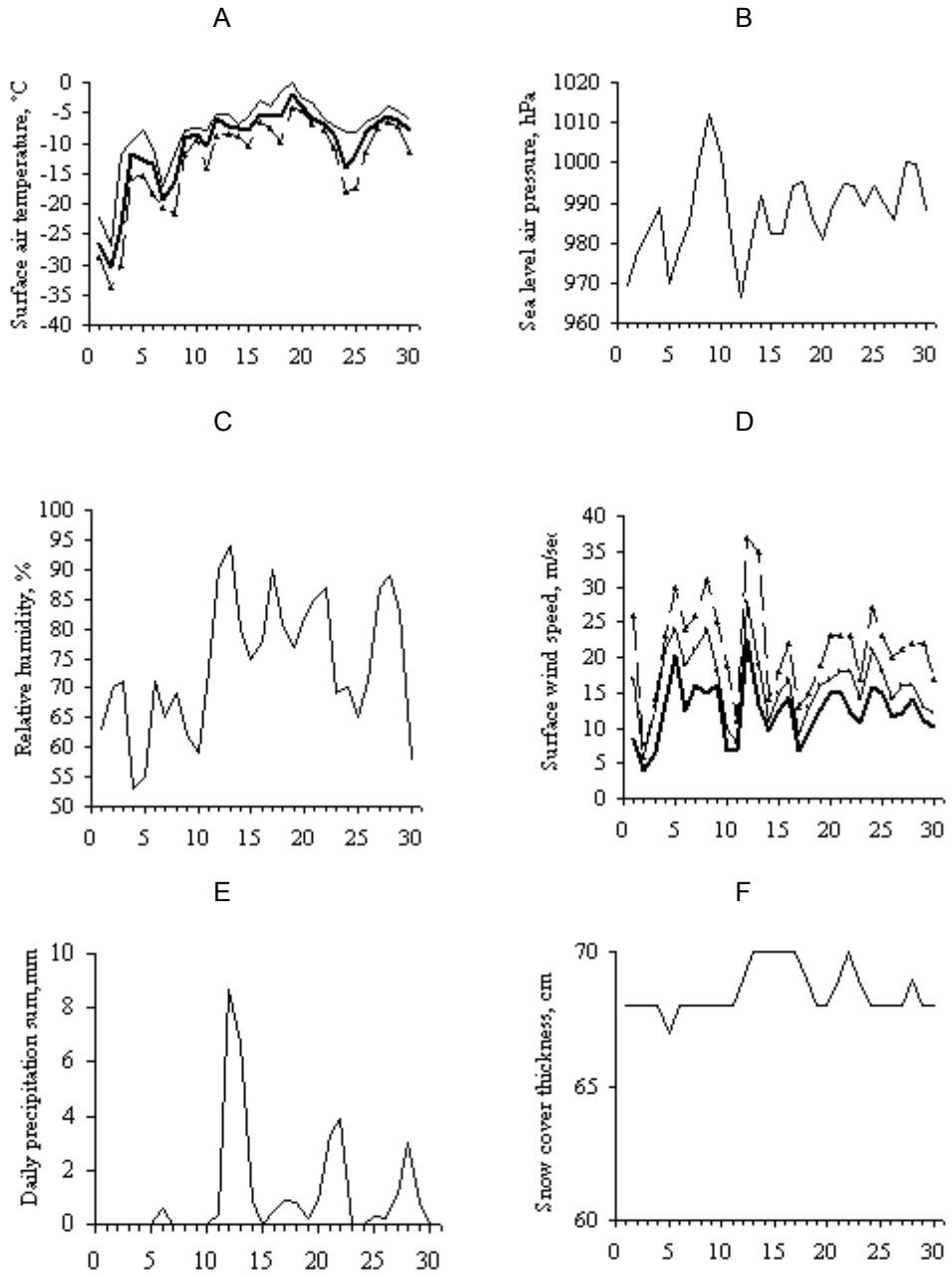

Fig. 1.19. Variations of daily mean values of surface temperature (A, bold line), maximum (A, thin line), minimum (A, dashed line) air temperature, sea level air pressure (B), relative humidity (C), mean (D, thick line), maximum (D, thin line) values of surface wind speed, maximum wind gust (D, dashed line), precipitation (E) and snow cover thickness (F). Mirny station. September 2013.

Table 1.20

Results of aerological atmospheric sounding (from CLIMAT-TEMP messages)

Mirny, September 2013

Isobaric surface, P hPa	Isobaric surface height, H m	Temperature, T ^{0}C	Dew point deficit, D ^{0}C	Resultant wind direction, deg	Resultant wind speed, m/s	Wind stability parameter,%	Number of days without temperature data	Number of days without wind data
984	39	-11.1	2.5					
925	511	-11.1	2.7	89	15	94	0	1
850	1155	-14.2	2.9	84	15	92	0	1
700	2609	-19.9	3.4	71	9	68	0	0
500	5035	-33.5	4.1	43	8	49	0	0
400	6564	-44.5	4.2	29	9	51	0	0
300	8427	-58.2	4.3	16	9	50	0	0
200	10912	-65.4	4.4	334	9	56	0	0
150	12660	-65.3	4.6	309	15	74	0	0
100	15130	-64.0	4.9	291	25	85	0	0
70	17343	-59.5	5.6	288	37	89	1	1
50	19465	-55.6	6.7	284	47	91	2	2
30	22726	-50.9	9.3	282	56	89	4	4
20	25385	-46.6	11.7	279	59	91	8	8

Table 1.21

Anomalies of standard isobaric surface heights and temperature

Mirny, September 2013

P hPa	$H-H_{avg}$, m	$(H-H_{avg})/\sigma_H$	$T-T_{avg}$, °C	$(T-T_{avg})/\sigma_T$
850	66	1.7	4.9	2.5
700	82	1.9	3.4	2.1
500	113	2.0	4.2	2.4
400	138	2.0	3.6	2.2
300	153	2.1	1.8	1.4
200	177	2.1	3.8	2.1
150	213	2.4	5.2	2.2
100	285	3.3	6.4	1.8
70	384	3.8	9.2	1.8
50	461	3.3	10.8	1.8
30	583	2.5	9.9	1.4
20	666	1.9	8.4	1.1

NOVOLAZAREVSKAYA STATION

Table 1.22

Monthly averages of meteorological parameters (f) and their deviations from the multiyear averages (f_{avg})

Novolazarevskaya, September 2013

Parameter	f	f_{max}	f_{min}	Anomaly $f-f_{avg}$	Normalized anomaly $(f-f_{avg})/\sigma_f$	Relative anomaly f/f_{avg}
Sea level air pressure, hPa	991.6	1011.3	968.0	7.4	1.6	
Air temperature, ^{0}C	-12.3	-3.7	-22.4	4.9	2.5	
Relative humidity, %	36			-15.1	-2.2	
Total cloudiness (sky coverage), tenths	5.9			0.5	0.5	
Lower cloudiness(sky coverage),tenths	1.7			0.9	1.0	
Precipitation, mm	1.4			-43.7	-0.8	0.0
Wind speed, m/s	10.6	22.0		0.7	0.4	
Maximum wind gust, m/s		28.0				
Prevailing wind direction, deg	135					
Total radiation, MJ/m^2	202.9			28.9	1.8	1.2
Total ozone content (TO), DU	199	234	160			

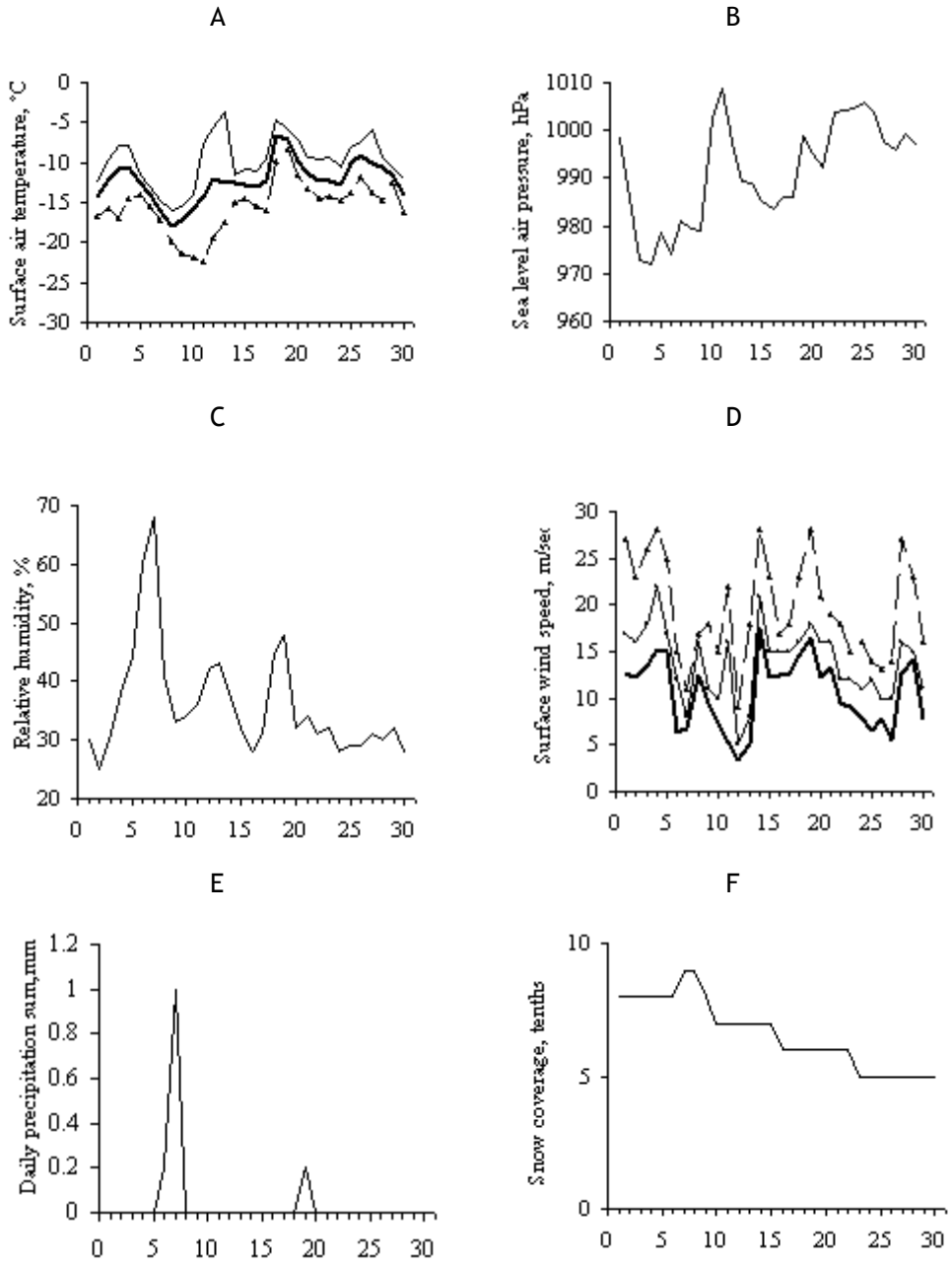

Fig. 1.20. Variations of daily mean values of surface temperature (A, bold line), maximum (A, thin line), minimum (A, dashed line) air temperature, sea level air pressure (B), relative humidity (C), mean (D, thick line), maximum (D, thin line) values of surface wind speed, maximum wind gust (D, dashed line), precipitation (E) and snow coverage (F). Novolazarevskaya station, September 2013.

Table 1.23

Results of aerological atmospheric sounding (from CLIMAT-TEMP messages)

Novolazarevskaya, September 2013

Isobaric surface, P hPa	Isobaric surface height, H m	Temperature, T ^{0}C	Dew point deficit, D ^{0}C	Resultant wind direction, deg	Resultant wind speed, m/s	Wind stability parameter,%	Number of days without temperature data	Number of days without wind data
976	122	-12.4	11.6					
925	527	-13.2	10.6	109	16	97	1	1
850	1163	-18.3	9.8	100	17	99	1	1
700	2585	-25.3	6.0	102	13	97	1	2
500	4965	-38.1	6.1	111	6	60	1	1
400	6463	-49.0	6.6	129	6	52	1	1
300	8292	-61.5	6.2	147	6	43	1	1
200	10728	-72.5	6.0	179	6	47	1	1
150	12404	-75.4	5.9	228	6	49	2	2
100	14736	-77.7	5.9	252	8	65	2	2
70	16767	-78.4	6.0	269	13	82	2	2
50	18681	-77.6	5.9	276	18	87	3	3
30	21624	-73.6	6.0	287	28	94	5	5
20	24032	-65.5	6.5	292	39	94	6	7

Table 1.24

Anomalies of standard isobaric surface heights and temperature

Novolazarevskaya, September 2013

P hPa	$H-H_{avg}$, m	$(H-H_{avg})/\sigma_H$	$T-T_{avg}$, °C	$(T-T_{avg})/\sigma_T$
850	62	1.7	2.8	2.1
700	69	1.7	2.1	1.6
500	84	1.7	2.0	1.8
400	93	1.7	1.3	1.2
300	94	1.5	0.5	0.4
200	93	1.4	-0.2	-0.1
150	89	1.3	-0.5	-0.3
100	80	1.0	-0.4	-0.2
70	72	0.8	-0.2	-0.1
50	48	0.4	0.6	0.2
30	18	0.1	1.4	0.3
20	-30	-0.1	3.3	0.6

BELLINGSHAUSEN STATION

Table 1.25

Monthly averages of meteorological parameters (f) and their deviations from the multiyear averages (f_{avg})

Bellingshausen, September 2013

Parameter	f	f_{max}	f_{min}	Anomaly $f-f_{avg}$	Normalized anomaly $(f-f_{avg})/\sigma_f$	Relative anomaly f/f_{avg}
Sea level air pressure, hPa	998.3	1028.9	967.7	7.2	2.1	
Air temperature, ^{0}C	-5.0	0.4	-18.8	-0.6	-0.3	
Relative humidity, %	90			1.3	0.5	
Total cloudiness (sky coverage), tenths	9.0			0.2	0.4	
Lower cloudiness(sky coverage),tenths	8.6			0.7	1.0	
Precipitation, mm	26.5			-36.3	-1.8	0.4
Wind speed, m/s	6.9	16.0		-1.1	-1.1	
Maximum wind gust, m/s		21.0				
Prevailing wind direction, deg	360					
Total radiation, MJ/m^2	227.4			13.4	0.7	1.1

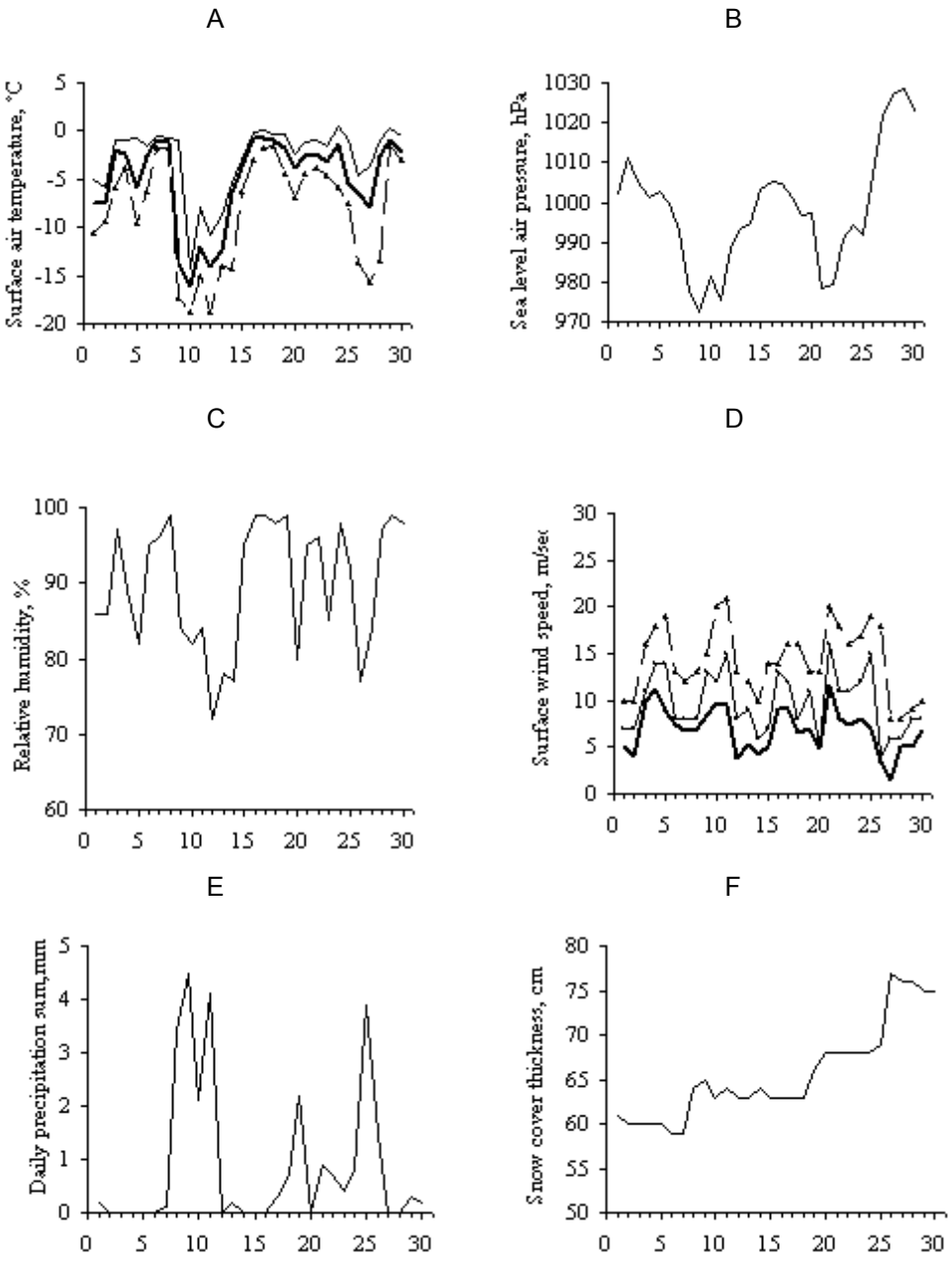

Fig. 1.21. Variations of daily mean values of surface temperature (A, bold line), maximum (A, thin line), minimum (A, dashed line) air temperature, sea level air pressure (B), relative humidity (C), mean (D, thick line), maximum (D, thin line) values of surface wind speed, maximum wind gust (D, dashed line), precipitation (E) and snow cover thickness (F). Bellingshausen station. September 2013.

PROGRESS STATION

Table 1.26

Monthly averages of meteorological parameters (f)

Progress, September 2013

Parameter	f	f_{max}	f_{min}
Sea level air pressure, hPa	990.1	1007.0	962.8
Air temperature, ^{0}C	-10.0	-1.7	-23.9
Relative humidity, %	62		
Total cloudiness (sky coverage), tenths	6.7		
Lower cloudiness(sky coverage),tenths	3.2		
Precipitation, mm	13.7		
Wind speed, m/s	7.1	22.0	
Maximum wind gust, m/s		34.0	
Prevailing wind direction, deg	90		
Total radiation, MJ/m^2	186.0		

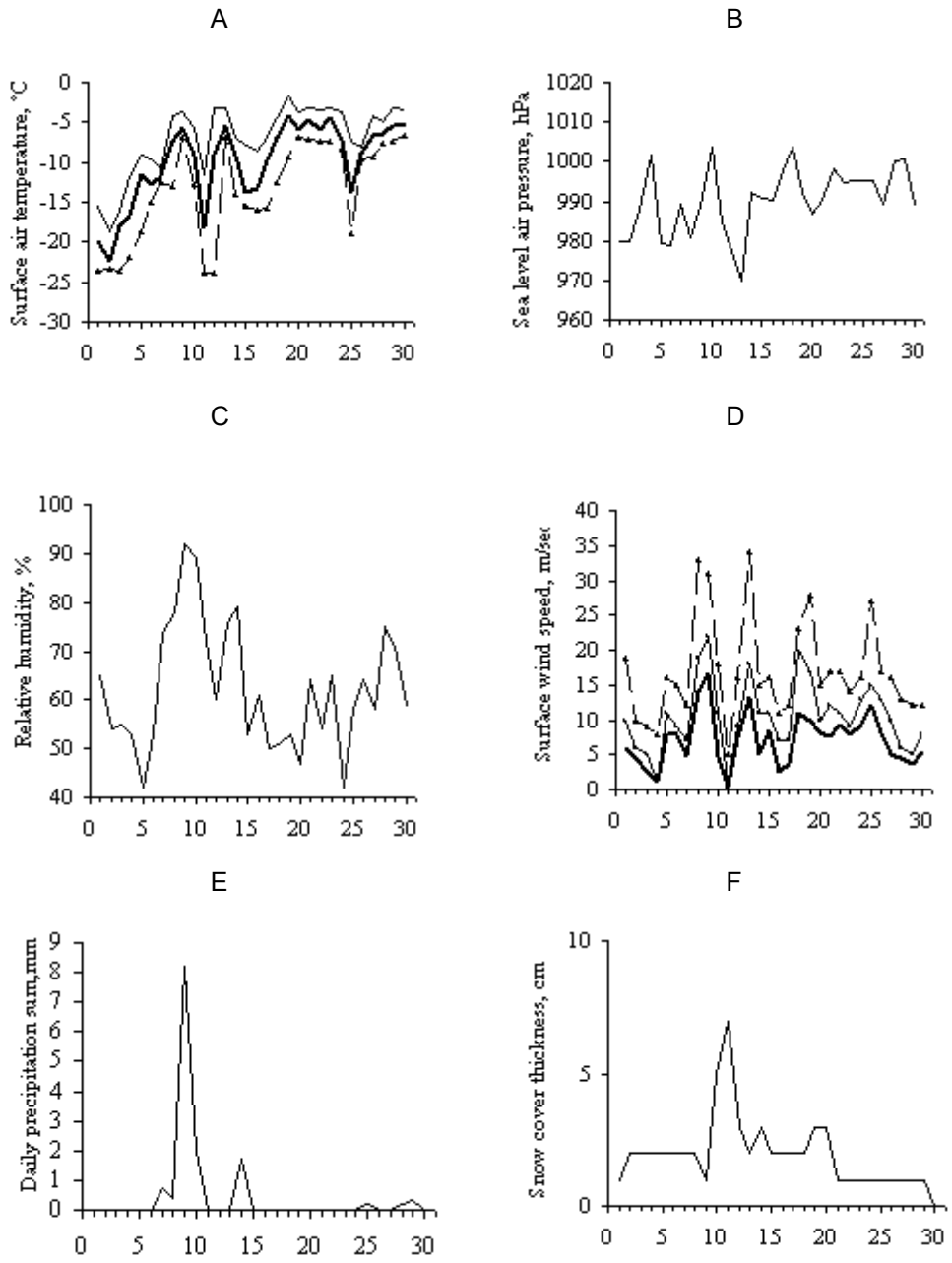

Fig. 1.22. Variations of daily mean values of surface temperature (A, bold line), maximum (A, thin line), minimum (A, dashed line) air temperature, sea level air pressure (B), relative humidity (C), mean (D, thick line), maximum (D, thin line) values of surface wind speed, maximum wind gust (D, dashed line), precipitation (E) and snow cover thickness (F). Progress station. September 2013.

VOSTOK STATION

Table 1.27

Monthly averages of meteorological parameters (f) and their deviations from the multiyear averages (f_{avg})

Vostok, September 2013

Parameter	f	f_{max}	f_{min}	Anomaly $f-f_{avg}$	Normalized anomaly $(f-f_{avg})/\sigma_f$	Relative anomaly f/f_{avg}
Ground level air pressure, hPa	633.2	650.1	619.8	15.2	3.3	
Air temperature, °C	-59.7	-39.4	-77.4	6.0	1.7	
Relative humidity, %	57			-12.0	-2.8	
Total cloudiness (sky coverage), tenths	4.7				0.8	
Lower cloudiness(sky coverage),tenths	0.0			-0.1	-0.5	
Precipitation, mm	3.5			0.5	0.2	1.2
Wind speed, m/s	3.6	7.0		-1.9	-2.1	
Maximum wind gust, m/s		11.0				
Prevailing wind direction, deg	292					
Total radiation, MJ/m^2	101.9			2.8	0.2	1.0
Total ozone content (TO), DU	205	256	149			

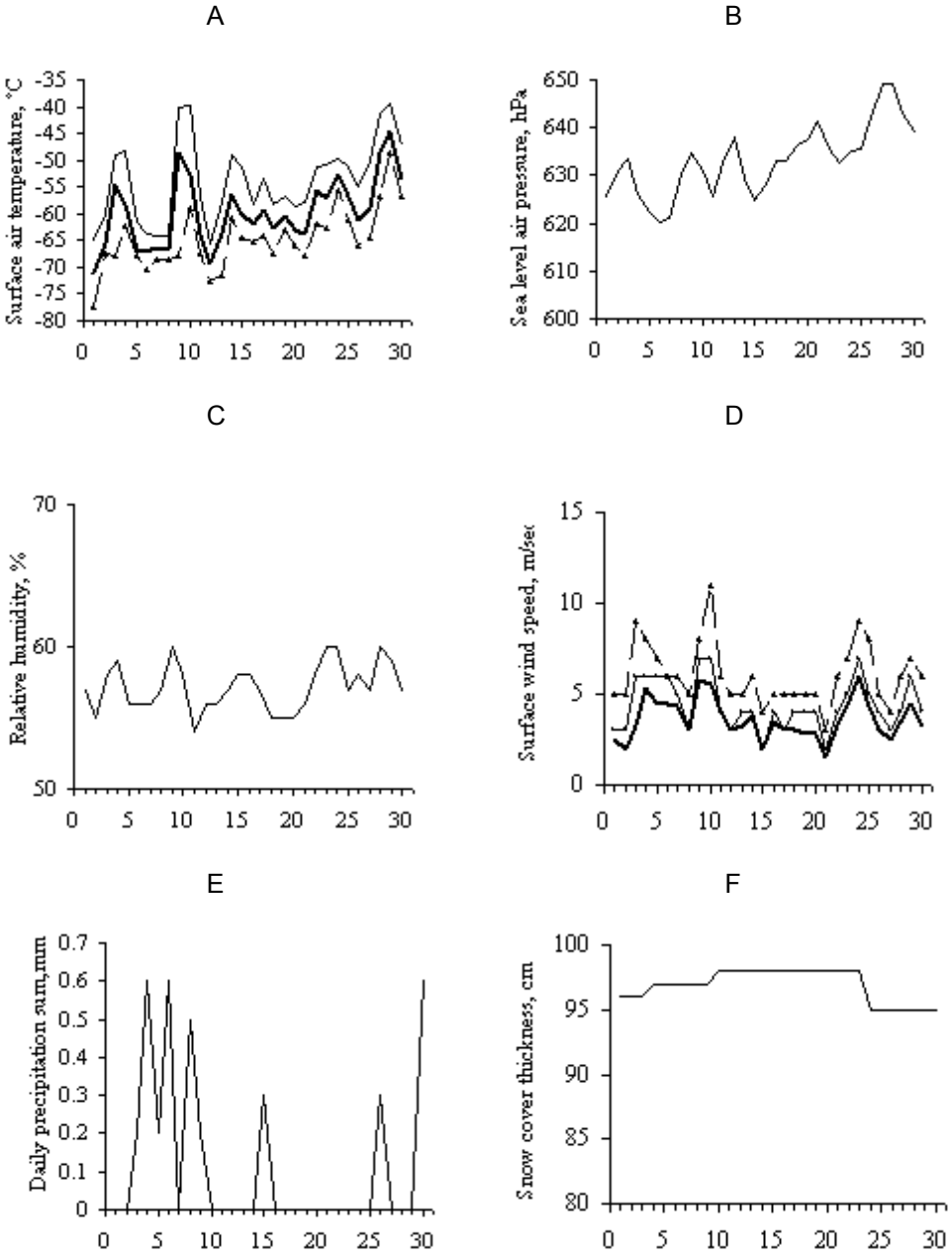

Fig. 1.23. Variations of daily mean values of surface temperature (A, bold line), maximum (A, thin line), minimum (A, dashed line) air temperature, ground level air pressure (B), relative humidity (C), mean (D, thick line), maximum (D, thin line) values of surface wind speed, maximum wind gust (D, dashed line), precipitation (E) and snow cover thickness (F).

Vostok station. September 2013.

S E P T E M B E R 2013

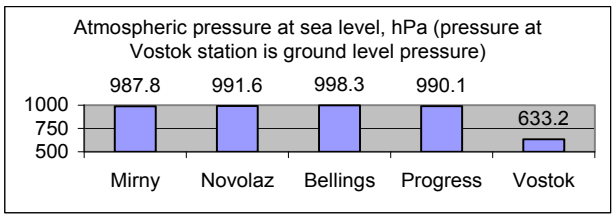

(f-favg)/σ_f	1.2	1.6	2.1	3.3

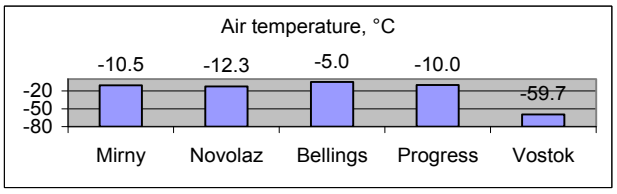

(f-favg)/σ_f	2.4	2.5	-0.3	1.7

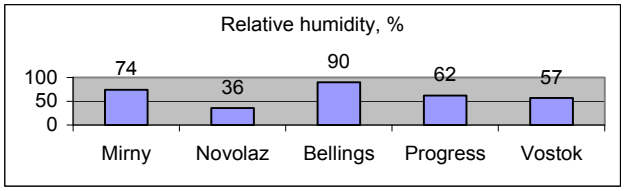

(f-favg)/σ_f	0.6	-2.2	0.5	-2.8

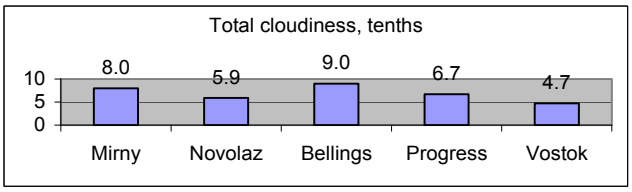

(f-favg)/σ_f	1.4	0.5	0.4	0.8

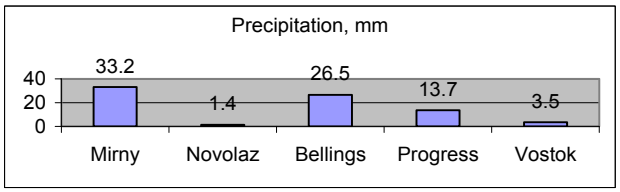

f/favg	0.5	0.0	0.4	1.2

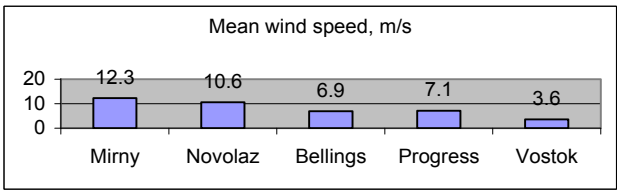

(f-favg)/σ_f	0.1	0.4	-1.1	-2.1

Fig.1.24. Comparison of monthly averages of meteorological parameters at the stations. September 2013.

2. METEOROLOGICAL CONDITIONS IN JULY-SEPTEMBER 2013

Figure 2.1 characterizes the air temperature conditions in July-September 2013 at the Antarctic continent. It presents monthly averages, anomalies and normalized anomalies of surface air temperature at the Russian and non-Russian meteorological stations. The actual data of the Russian Antarctic Expedition contained in /1/ were used for the Russian Antarctic stations and data contained in /2, 3/ were used for the foreign stations. The multiyear averages over the period 1961-1990 were adopted from /4/.

In **July** as compared with June there was a decrease of the number of stations with the above zero anomalies of mean monthly air temperature. The below zero air temperature anomalies embraced the coastal areas of East Antarctica (Victoria Land, Wilkes Land, Queen Mary Land, Enderby Land). The largest values of below zero anomalies were noted at Dumont D'Urville (-4.6°C, -2.0 σ) and Casey (-4.4°C, -1.4σ) stations. July 2013 at these stations was correspondingly the first and the sixth coldest July for the entire period of operation of the stations. In the regions of East Antarctica, one observed the above zero anomalies of air temperature (less or about 1σ). The largest anomaly was observed in the Ross Sea area at McMurdo station (3.5°C, 1.2 σ).

In **August,** small (less than 1σ) below zero anomalies of air temperature were observed at the stations of the eastern part of the Indian Ocean coast of East Antarctica and in the Weddell Sea area. In the central part of Antarctica and on the west coast of East Antarctica an area with the above zero anomalies was noted. The largest anomalies were observed in the inland part of Antarctica in the vicinity of Amundsen-Scott station (6.2°C, 2.1 σ). August 2013 at Amundsen-Scott station was the warmest August for the entire observation period.

In **September,** the area of the above zero air temperature anomalies increased. Significant heat anomalies were observed at the stations almost over the entire territory of Antarctica. The largest anomalies were recorded in the central part of the coast of East Antarctica and in the inland areas. September 2013 has become the warmest September at Amundsen-Scott (8.1°C and 3.3 σ), Mirny (6.2°C, 2.4 σ), Casey (6.0°C, 2.2 σ), McMurdo (6.2ºC, 2.1 σ), Mawson (4.9°C, 2.0 σ) and Davis (5.3°C, 1.9 σ) stations. At Novolazarevskaya station (4.9°C, 2.5 σ), September 2013 was the second warmest September for the operation period of the station. In the region of the Antarctic Peninsula, an area of small (less than 1σ) below zero air temperature anomalies was preserved.

An assessment of the temporal changes in mean monthly air temperature at the Russian stations for these months reveals a statistically significant trend at Bellingshausen and Novolazarevskaya stations for August and at Mirny station for September (Fig. 2.2-2.4). The air temperature increase for August at Bellingshausen and Novolazarevskaya stations comprised 2.1°C/46 years and 2.0°C/53 years, respectively and at Mirny station for September - 3.1°C/57 years (Table 2.1).

The atmospheric pressure in July at Bellingshausen, Novolazarevskaya and Vostok stations was characterized by small (less or around 1σ) negative deviations from a multiyear average. In August-September at these stations and at Mirny station also in July, the positive air pressure anomalies were recorded. The largest anomalies were observed in September at Bellingshausen (7.2 hPa, 2.1 σ) and Vostok stations (15.2 hPa, 3.3 σ). For Vostok station such air pressure increase in September was noted for the first time over the entire period of observations from 1958 (the previous largest positive anomaly was noted in 1961 (8.6 hPa, 1.9 σ).

At all Russian stations for July a tendency of the atmospheric pressure decrease prevails, for August – at Mirny and Novolazarevskaya stations, and for September only at Mirny station. However the statistically significant linear trends of the air pressure decrease are preserved for July only at Novolazarevskaya station (5.1 hPa/53 years) and for August only at Mirny station. The statistically significant air pressure increase is noted for September at Bellingshausen (5.5 hPa/46 years) and Vostok (1.2.hPa/52 years) stations.

The amount of precipitation at the Russian stations in July was below the multiyear average (by 10-30 %). In August, at Bellingshausen and Novolazarevskaya stations, precipitation comprised about 1.5 multiyear averages, at Mirny station, the precipitation amount comprised only half of the monthly multiyear average. In September, the precipitation amount was 20 % higher than the multiyear average at Vostok station and much less than the multiyear average at Mirny and Bellingshausen stations (about 40-50% of the multiyear average). At Novolazarevskaya station, no precipitation was recorded in September.

.

Table 2.1

Linear trend parameters of mean monthly surface air temperature

Station, operation period	Parameter	VII	VIII	IX	VII	VIII	IX
		Entire observation period			2004-2013		
Novolazarevskaya 1961-2013	°C/10 years	0.33	0.38	0.31	2.96	0.33	3.75
	%	17.7	25.2	24.8	27.2	3.9	71.5
	P		90	90	-	-	95
Mirny 1957-2013	°C/10 years	0.19	0.14	0.54	0.06	-2.36	3.97
	%	10.6	8.6	34.5	0.5	32.9	50.0
	P	-	-	95	-	-	-
Vostok 1958-2013	°C/10 years	0.31	0.36	0.10	1.21	-1.54	0.42
	%	13.8	15.2	4.9	10.4	12.5	4.5
	P	-	-	-	-	-	-
Bellingshausen 1968-2013	°C/10 years	0.13	0.46	0.03	-1.82	-2.23	-2.35
	%	5.8	26.8	2.1	19.8	36.9	48.0
	P	-	90	-	-	-	-

First line: the linear trend coefficient;
Second line: the dispersion value explained by the linear trend;
Third line: P=1-α, where α is the level of significance (given if P exceeds 90%).

References:

1. http://www.south.aari.nw.ru
2. http://www.ncdc.noaa.gov/ol/climate/climatedata.html
3. http://www.nerc-bas.ac.uk/public/icd/metlog/jones_and_limbert.html
4. Atlas of the Oceans. The Southern Ocean. GUNiO MO RF, St. Petersburg, 2005

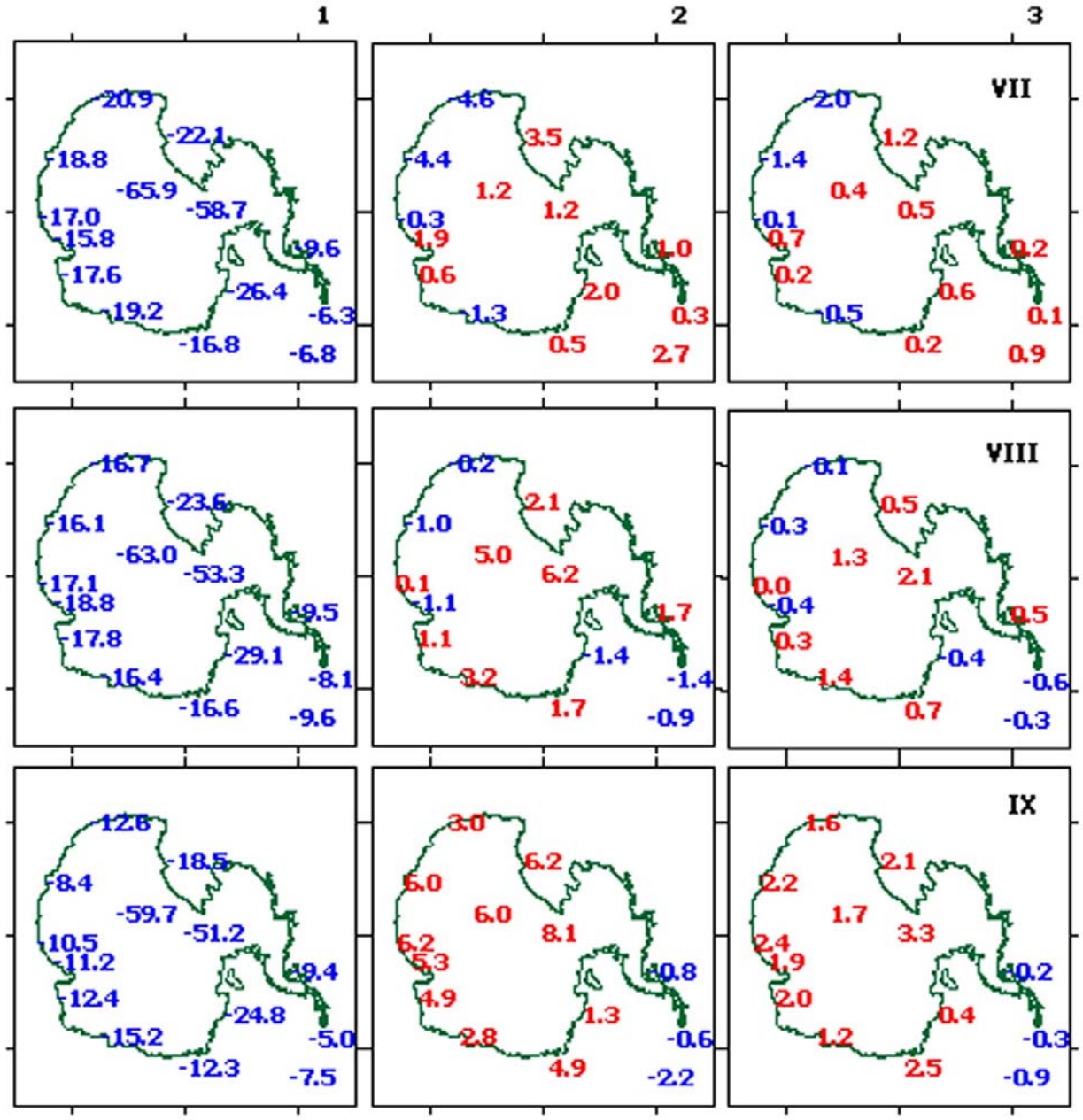

Fig.2.1. Mean monthly values (1) of surface air temperature and their anomalies (2) and normalized anomalies (3) in July (VII), August (VIII) and September (IX) 2013 from data of permanent meteorological stations in the South Polar Area.

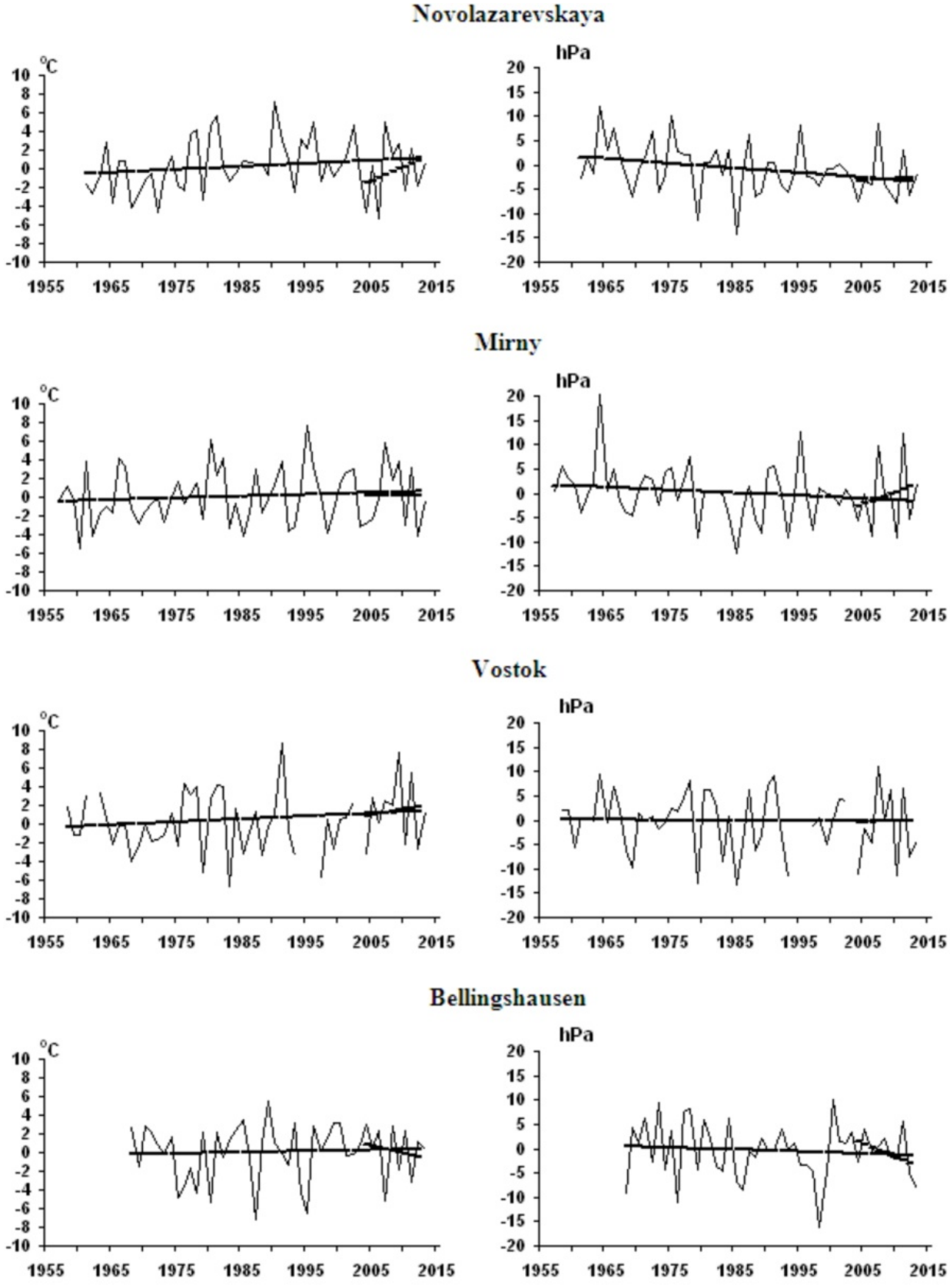

Fig. 2.2. Interanual variations of anomalies of air temperature and atmospheric pressure at the Russian Antarctic stations. July.

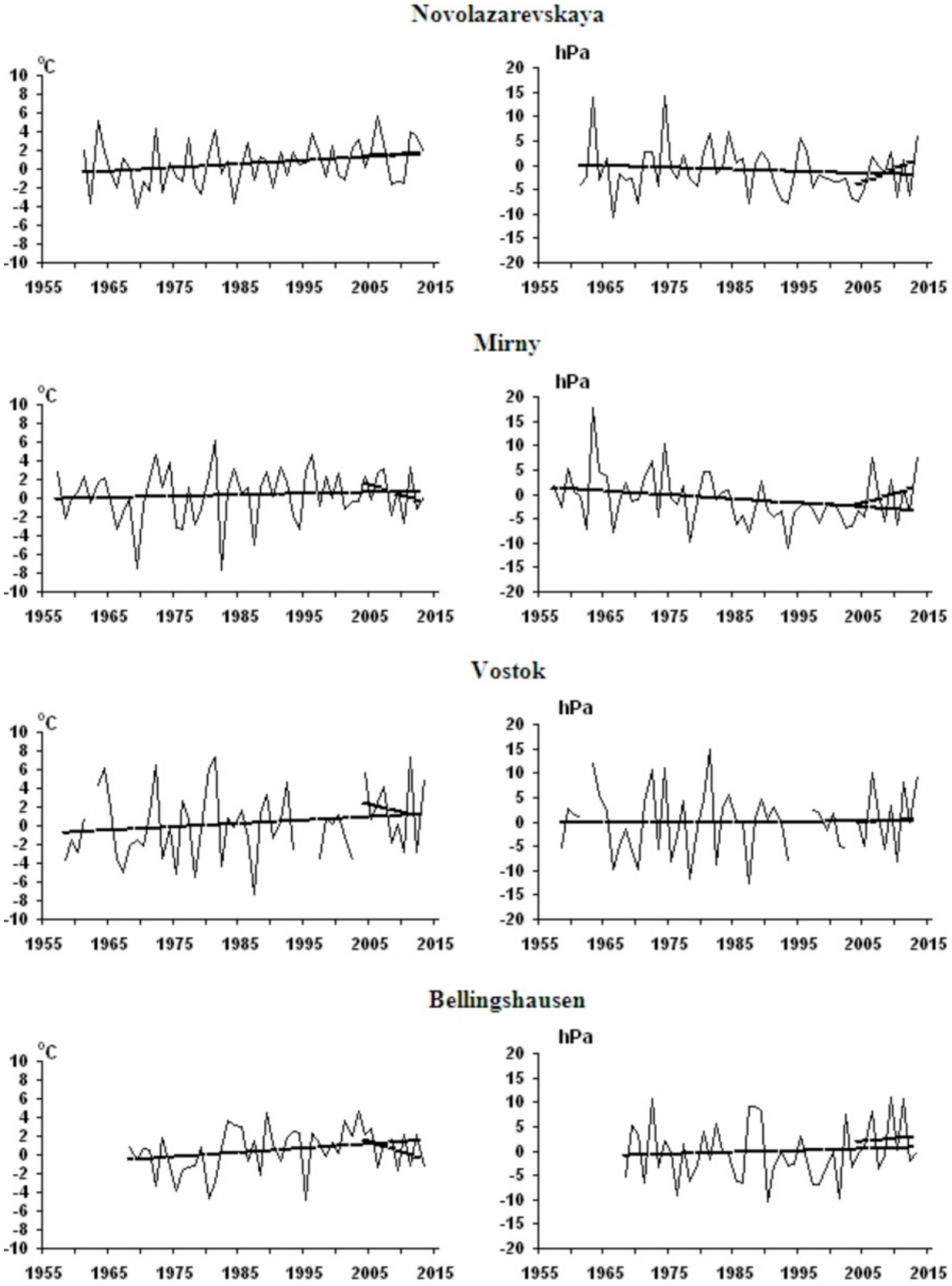

Fig. 2.3. Interanual variations of anomalies of air temperature and atmospheric pressure at the Russian Antarctic stations. August.

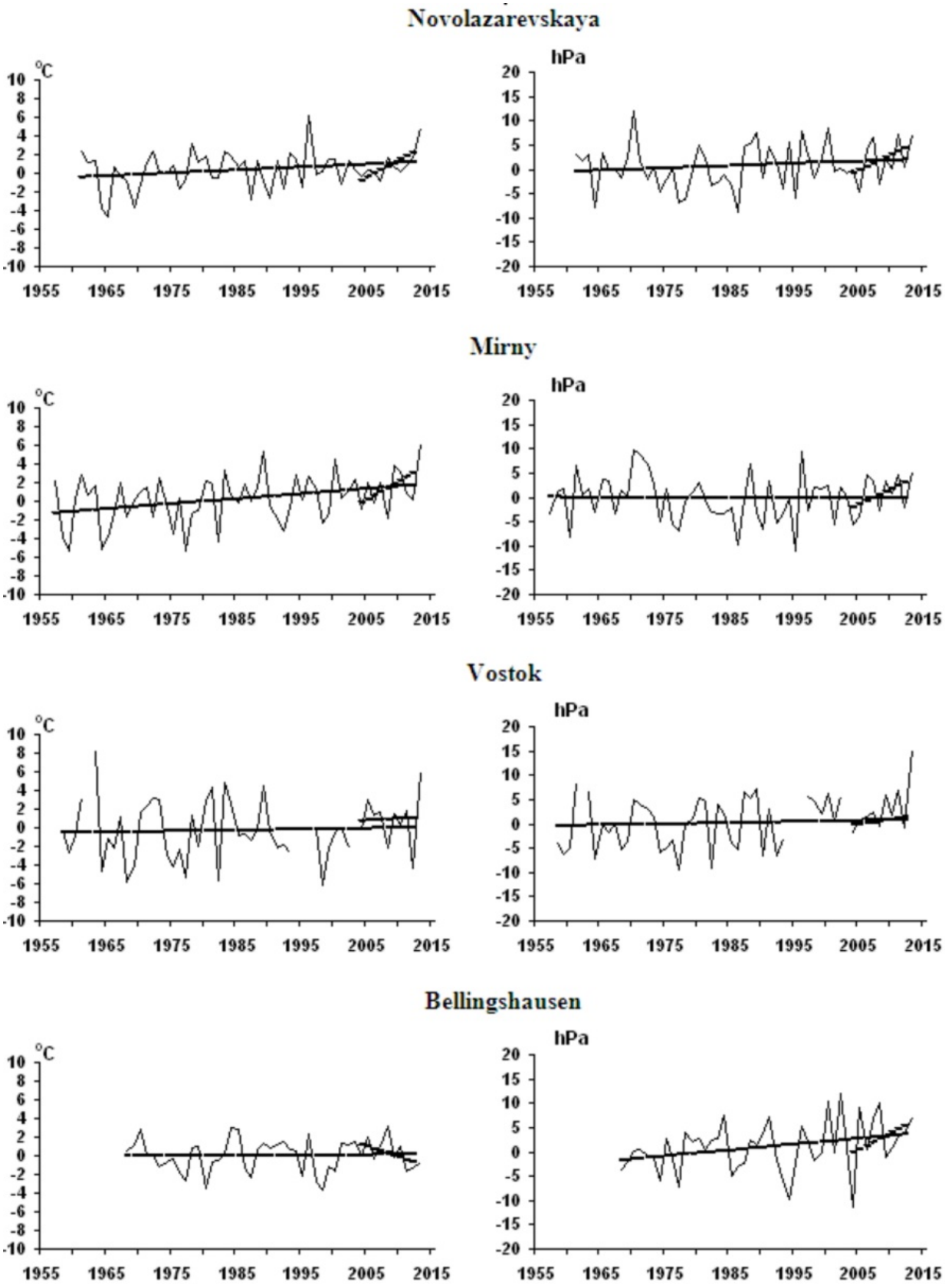

Fig. 2.4. Interanual variations of anomalies of air temperature and atmospheric pressure at the Russian Antarctic stations. September.

3. REVIEW OF THE ATMOSPHERIC PROCESSES OVER THE ANTARCTIC IN JULY-SEPTEMBER 2013

The middle of the Antarctic winter (the period under consideration presents its central months) determines in many aspects the character and the general assessment of the entire cold season.

In ***July***, the intensity of the atmosphere circulation processes and the frequency of occurrence of the circulation forms of the southern hemisphere (Table 3.1) were close to their mean multiyear state. The cyclonic activity was mainly observed at zonal trajectories, and at the development of meridionality – at the Falkland, South African, Kerguelen, New Zealand and central and eastern Pacific trajectories. One can only note several cases of the passage of deep cyclones to the coast of East Antarctica causing prolonged storm weather at significant wind increase and significant precipitation amount. These movements of cyclones occurred along the South African and Kerguelen branches of the trajectories. Predominantly shallow cyclones reached the coasts of the Antarctic continent which developed at the Antarctic front. One can nevertheless note a series of deep cyclones passing from the Pacific Ocean Basin to the Atlantic sector across the Drake Passage.

The field of atmospheric pressure anomalies in July reflected the aforementioned circulation peculiarities. The pressure anomalies along the coast of East Antarctica to the south of the Polar Circle were close to mean multiyear values. In high latitudes of the Pacific Ocean in the West Antarctic sector one observed a belt of negative anomalies extending across the Drake Passage and the Antarctic Peninsula to the northern part of the Weddell Sea [2]. The Antarctic High was attenuated at this.

The thermal regime was close to a multiyear average. Of interest is a center of the below zero anomalies of surface air temperature above he Mawson and D'Urville Seas and a slightly elevated background temperature above the Antarctic Plateau [3]. The precipitation deficit was noted for most regions.

Table 3.1

Frequency of occurrence of the atmospheric circulation forms of the Southern Hemisphere and their anomalies (days) in July-September 2013

Months	Frequency of occurrence			Anomalies		
	Z	M_a	M_b	Z	M_a	M_b
July	11	10	10	1	-2	1
August	13	11	7	1	0	-1
September	15	7	8	3	-4	1

In ***August***, the picture of development of the atmospheric processes close to mean multiyear was preserved. This was expressed both in the frequency of occurrence of the circulation forms (Table 3.1), and in the low intensity of cyclonic activity above the south-polar area. The zonal circulation form in August was mainly developed in middle latitudes. One can identify among the meridional trajectories the Falkland and central Pacific branches, the cyclones moved more rarely along the South African and New Zealand trajectories. One observed a belt of positive anomalies of the atmospheric pressure over the coast of Antarctica. The largest center of positive anomalies was located above the Ross Sea [2]. The air pressure anomalies above the Drake Passage, the Antarctic Peninsula, water areas of the Scotia Sea and the northern areas of the Weddell Sea were close to a multiyear average or were slightly less. The air temperature anomalies over most regions of the South Polar area were close to mean multiyear values. The positive deviations from a multiyear average were observed over the coast of the Ross Sea and the Antarctic Plateau. This is connected with the development of the central Pacific high pressure ridge and the subsequent motion of cyclones along the meridional New Zealand trajectory with penetration of cyclones deep inland accompanied by the outflow of warm air masses. In such synoptic situation the mean daily temperature at Vostok station increased from -24.5ºC on 5 August to -6.8ºC on 9 August.

The precipitation amount over the coast of Antarctica was mainly deficit due to the attenuated cyclonic activity in high latitudes. The exception was the Antarctic Peninsula, where the precipitation amount exceeded the multiyear average.

In ***September,*** as can be seen from Table 3.1, there was some intensification of zonal atmospheric circulation at the decreased activity of the meridional form M_a, which is not typical for the winter season. The cyclonic activity was mainly observed at zonal trajectories. Zonality was predominantly of the middle-latitudinal character and the cyclones moved in the zonal flow along the more northern trajectories than usually. Among the active meridional cyclonic trajectories one can identify the Falkland, South African, Kerguelen, New Zealand and to a lesser extent the Pacific branches. At the decreased intensity of the atmospheric circulation in September this month can be considered the quietest month during the whole current year.

The displacement of cyclones to temperate latitudes resulted in the formation of the circumpolar belt of positive pressure anomalies over the entire coast of Antarctica.

The field of anomalies of the air temperature above most regions including the Antarctic Plateau, had a positive

background reaching sometimes the extreme values [1, 2]. The exception is the area of the Antarctic Peninsula, where small below zero anomalies were recorded. The field of atmospheric precipitation remained deficient.

References:

1. http://www.aari.aq
2. http://www.bom.gov.au/cgi-bin/climate/cmb.cgi?/page
3. Section 2 of this bulletin

4. BRIEF REVIEW OF ICE PROCESSES IN THE SOUTHERN OCEAN FROM DATA OF SATELLITE AND COASTAL OBSERVATIONS AT THE RUSSIAN ANTARCTIC STATIONS IN JULY - SEPTEMBER 2013

Throughout the entire winter period the area of ice extent in the Southern Ocean continued to exceed the multiyear average by approximately 0.8 mln km^2. This corresponded to the deviation from the multiyear average of the residual sea ice extent level reached by the end of summer in February 2013. The total sea ice extent values observed in winter became maximum for the entire 35-year period of satellite microwave measurements in the Antarctic. By the end of July the sea ice area increased for the month from 15.2 to 17.4 mln km^2, in August – to 19 mln km^2, and in September, the last year maximum of the sea ice extent was repeated and comprised 19.5 mln km^2.

The most significant event was a transfer of the leadership in formation of the increased background sea ice extent of the Southern Ocean from the Atlantic to the Pacific Ocean sector where, beginning from June, the record areas of the ice cover were observed. In September, both sectors became equal in the absolute expression – by 7.5 mln km^2 of ice in each. However, while the Atlantic massif was developed in accordance with the multiyear average, the area of the Pacific ice massif was greater than the multiyear average approximately by 10% (Fig. 4.1). This comprised about $^4/_5$ of the observed positive sea ice extent anomaly of the ocean in total. The ice belt in the Somov Sea, in the vicinity of Russkaya station and in the Drake Passage, where the ice edge reached the 60th parallel, was distinguished by the especially increased size.

Probably the restoration of the Pacific ice massif that had strongly degraded from 2009 began. In this respect quite indicative appears the development of the ice events in the area of Bellingshausen station. The ice tongue, which began to develop in June from the area of Marguerite Bay in the direction of the Drake Passage (see a similar review for the previous quarter) reached in a month the South Shetland Islands Archipelago. Surrounding King-George Island by ice from all sides in the middle of July was immediately manifested in the formation of stable landfast ice in Ardley Bay (Table 4.1). As a result, in spite of a month delay in the formation of landfast ice due to the weakened advection of the Weddell Sea water and ice to Bransfield Strait in autumn-winter, the whole bay was rapidly covered by landfast ice by 1 August, which bound it for almost 2.5 months.

It is of interest that the winter intensity of the landfast ice growth near Bellingshausen station was the same as at the roadstead of Mirny station in autumn. As a result the landfast ice thickness in Ardley Bay by late September comprised more than 60 cm in spite of large snow concentration (Table 4.2), which was a local multiyear average before the onset of "warm" winters in 1996-2006. At the rest of the stations the landfast ice thickness throughout the winter was less than mean multiyear value by almost 10 cm.

Completing the topic of the probable beginning of reconstruction of the Pacific ice massif, one should note stable formation of landfast ice within the maximum possible boundaries near the west coast of the Antarctic Peninsula in the middle of September, which has not been observed for a long time. Marguerite Bay was completely frozen along the line Cape Russky on the Alexander I Land to the southern tip of Adelaide Island. Short-term establishment of landfast ice was also observed over the entire coastal water area from Adelaide Island to Anvers Island along the Biscoe Islands. Besides based on the updated data, there was reconstruction of a typical jugged protrusion of landfast ice between Cape Burks and the concentration of icebergs on the Aristov Bank that had disappeared in 2009. In the case of existence of this protrusion of about 60 km long, which makes the western coastal ice advection here difficult, heavy ice conditions of navigation are created.

As unordinary ice event in winter of 2013, one should mention the transformation of Sannefjord Inlet in Prydz Bay to the inaccessible ice inlet surrounded from all sides by glacier ice. At the beginning of April, the entry to the inlet that had narrowed by that time to 14 km between the extending to the northeast the Amery ice shelf and the outlet glacier Polar-Record was plugged by a giant iceberg. This iceberg 10x15 km in size was formed as a result of calving of the super-tongue of the outlet glacier Publication at the head of Sannefjord Inlet on 26 March 2013. As a result, the configuration of the ice coast in Prydz Bay attains the increasing similarity to that of the ice coast, which had existed here during the voyage of the diesel-electric ship "Lena" in summer of 1957 and preserved until the catastrophic calving of the Amery ice shelf in 1964.

Finally an exceptionally rare situation occurred in the area of Novolazarevskaya station. In winter the water area of Leningradsky Bay was completely covered with landfast ice at 12-14°E up to 69°30′ S, where one of the most stable recurring polynyas in Antarctica is usually preserved.

Table 4.1

Dates of the onset of main ice phases in the area of Bellingshausen station in winter of 2013

Station (water body)		Ice formation		Landfast ice		Freeze up		Landfast ice breakup		Clearance	
		First	Stable	First	Stable	First	Final	Start	Final	First	Final
Bellingshausen (Ardley Bay)	Actual	24.05	20.06	04.07	17.07	01.08	01.08	10.10	NO[1]	-	-
	Multiyear average	12.05	06.06	09.06	17.06	05.07	30.06	14.09	13.10	21.10	01.11

Note:[1] - phenomenon was absent (did not occur).

Table 4.2

First-year landfast ice thickness and snow depth (cm) on it in the areas of the Russian Antarctic stations in winter of 2013

Station	Characteristics		Months			
			VI	VII	VIII	IX
Mirny	Ice	Actual	72	85	112	128
		Multiyear average	84	101	121	139
	Snow	Actual	11	28	17	17
		Multiyear average	18	18	19	20
Progress	Ice	Actual	90	107	122	135
		Multiyear average	97	117	132	145
	Snow	Actual	10	25	16	14
		Multiyear average	5	6	7	7
Bellingshausen	Ice	Actual		≈14	55	64
	Snow	Actual		≈1	16	17

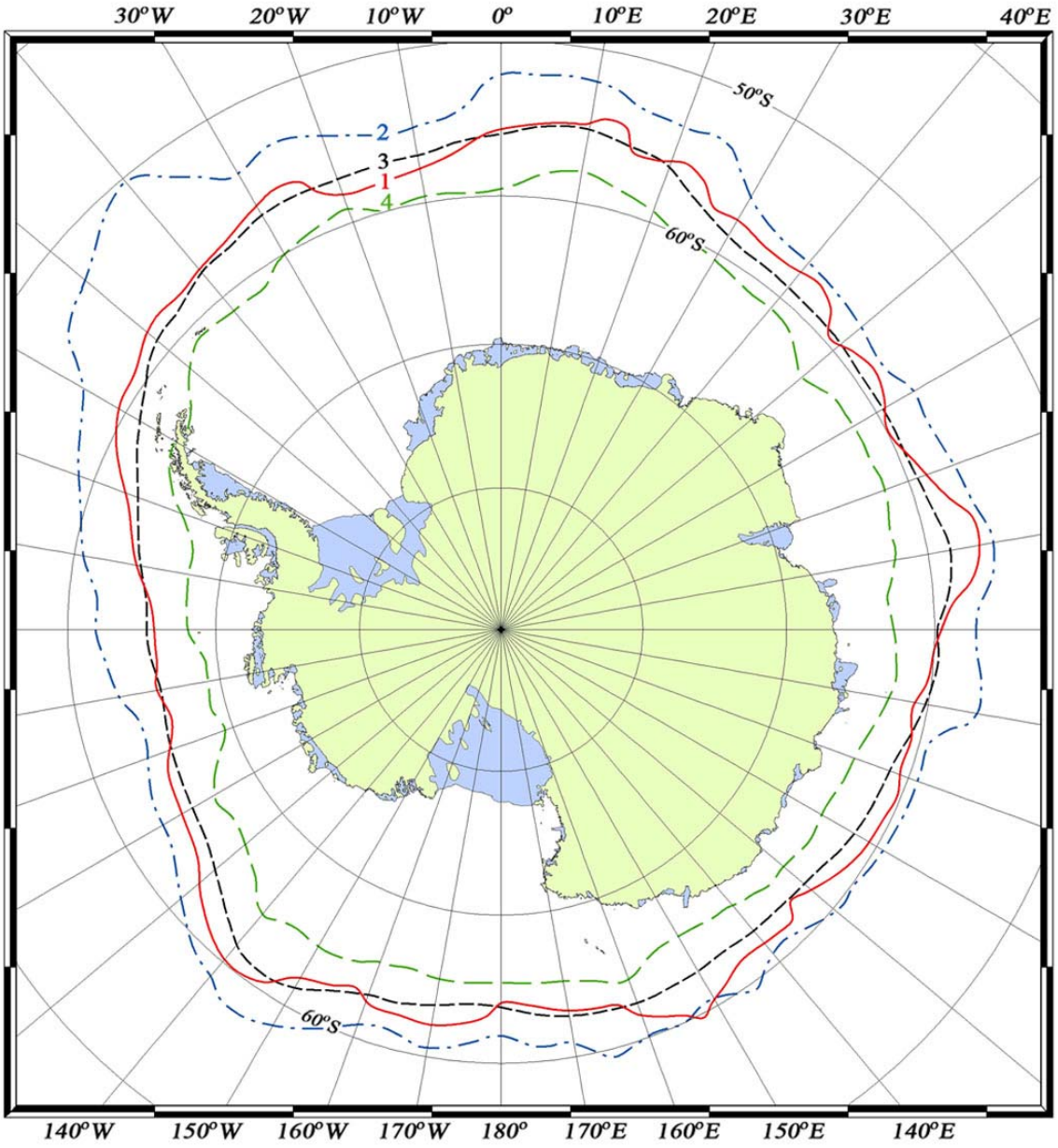

Fig. 4.1. Mean monthly location (1) of the external northern sea ice edge in September 2013 relative to its maximum (2), average (3) and minimum (4) spreading in the Southern Ocean for a multiyear period.

5. RESULTS OF TOTAL OZONE MEASUREMENTS AT THE RUSSIAN ANTARCTIC STATIONS IN THE THIRD QUARTER OF 2013

After the end of the polar night the Russian stations in Antarctica resumed measurements of total ozone (TO) at Mirny station – from 1 August, at Novolazarevskaya station – from 15 August and at Vostok station – from 6 September.

In 2013, the ozone hole area in the first part of August increased slower than in recent years, however it increased more rapidly in the second part of the month than in 2010-2012. The ozone hole area achieved its maximum (from data in [1]) on 16 September (24 mln km^2). For the last twenty years the ozone hole area was less than in the current year only four times (in 2002, 2004, 2010 and 2012).

In spring 2013, a significant decrease of ozone concentration occurred at the Russian Vostok and Novolazarevskaya stations, which is usual in the last years (Fig. 5.1). One should note the significant TO fluctuations at Mirny station in the spring period and also a very high ozone concentration at this station on some days when the TO values were maximum for the entire observation period (27-28 August and 17-22 September). At this station, especially in recent years one observes very large ozone concentration variations from day-to-day and much higher TO values in spring compared to the other stations. This variability of ozone concentration at Mirny station is explained by its peripheral location relative to the most often observed geographical location of the ozone hole. This is well seen in Fig. 5.2, where the TO charts based on satellite data are presented [2] for the days when the TO value at Mirny station was minimum in the current year (219 DU on 9 August) and maximum (455 DU on 20 September). The location of Mirny station on these charts is denoted by a blue point.

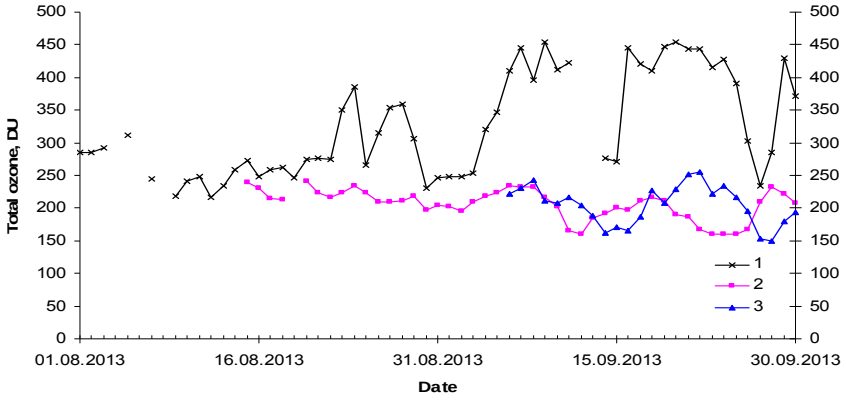

Fig. 5.1. Mean daily TO values at the Russian stations in the third quarter of 2013.

1 – Mirny, 2 – Novolazarevskaya, 3 – Vostok

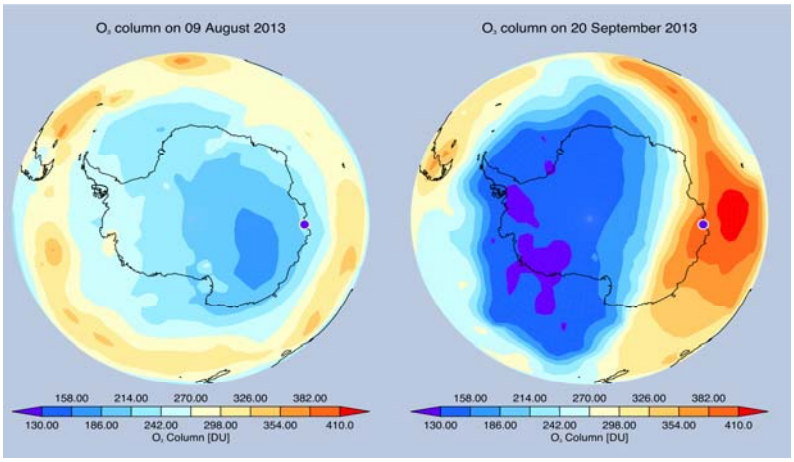

Fig. 5.2. Charts of total ozone concentration above the Antarctic obtained from the measurement data of Aura satellite [2].

The multiyear variations of normalized deviations of mean monthly TO values in September at the stations in Antarctica are shown in Fig. 5.3. The mean multiyear TO values are calculated for the period 1981-2010. For construction of this Figure in addition to the measurement data at the Russian stations in Antarctica, data of foreign stations presented at the site [3] were used.

One should note a large variability of the TO anomalies in Antarctica, which is quite well described by the polynomial to the power of 3 (R^2=0.71). As follows from the Figure, the negative TO anomalies observed in Antarctica from the beginning of the 1990s have a tendency at the present time for a sign change. One can speak about some change in the size of the ozone hole annually forming above Antarctica and the extent of destruction of the ozone layer during the last two years and about the stabilized manifestation of the ozone anomaly above the Antarctic during the last decade.

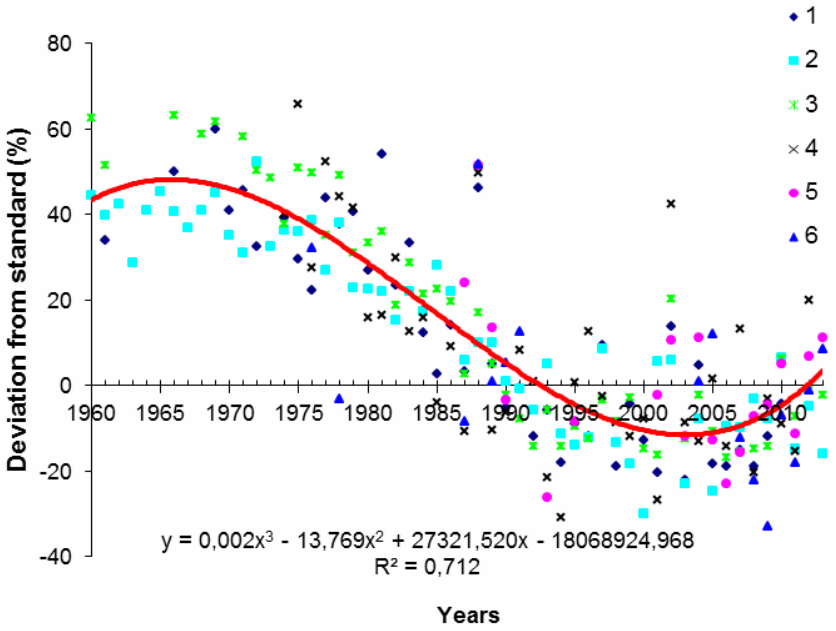

Fig. 5.3. Interannual variability of normalized deviations of mean monthly TO values in September (the multiyear averages were calculated for the period 1981-2010) at the Russian and foreign stations in Antarctica
1 – Mirny, 2 – Novolazarevskaya, 3 – Vostok, 4 – Syowa, 5 – Vernadsky, 6 – Halley.

The role of dynamic factors (circulation of the stratosphere) in the processes of TO regulation above the Antarctic is significant. Of interest in Fig. 5.3 are the values of TO anomalies in 1988 and 2002. In these years one observes sufficiently large positive anomalies at all stations under analysis, and the ozone holes developed according to the non-typical scenarios for most of the years under consideration. In 1988, the stratospheric circumpolar vortex was destroyed already in early spring and the ozone hole was not even formed. In 2002, there was a dramatic temperature increase in the stratosphere, accompanied with the TO increase resulting in a sharp decrease of the hole size and even its division into two parts by the end of September [4]. One should also note the positive TO anomalies at some stations, for example, at Mirny station in 2007, 2012 and especially in 2013.

References:

1 *http://ozone-watch.gsfc.nasa.gov/*
2 Antarctic Ozone Bulletin, 2013, No.1-3 *http://www.wmo.int/pages/prog/arep/gaw/ozone/index.html*
3 *http://www.woudc.org/data_e.html/*
4 Sibir E.E., Radionov V.F. Total ozone concentration in the Antarctic during the period of the International Polar Year 2007/2008. /In: Contribution of Russia to the International Polar Year 2007/2008. Meteorological and geophysical studies. M.- St. Petersburg: OOO "Paulsen". –2011 – P.178-186.

6. GEOPHYSICAL OBSERVATIONS AT THE RUSSIAN ANTARCTIC STATIONS IN JULY-SEPTEMBER 2013

Analysis of geophysical materials of the Antarctic stations for the 3rd quarter of 2013

Geomagnetic data

The geomagnetic observations in the third quarter of 2013 were carried out at Vostok, Novolazarevskaya, Mirny and Progress stations under the standard program.

As can be seen from the presented data, the average quarter absolute values of the Earth's magnetic field components (EMF) at Mirny, Vostok and Progress stations have not practically changed compared to the second quarter of 2013. They are not greater than 20 nT and can be explained by the general change of magnetic activity in the second and third quarters. The largest changes similar to the previous quarter were noted at Novolazarevskaya station – the vertical component value has decreased (by module) by 22 nT.

At all stations, the measurements of the basis values of variometers were regularly carried out. At Novolazarevskaya, Mirny and Progress stations, the basis values are stable and the random error of their measurements is within the permissible bounds. However at Vostok station one should undertake measures to reduce the measurement errors. At Mirny station, due to the damage of the geomagnetic variation system of the main series (automatic digital geomagnetic variation system), the data on its basis values for the period 1 to 15 September are absent.

The state of the magnetosphere is characterized by the PC-index, proposed at the AARI Department of Geophysics and adopted in August 2013 at the 12th session of the International Association of Geomagnetism and Aeronomy (IAGA) as a new international index of magnetic activity. The PC-index values are calculated at the Department of Geophysics in real time and are posted as a diagram to the AARI site. Fig. 6.1 presents the index values for the entire third quarter of 2013. The index value of 2 mV/m denoted on this diagram by a blue line, determines the level after the excess of which the processes of magneto-ionospheric perturbations are manifested at the Earth's surface, characterizing the state of the magnetosphere and the "space weather" in general. Fig. 6.2 presents at a larger scale than Fig.6.1 the PC-index values for the period 14 August to 18 August, and Fig. 6.3 – the manetogram of Novolazarevskaya station for the same time. As can be seen, a strong magnetic perturbation is observed during the period of large PC-index values.

All ionospheric perturbations noted from the data of riometers are also observed on the magnetograms of these stations.

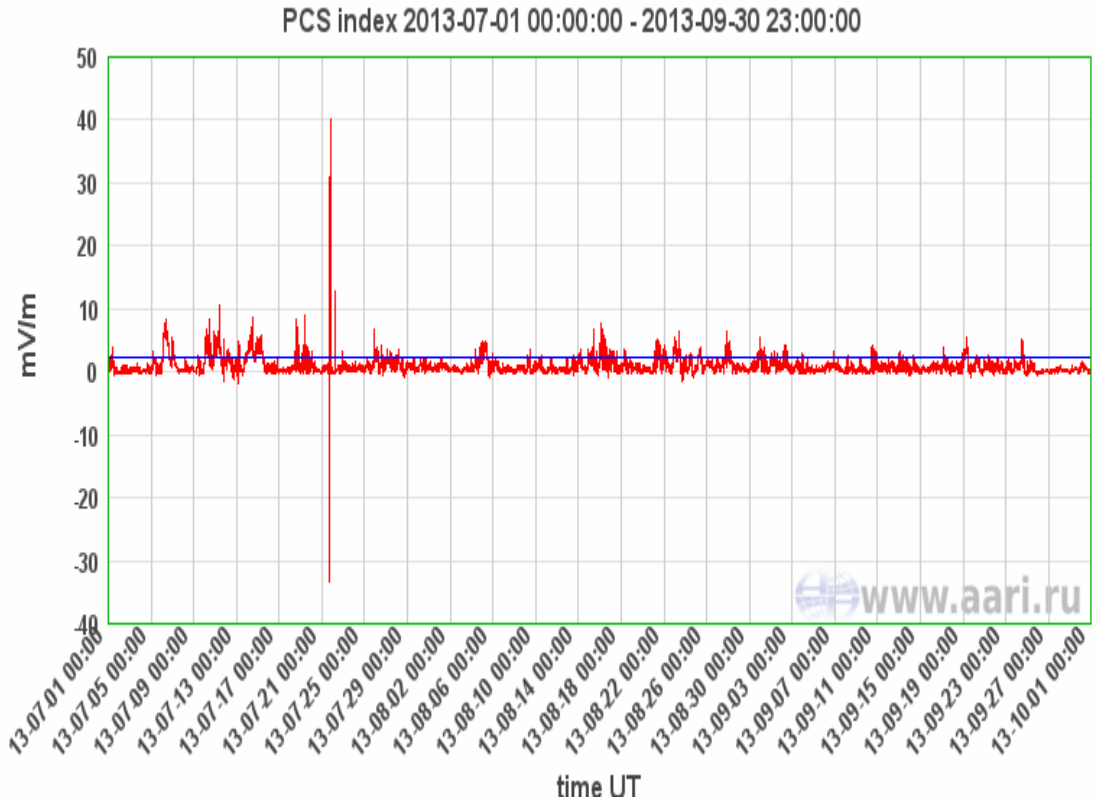

Fig. 6.1. PC-index for the 3rd quarter of 2013.

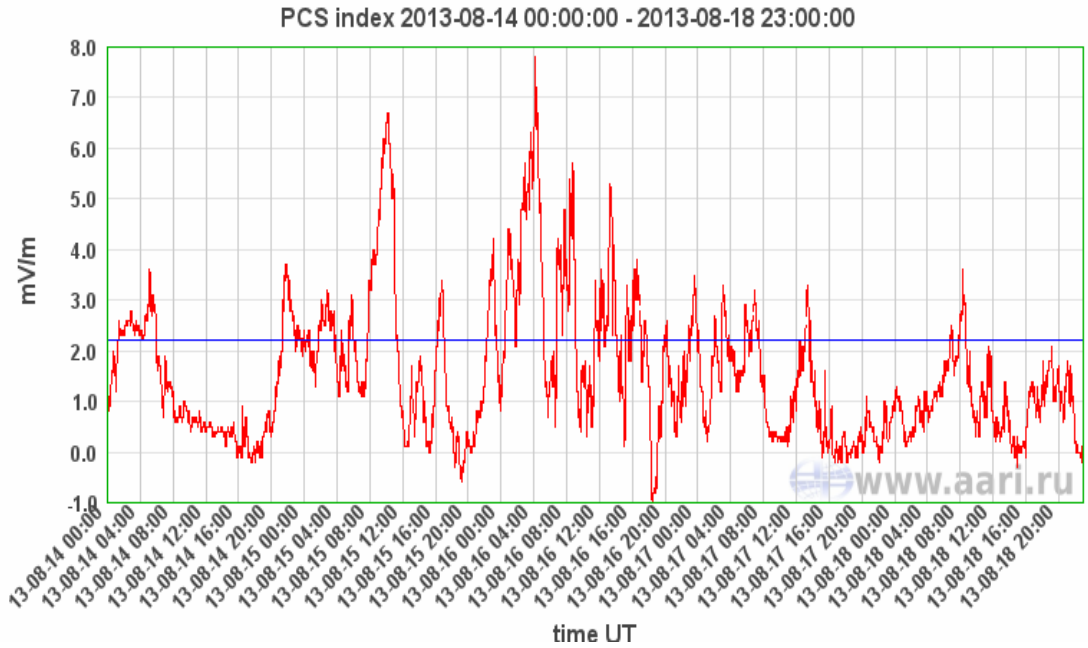

Fig. 6.2. PC-index for the period 14 to 18 August 2013.

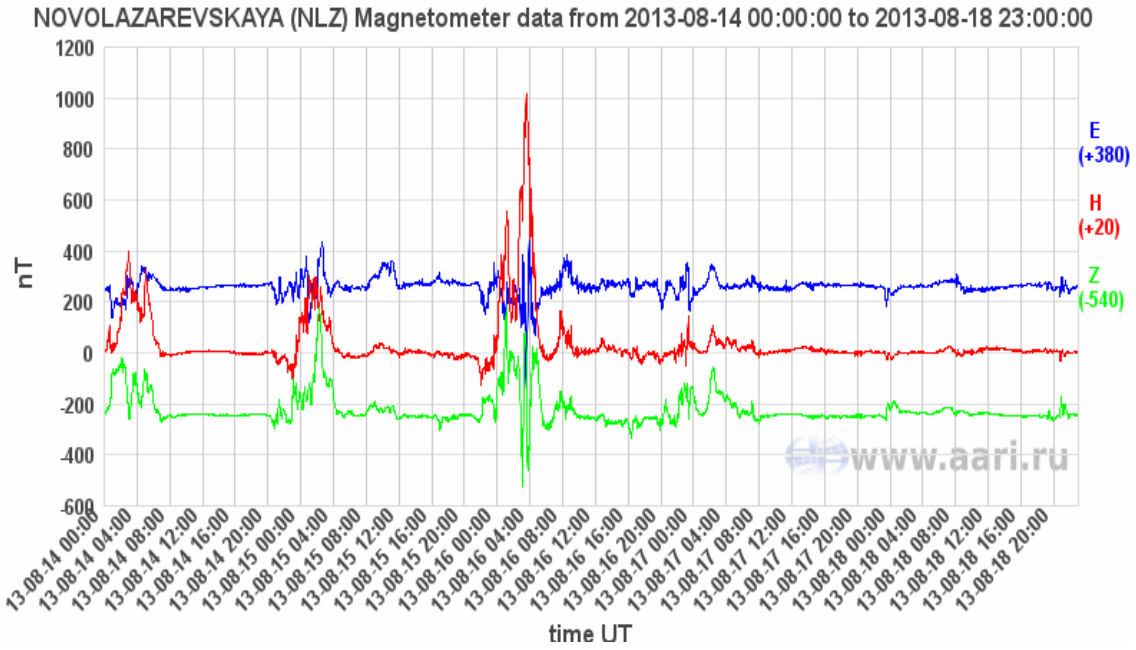

Fig. 6.3. Magnetogram of Novolazarevskaya station for the period 14 to 18 August 2013.

Analysis of riometer data of Antarctic stations Vostok, Mirny, Progress and Novolazarevskaya for the period July – September 2013 (based on the data of maximum absorption values for each 24 h)

A monthly set of the maximum (for each 24 h) absorption values is analyzed**.** The analysis presents an assessment of the work of riometers in general and the classification of riometer absorption increases depending on the factors influencing these increases. The increases with the amplitude greater than 0.5 dB were analyzed.

The main abbreviations used in the analysis:

(1) SPE (solar proton event) – a phenomenon of the increase of solar proton fluxes after strong solar bursts, registered in the interplanetary space and in the Earth's magnetosphere; fluxes of protons with the energy of 10 MeV (in the integral measurement of F> 10 MeV) make the largest contribution to the absorption; during the analysis such SPE were considered, which had the maximum intensity of F_{max} (> 10 MeV) ≥ 5 particles/cm^2 s steradian.

(2) PCA (type of polar cap absorption) – a phenomenon of the increase of absorption determined by the proton fluxes during the SPE.

(3) GA (geomagnetic activity) – level of geomagnetic field perturbation.

(4) GP (geomagnetic perturbation) – a phenomenon of the increase of geomagnetic activity; intensity of GP is assessed by the Kp index, which reflects a global character of geomagnetic perturbation; as a significant geomagnetic perturbation, the periods were considered where Kp≥3$_0$.

(5) AA (auroral absorption) – a phenomenon of the increase of absorption determined by the fluxes of magnetospheric particles at the time of global or local geomagnetic perturbations.

(6) QDC (Quiet day curve) – a non-perturbed level of the space noise registered by riometers. It is determined by a special algorithm.

(7) BA (Background absorption) – a stable increased or decreased absorption, which is approximately the same for several days, determined by unstable performance of riometer

(8) BV (background variations) – periodic (daily) absorption variations with the amplitude of 0.2 – 0.4 dB; the BV are determined by inaccuracy of processing, due to inaccuracy of QDC selection; the BV often have a sinusoid shape but in some cases differ significantly from it.

The absorption increases of the impulse character can be caused by the global factors (SPE and GP), or the local factors (local increase of geomagnetic activity, increase of the level of interference or malfunction of riometer work). The prolonged increased (or decreased) similar absorption values can be caused by riometer fault (BA) or inaccuracy of the QDC (BV).

The Internet data on the fluxes of solar protons (with the energy of 1 – 100 MeV) and on the level of geomagnetic activity (K_p index) were used in the analysis. The maximum for the day absorption values were compared with variations of

every minute absorption values presented at the site of the Department of Geophysics of the AARI.

July

During this month no SPE phenomena were observed. There were registered 5 geomagnetic perturbations: on 5 – 6 July with the maximum on 6 July ($K_p = 5_-$), on 9 – 13 July with the maximum on 11 July ($K_p = 5_-$), on 13 – 15 July with the maximum on 15 July ($K_p = 5_0$), on 18 – 19 July with the maximum on 18 July ($K_p = 5_-$) and on 25 – 28 July with the maximum on 25 July ($K_p = 4_0$).

Vostok (32 MHz). No increases of absorption, connected with anomalous phenomena were registered.

Mirny (32 MHz). Two increases of absorption were registered with the maximums on 18 and 27 July (with amplitudes of 2.0 and 10 dB, respectively). Both increases are AA and are determined by the increase of the level of global GA.

Progress (32 MHz). A number of increases of absorption were registered with the maximums on 11, 16, 18, 21, 27 and 30 July, determined by the increased global or local geomagnetic activity. The record level is elevated approximately by 0.5 dB due to some instability of riometer functioning.

Novolazarevskaya (32 MHz). Four increases of absorption were registered, determined by the increased global GA.

August

During August 2013 no strong SPE phenomena were observed. Five geomagnetic perturbations were registered: on 5 – 6 August with the maximum on 5 August ($K_p = 4_+$), on 14 – 17 August with the maximum on 16 August ($K_p = 5_+$), on 20 – 25 August with the maximum on 21 August ($K_p = 4_0$), on 27 – 28 August with the maximum on 27 August ($K_p = 5_0$) and on 30 – 31 August with the maximum on 31 August ($K_p = 4_0$).

Vostok (32 MHz). No absorption increases connected with the anomalous phenomena were registered.

Mirny (32 MHz). Two absorption increases were registered with the maximums on 15 and 22 August (the amplitudes of 4.3 and 2.5 dB, respectively). Both increases are AA determined by the increased level of the global GA.

Progress (32 MHz). Five absorption increases were registered with the maximums on 4, 14, 18, 22 and 31 August, which are determined by the increase of the global or local GA.

Novolazarevskaya (32 MHz). Several increases were registered, which are AA, determined by the increased level of the global and local GA.

September

During September 2013, one SPE phenomenon was recorded that began on 30 September (F_{max} (>10 MeV) = 10 particles/cm^2 s steradian) and ended in the next month. Two geomagnetic perturbations were registered: on 19 – 22 September with the maximum on 19 September ($K_p = 4_0$) and on 24 – 25 September with the maximum on 24 September ($K_p = 4_0$).

Vostok (32 MHz). One absorption increase was registered with the maximum on 30 September (the amplitude of 3.3 dB), which is the PCA determined by the SPE proton fluxes. The other increases (on 10 and 27 September) present the AA, determined by the local GA.

Mirny (32 MHz). Two absorption increases were registered with the maximum on 13 and 30 September (the amplitudes are 0.6 and 1.2 dB, respectively). The first increase is the AA, determined by the global GA and the second is the PCA determined by the SPE phenomenon.

Progress (32 MHz). A series of increases was registered, determined by the global and local GA. The increase on 30 September (the amplitude of 2.8 dB) is determined by the SPE phenomenon.

Novolazarevskaya (32 MHz). A series of absorption increases was registered with the maximums on 3, 13, 19, 23 September, which present the AA determined by the increase of the global and local GA.

Conclusions

During the period under consideration the following phenomena were registered:

One PCA phenomena determined by the SPE proton fluxes,

Some AA events determined by the global and local GA.

In general, the riometers at Vostok, Mirny and Novolazarevskaya stations functioned normally. At Progress station, the riometer performance has improved.

CURRENT OBSERVATIONS

MIRNY STATION
Mean monthly absolute geomagnetic field values

	Declination	*Horizontal component*	*Vertical component*
July	*88°17.5′W*	*13668 nT*	*-57646 nT*
August	*88°20.6′W*	*13661 nT*	*-57634 nT*
September	*88°17.6′W*	*13668 nT*	*-57642 nT*

Main variometer reference values

Date	D deg.	H, nT	Z, nT
05.07.2013	-87.0483	13902	-57626
11.07.2013	-87.0533	13904	-57622
17.07.2013	-87.0650	13904	-57625
23.07.2013	-87.0700	13902	-57626
29.07.2013	-87.0483	13907	-57626
04.08.2013	-87.0550	13906	-57624
10.08.2013	-87.0550	13904	-57625
16.08.2013	-87.0317	13909	-57627
22.08.2013	-87.0367	13902	-57628
28.08.2013	-87.0083	13901	-57622
03.09.2013			
09.09.2013			
15.09.2013			
21.09.2013	-87.0217	13896	-57623
27.09.2013	-87.0250	13893	-57626
Averages	-87.0432	13903	-57625
σ	0.0178	4.2	1.8

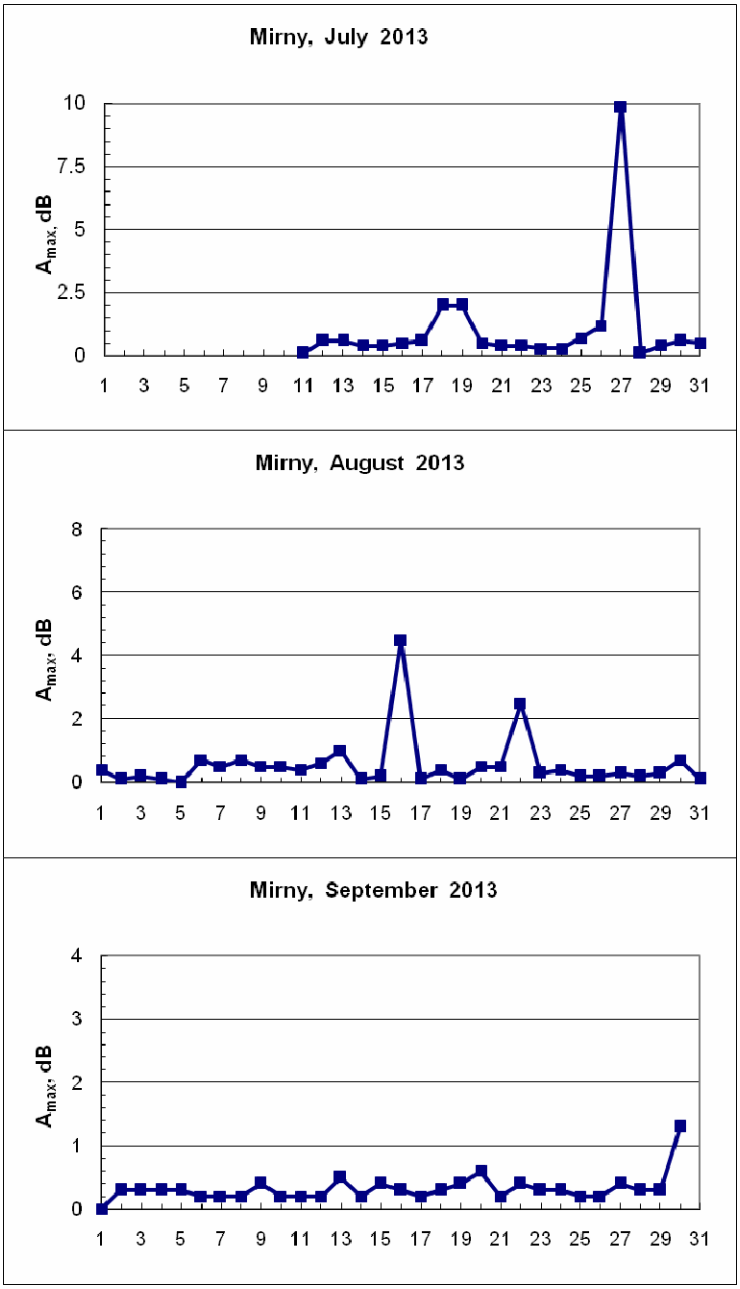

Fig. 6.4. Maximum daily space radio-emission absorption at the 32 MHz frequency from riometer observations at Mirny station.

NOVOLAZAREVSKAYA STATION

Mean monthly absolute geomagnetic field values

	Declination	*Horizontal component*	*Vertical component*
July	*29°20.3′W*	*18548 nT*	*-34492 nT*
August	*29°19.8′W*	*18543 nT*	*-34486 nT*
September	*29°20.2′W*	*18542 nT*	*-34474 nT*

Main variometer reference values

Date	D deg	H, nT	Z, nT
04.07.2013	-29.6810	18537	-34786
12.07.2013	-29.6897	18529	-34777
20.07.2013	-29.7132	18536	-34781
24.07.2013	-29.6825	18543	-34783
30.07.2013	-29.6840	18537	-34784
06.08.2013	-29.6882	18535	-34787
10.08.2013	-29.6677	18531	-34787
17.08.2013	-29.6618	18540	-34781
26.08.2013	-29.6677	18542	-34780
30.08.2013	-29.7132	18542	-34778
04.09.2013	-29.6990	18542	-34780
09.09.2013	-29.7242	18542	-34780
16.09.2013	-29.7208	18544	-34780
22.09.2013	-29.6495	18547	-34779
28.09.2013	-29.7152	18543	-34782
Averages	-29.6905	18539.3	-
σ	0.0232	5.0	3.1

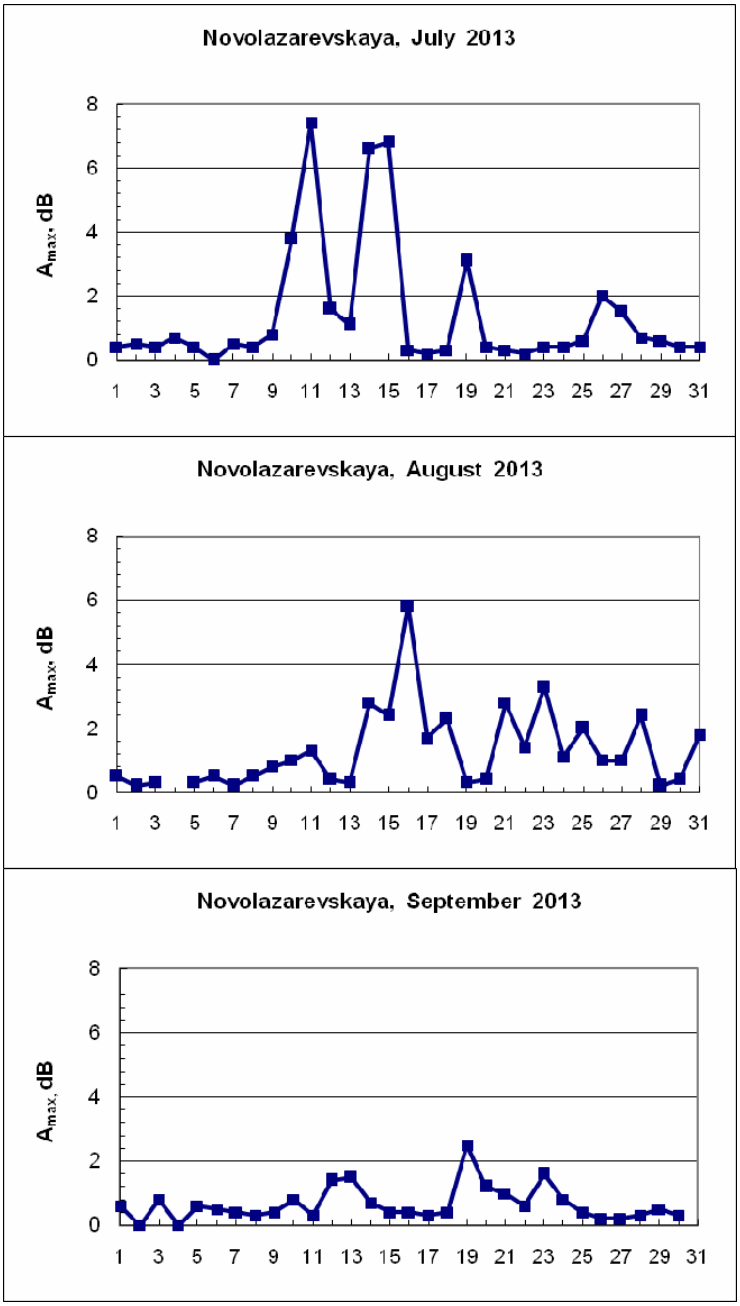

Fig. 6.5. Maximum daily space radio-emission absorption at the 32 MHz frequency from riometer observations at Novolazarevskaya station.

PROGRESS STATION

Mean monthly absolute geomagnetic field values

	Declination	*Horizontal component*	*Vertical component*
July	*79°04.9′W*	*16972 nT*	*-50843 nT*
August	*79°06.1′W*	*16990 nT*	*-50848 nT*
September	*79°05.8′W*	*16996 nT*	*-50848 nT*

Main variometer reference values

Date	D, deg.	H, nT	Z, nT
01.07.2013	-78.8803	119.0	-42.5
05.07.2013	-78.8836	117.1	-42.5
10.07.2013	-78.8789	120.8	-41.1
15.07.2013	-78.8886	119.8	-41.7
21.07.2013	-78.8789	118.5	-43.2
27.07.2013	-78.8922	118.3	-42.5
29.07.2013	-78.8931	117.9	-42.9
01.07.2013	-78.8803	119.0	-42.5
05.07.2013	-78.8836	117.1	-42.5
10.07.2013	-78.8789	120.8	-41.1
15.07.2013	-78.8886	119.8	-41.7
21.07.2013	-78.8789	118.5	-43.2
27.07.2013	-78.8922	118.3	-42.5
29.07.2013	-78.8931	117.9	-42.9
01.08.2013	-78.8972	117.2	-41.2
05.08.2013	-78.8856	113.5	-42.8
06.08.2013	-78.8883	116.5	-43.2
12.08.2013	-78.8892	116.5	-43.6
17.08.2013	-78.8983	115.4	-43.1
22.08.2013	-78.8917	116.0	-43.4
26.08.2013	-78.8908	115.1	-43.1
29.08.2013	-78.8933	111.6	-43.5
03.09.2013	-78.8844	116.8	-43.0
06.09.2013	-78.8694	116.6	-42.9
09.09.2013	-78.8608	119.4	-41.5
16.09.2013	-78.8553	118.4	-42.2
20.09.2013	-78.8550	118.6	-42.2
23.09.2013	-78.8528	120.3	-41.5
Averages	-78.8814	117.7	-42.5
σ	0.0134	2.07	0.72

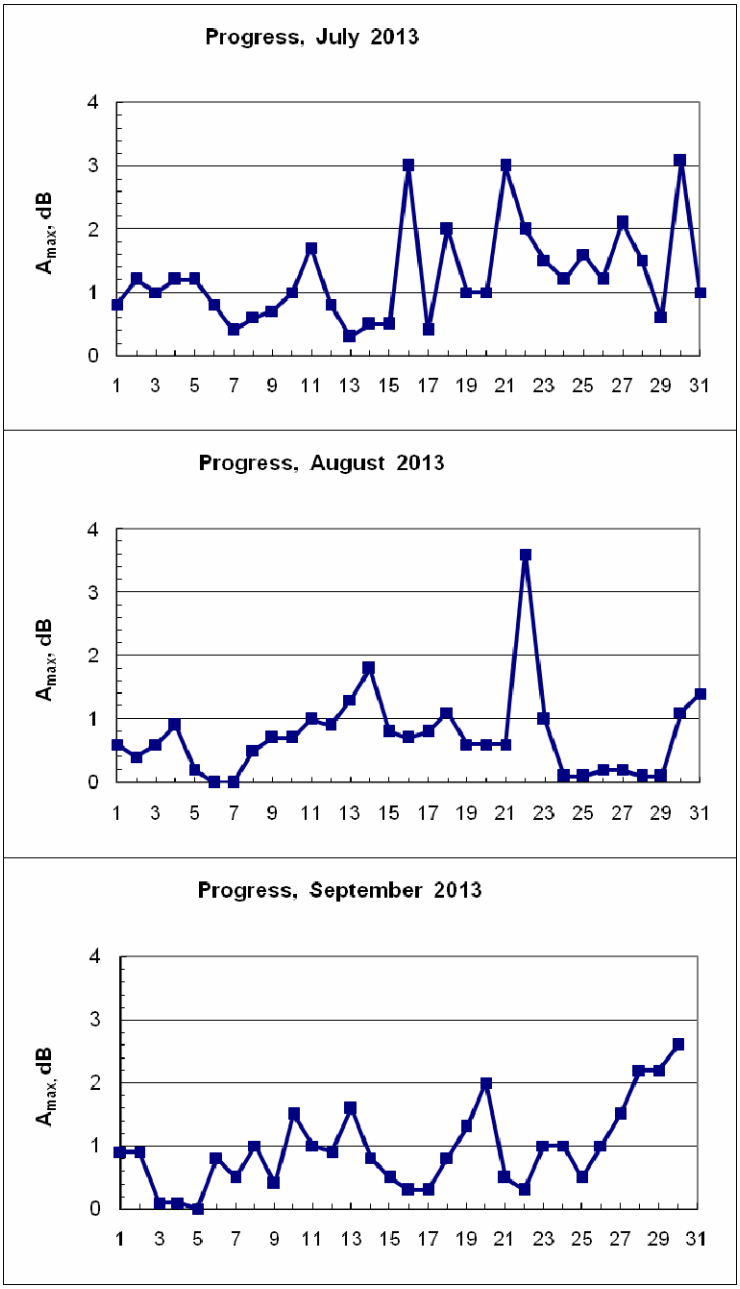

Fig. 6.6. Maximum daily space radio-emission absorption at the 32 MHz frequency from riometer observations at Progress station.

VOSTOK STATION

Mean monthly absolute geomagnetic field values

	Declination	*Horizontal component*	*Vertical component*
July	*123°20.2′W*	*13595 nT*	*-57834 nT*
August	*123°20.3′W*	*13593 nT*	*-57823 nT*
September	*123°26.1′W*	*13588 nT*	*-57819 nT*

Main variometer reference values

Date	D, deg.	H, nT	Z, nT
09.07.2013	-122.5858	13570	-57908
16.07.2013	-122.5886	13570	-57909
17.07.2013	-122.5953	13572	-57908
20.07.2013	-122.5928	13570	-57908
24.07.2013	-122.5831	13572	-57905
01.08.2013	-122.6028	13570	-57905
03.08.2013	-122.6011	13570	-57906
08.08.2013	-122.6014	13573	-57907
10.08.2013	-122.6064	13572	-57905
14.08.2013	-122.6036	13575	-57906
20.08.2013	-122.5936	13575	-57908
07.09.2013	-122.6139	13579	-57910
15.09.2013	-122.6081	13576	-57908
25.09.2013	-122.6119	13576	-57907
27.09.2013	-122.6225	13574	-57906
26.09.2013	-122.6042	13576	-57909
29.09.2013	-122.6056	13575	-57906
Averages	-122.6012	13573.2	-57907.1
σ	0.0104	2.8	1.4

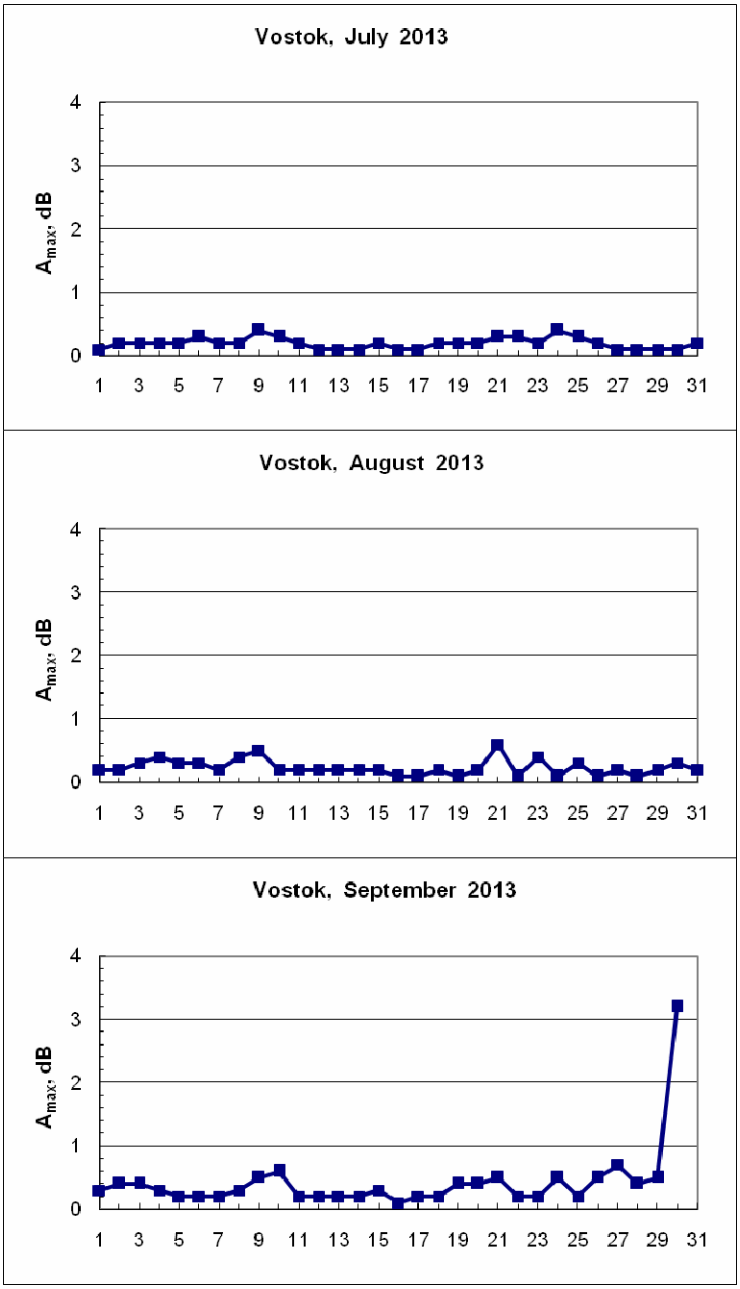

Fig. 6.7. Maximum daily space radio-emission absorption at the 32 MHz frequency from riometer observations at Vostok station.

7. SEISMIC OBSERVATIONS IN ANTARCTICA IN 2012

In 2012, the seismic observations in Antarctica were continued at the stationary stations of the Geophysical Service (GS) of RAS Mirny and Novolazarevskaya. At Mirny station, seismic observations have been carried out from 1956 and observations at Novolazarevskaya station from 1962. These stations are within the teleseismic network of GS RAS /1/, its main objective being provision of continuous monitoring of the Earth's seismic active zones, including Russia.

The Antarctic seismic stations perform the following functions:

– Monitoring of strong earthquakes at Earth with a magnitude $MPSP^1 > 6$;

– Registration of earthquakes in the territory around Antarctica;

– Registration of local phenomena in Antarctica including local earthquakes and ruptures in the ice sheet.

The equipment of Mirny station is represented by a set of analogue instrumentation – seismometer with a highly sensitive short-period channel SKM-3 and a medium-period seismograph SKD with a channel of decreased sensitivity/1/. The seismograms obtained as a result of continuous observations are subjected to preliminary processing, which includes keeping the registration log of the change of the seismograms, separation of the precise time signals and determination of time corrections and registration of seismograms. Then interpretation of the records of earthquakes was performed. Upon the return of the expedition, the seismograms were passed to the archive of the GS RAS.

At the Novolazarevskaya seismic station, observations are carried out using a broadband seismometer SKD in a set with a 16-charge digital seismic station SDAS, developed and produced by the GS RAS (Obninsk) jointly with the Scientific-Production Association "Geotekh" /2/. These instruments with a bandwidth of 0.04–3 *Hz*, sampling rate of 20 readouts a second and the dynamic range of about 90 *dB* allow applying a modern digital level of collection, storage and processing of seismic records /1/. The digital records of earthquakes are computer-processed and archived on CD-ROMs, which upon the return of the expeditions are passed to the archive of GS RAS.

Processing of the records of earthquakes at Mirny and Novolazarevskaya stations was carried out in accordance with the methodology /3/ and included identification of arrivals of seismic waves, determination of the time and precision of arrivals, identification of seismic waves and determination of the main parameters of earthquakes (time in the source, distance to the epicenter and magnitudes). The interpretation results were recorded in the station logs (Mirny) and in the electronic database (Novolazarevskaya), and on their basis daily operational reports were prepared and sent to the Information-Processing Center (IPC) of GS RAS. These data were used in the summary processing of earthquakes in preparation of the Seismological Bulletins of GS RAS /4/.

From 1 January to 26 December 2012 (until the stop of equipment operation) 1003 earthquakes and separate arrivals were recorded at Mirny station. Complete processing was carried out with determination of the main source parameters for 99 earthquakes. Data of this station were used for a summary processing at the IPC of GS RAS of 291 earthquakes, of them 60 – with $MPSP \geq 6.0$, including 11 – with $MPSP \geq 6.5$ (Table 7.1). In addition, at Mirny station there was daily observation of the level of microseisms and identification from records of short-period fluctuations connected with the Antarctic ice sheet ruptures. The distribution of these events by months of 2012 is shown in Fig. 7.1.

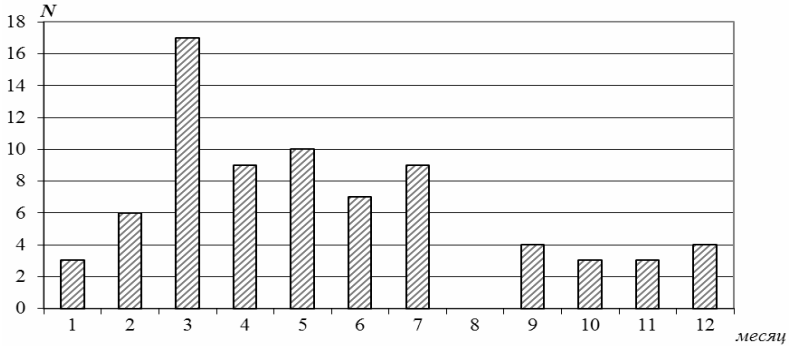

Fig. 7.1. Distribution of ice shears by months of 2012 from data of Mirny station.

At Novolazarevskaya station, 3382 earthquakes together with separate arrivals were registered in 2012. Complete processing was carried out with determination of the main source parameters for 1424 earthquakes. Data of this station were used for a summary processing at the IPC of GS RAS of 683 earthquakes, of them with $MPSP \geq 6.0$ – 94 events, including 16 events with $MPSP \geq 6.5$ (Table 7.1). Records of ruptures in the ice cover were processed, and in total 329 intervals of the "possible" ruptures of the ice cover were identified with duration of several seconds to three minutes the problem of their

unambiguous interpretation remained, as the frequency composition of these records coincides with the frequency composition of noises..

The Table presents the main parameters of strong earthquakes according to data of the Seismological Bulletins /4/ and it is shown which of them were registered by the Russian Antarctic stations.

Table 7.1

Earthquakes with the magnitude of *MPSP*≥6.0, recorded by Mirny and Novolazarevskaya stations in 2012

No.	Date dd.mm	Time in the source (Greenwich) hh:mm:ss	Epicenter coordinates		**DEPTH** *h*, *km*	Magnitude ***MPSP***	Epicentral distance to the station (Δ, °)	No.	
			φ, °	λ, °				**NVL**	MIR
1	01.01	05:27:53	31.448	138.182	358	6.4	Southeast of Honshu, Japan	131.13[2]	–[3]
2	09.01	04:07:14	–10.582	165.144	36	6.4	Santa Cruz Islands	96.83	–
3	10.01	18:36:58	2.404	93.163	22	6.7	Near the west coast of North Sumatra	89.39	–
4	12.01	03:20:50	37.109	141.154	30	6.1	East coast of Honshu, Japan	137.28	–
5	15.01	13:40:19	–61.070	–56.313	10	6.1	South Shetland Islands	27.82	50.70
6	21.01	18:47:10	14.991	–92.995	44	6.0	Coast of Chiapas, Mexico	+[4]	128.33
7	28.01	17:42:53	–29.144	–177.302	33	6.0	Kermadec Islands, New Zealand	80.16	+
8	30.01	05:10:58	–14.114	–75.816	33	6.2	Coast of Peru	76.01	–
9	02.02	13:34:39	–17.794	167.055	29	6.4	Vanuatu Islands	90.00	67.47
10	05.02	16:40:42	–17.820	167.142	33	6.1	Vanuatu Islands	89.99	+
11	06.02	03:49:13	9.946	123.229	29	6.4	Negros, the Philippines	+	–
12	08.02	12:01:39	37.892	137.980	34	6.0	West coast of Honshu, Japan	137.03	–
13	13.02	10:55:07	9.323	–84.010	14	6.0	Costa-Rica	+	–
14	14.02	08:19:56	–10.289	161.079	72	6.3	Solomon Islands	96.48	71.95
15	22.02	10:45:22	–5.090	133.564	24	6.0	Area of Aru Islands, Indonesia	–	–
16	26.02	02:35:00	22.733	120.925	42	6.0	Taiwan	117.55	–
17	26.02	06:17:18	51.733	96.047	14	6.6	South West Siberia, Russia	135.90	–
18	03.03	12:19:55	–22.124	170.328	28	6.2	Southeast of Loyalty Islands	86.13	+
19	05.03	07:46:08	–28.248	–63.314	545	6.1	Province Santiago del Estero, Argentina	58.72	–
20	09.03	07:09:49	–19.193	169.640	19	6.1	Vanuatu Islands	88.95	+
21	10.03	14:10:39	55.100	–157.600	33	6.0	Alaska Peninsula	163.60	–
22	14.03	09:08:36	40.943	144.910	36	6.8	Near the east coast of Honshu, Japan	141.94	–
23	14.03	10:49:26	40.854	144.785	34	6.0	Near the east coast of Honshu, Japan	–	–
24	20.03	17:56:13	–3.771	140.228	33	6.3	West Irian, Indonesia	98.26	–
25	20.03	18:02:47	16.535	–98.245	33	6.7	Coast of Guerrero, Mexico	–	–
26	21.03	22:15:04	–6.190	146.052	115	6.4	Area of East New Guinea, Papua New Guinea	97.39	70.28
27	25.03	22:37:04	–35.137	–71.942	31	6.4	Central Chile	55.25	77.98
28	27.03	11:00:42	39.959	142.190	16	6.2	East coast of Honshu, Japan	140.22	–
29	01.04	14:04:24	37.210	141.007	53	6.0	East coast of Honshu, Japan	–	–
30	03.04	23:42:21	–5.611	133.858	33	6.0	Area of Aru Islands, Indonesia	94.77	67.03

[1] The *MPSP* magnitude –characteristic of the earthquake force, calculated from the measurements of amplitudes and periods at the maximum phase of longitudinal wave P using records of short-period (SP) instruments and corresponds to the international magnitude m_b.

[2] 131.13 (epicentral distance in degrees) – shown for the parameters of the sources, in the summary processing of which this station participated.

[3] – – results of processing of this event are absent in the station log.

[4] + – results of processing of this event are present in he station log, data have not participated in the summary processing due to different reasons.

No.	Date dd.mm	Time in the source (Greenwich) hh:mm:ss	Epicenter coordinates		**DEPTH** *h*, *km*	Magnitude ***MPSP***	Epicentral distance to the station (Δ, °)	No.	
			φ, °	λ, °				**NVL**	MIR
31	11.04	08:38:36	2.269	93.083	38	7.4	Near the west coast of North Sumatra	89.24	68.66
32	11.04	09:01:04	2.228	89.509	10	6.0	North Indian Ocean	–	–
33	11.04	09:27:54	1.266	91.794	10	6.1	North Indian Ocean	–	–
34	11.04	10:43:08	0.798	92.445	26	7.1	Near the west coast of North Sumatra	87.65	–
35	11.04	11:53:33	2.922	89.491	10	6.0	North Indian Ocean	–	–
36	11.04	22:55:09	18.215	–102.664	33	6.0	Michoacan, Mexico	–	–
37	12.04	07:15:46	28.750	–113.050	10	6.3	Lower California, Mexico	128.16	138.95
38	12.04	14:50:52	37.612	141.700	37	6.0	East coast of Honshu, Japan	–	–
39	14.04	10:56:17	–57.599	–65.291	10	6.1	Drake Passage	33.40	55.11
40	14.04	19:26:42	–6.682	105.495	70	6.0	Sunda Strait, Indonesia	84.95	60.39
41	14.04	22:05:24	–18.933	168.722	10	6.1	Vanuatu Islands	89.09	67.10
42	15.04	05:57:39	2.573	90.274	33	6.2	Near the west coast of North Sumatra	88.61	68.99
43	17.04	03:50:13	–32.637	–71.572	25	6.3	Coast of Central Chile	+	80.42
44	17.04	07:13:49	–5.464	147.115	210	6.5	Area of East New Guinea, Papua New Guinea	+	71.32
45	17.04	19:03:59	–59.251	–17.019	33	6.0	East to the South Sandwich Islands	+	44.29
46	20.04	23:14:30	2.192	93.355	33	6.1	Near the west coast of North Sumatra	89.25	68.59
47	21.04	01:16:53	–1.602	134.347	35	6.3	Area of West Irian, Indonesia	98.73	70.98
48	23.04	21:21:43	0.360	125.356	49	6.0	North Molucca Sea	–	70.59
49	28.04	10:08:03	–18.658	–174.676	102	6.3	Tonga Islands	90.69	73.97
50	12.05	23:28:44	38.678	70.367	30	6.1	Afghanistan –Tajikistan border area	116.86	+
51	14.05	10:00:42	–17.511	–69.794	132	6.2	Peru–Bolivia border area	70.84	+
52	20.05	07:20:37	39.684	143.179	33	6.1	Near the east coast of Honshu, Japan	+	+
53	23.05	15:02:24	41.376	142.101	54	6.3	Hokkaido area, Japan	+	+
54	28.05	05:07:22	–28.043	–63.115	583	6.0	Province Santiago del Estero, Argentina	58.85	83.97
55	02.06	07:52:52	–22.032	–63.604	521	6.0	Province Salta, Argentina	64.58	89.94
56	04.06	00:45:16	5.727	–82.661	10	6.1	South to Panama	96.86	–
57	04.06	03:15:24	5.536	–82.746	10	6.0	South to Panama	96.70	–
58	04.06	11:18:13	–7.586	106.538	62	6.2	Java, Indonesia	84.45	59.61
59	05.06	19:31:33	34.948	141.183	23	6.3	Near the east coast of Honshu, Japan	135.29	+
60	07.06	04:05:06	–35.981	–70.925	23	6.0	Chile–Argentine border area	54.14	77.05
61	07.06	16:03:17	–15.837	–72.561	108	6.1	South Peru	73.32	–
62	09.06	21:00:17	24.626	122.452	79	6.3	Taiwan area	+	93.59
63	15.06	01:14:05	5.744	126.473	37	6.1	Mindanao, the Philippines	–	76.05
64	16.06	22:18:46	15.611	119.708	37	6.4	Luzon, the Philippines	110.51	84.29
65	17.06	03:43:10	–8.386	160.355	62	6.2	Solomon Islands	98.22	73.42
66	17.06	20:32:19	38.977	141.955	43	6.2	East coast of Honshu, Japan	139.25	+
67	19.06	15:56:33	53.275	171.519	38	6.2	Near Islands, the Aleutian Islands	160.23	+
68	23.06	04:34:52	3.044	98.003	105	6.2	North Sumatra, Indonesia	91.58	+
69	29.06	15:31:45	–24.657	–9.659	10	6.1	South Atlantic Ocean	47.78	–
70	29.06	21:07:32	43.435	84.712	23	6.4	North Xinjiang, China	125.12	–
71	06.07	02:28:23	–14.612	167.274	178	6.0	Vanuatu Islands	93.17	+
72	12.07	14:00:32	36.536	70.914	191	6.0	Hindu Kush area, Afghanistan	114.97	–
73	20.07	06:10:26	49.393	155.941	47	6.0	Kuril Islands	152.83	–
74	20.07	06:33:01	49.466	156.135	64	6.0	Kuril Islands	152.95	–
75	25.07	00:27:45	2.651	96.095	38	6.2	North Sumatra, Indonesia	90.59	69.08

No.	Date dd.mm	Time in the source (Greenwich) hh:mm:ss	Epicenter coordinates		**DEPTH** *h*, *km*	Magnitude ***MPSP***	Epicentral distance to the station (Δ, °)	No.	
			φ, °	λ, °				**NVL**	MIR
76	25.07	11:20:27	–9.672	159.794	36	6.5	Solomon Islands	96.86	72.03
77	28.07	20:03:55	–4.635	153.205	37	6.4	Area of New Ireland, Papua New Guinea	100.50	74.22
78	02.08	09:56:38	–4.650	153.318	33	6.1	Area of New Ireland, Papua New Guinea	100.51	74.25
79	10.08	18:37:44	52.699	–167.487	30	6.0	Fox Islands, the Aleutian Islands	+	+
80	11.08	12:23:16	38.360	46.813	11	6.2	Armenia–Azerbaijan–Iran border area	+	+
81	11.08	12:34:33	38.343	46.756	10	6.3	Armenia–Azerbaijan–Iran border area	+	–
82	12.08	10:47:05	35.666	82.544	14	6.1	Tibet	117.29	+
83	14.08	02:59:37	49.745	145.169	591	6.8	Sea of Okhotsk	149.94	122.55
84	19.08	22:41:48	–4.690	144.617	70	6.1	North coast of New Guinea, Papua New Guinea	98.49	71.20
85	25.08	14:16:15	42.336	142.988	61	6.0	Hokkaido area, Japan	142.64	–
86	26.08	15:05:33	2.201	126.847	66	6.5	North Molucca Sea	100.14	+
87	27.08	04:37:17	12.338	–88.616	10	6.0	Near the coast of Central America	+	+
88	29.08	19:05:07	38.403	141.811	32	6.1	East coast of Honshu, Japan	138.67	–
89	30.08	13:43:23	71.436	–10.892	13	6.3	Area of Jan-Mayen Islands	142.75	+
90	31.08	12:47:32	10.734	126.740	33	7.3	Area of the Philippines Islands	108.16	+
91	03.09	18:23:04	–10.673	114.003	22	6.4	South of Bali, Indonesia	83.98	57.60
92	05.09	14:42:08	10.387	–85.327	36	6.5	Costa-Rica	102.04	123.87
93	08.09	10:51:42	–3.167	135.116	20	6.0	Area of West Irian, Indonesia	97.46	69.71
94	11.09	16:36:52	11.864	143.135	33	6.0	South of the Marians	+	86.33
95	12.09	03:27:44	34.906	23.999	33	6.0	Crete, Greece	+	–
96	14.09	04:51:47	–3.222	100.630	33	6.3	South Sumatra, Indonesia	86.58	63.44
97	25.09	23:45:24	24.749	–110.125	20	6.0	Lower California, Mexico	123.52	135.73
98	26.09	23:39:56	51.629	–178.221	37	6.1	Andreanof Islands, the Aleutian Islands	160.25	135.34
99	30.09	16:31:32	1.984	–76.416	148	6.9	Columbia	91.28	+
100	08.10	11:43:34	–4.453	129.042	38	6.5	Banda Sea	94.49	66.84
101	12.10	00:31:29	–4.835	134.055	33	6.5	Area of West Irian, Indonesia	95.57	67.82
102	16.10	12:41:25	49.693	156.452	92	6.2	Kuril Islands	153.24	125.49
103	20.10	23:00:30	–13.534	166.518	33	6.1	Vanuatu Islands	94.12	71.12
104	28.10	03:04:07	52.631	–132.299	21	6.6	Area of the Queen Charlotte Islands	155.73	153.90
105	28.10	18:54:19	52.567	–132.708	11	6.1	Area of the Queen Charlotte Islands	155.80	153.69
106	30.10	02:49:00	52.248	–132.111	10	6.0	Area of the Queen Charlotte Islands	155.34	153.68
107	02.11	18:17:32	9.204	126.149	53	6.3	Mindanao, the Philippines	+	79.32
108	07.11	16:35:49	14.076	–91.834	53	6.6	Guatemala	+	127.48
109	10.11	14:57:47	–8.777	–75.155	104	6.1	Central Peru	80.78	–
110	11.11	01:12:38	22.932	95.847	27	6.2	Myanmar	+	89.23
111	12.11	20:42:13	57.783	–142.835	10	6.1	Alaska Bay	163.16	153.40
112	14.11	19:02:04	–29.041	–71.326	53	6.4	Coast of Central Chile	60.64	–
113	15.11	09:20:18	18.326	–100.333	33	6.0	Guerrero, Mexico	+	–
114	16.11	18:12:41	49.223	155.523	62	6.4	Kuril Islands	152.55	–
115	19.11	09:44:36	–5.654	151.523	35	6.0	Area of New Britain, Papua New	99.16	72.68

No.	Date dd.mm	Time in the source (Greenwich) hh:mm:ss	Epicenter coordinates		**DEPTH** *h*, *km*	Magnitude ***MPSP***	Epicentral distance to the station (Δ, °)	No.	
			φ, °	λ, °				**NVL**	MIR
							Guinea		
116	28.11	08:56:13	–5.325	131.087	42	6.1	Banda Sea	94.26	66.54
117	02.12	00:54:21	–16.953	167.651	33	6.2	Vanuatu Islands	90.91	–
118	07.12	08:18:20	37.953	144.046	25	7.2	Near the east coast of Honshu, Japan	138.92	111.24
119	07.12	08:31:13	38.161	143.766	24	6.3	Near the east coast of Honshu, Japan	+	–
120	10.12	16:53:07	–6.529	129.790	150	6.6	Banda Sea	92.74	65.04
121	11.12	06:18:26	0.556	126.189	33	6.2	North Molucca Sea	98.38	70.97
122	14.12	10:35:59	31.159	–119.681	13	6.4	Near the west coast of Lower California	132.38	139.51
123	15.12	04:49:27	52.290	174.067	22	6.0	Near Islands, the Aleutian Islands	159.78	–
124	15.12	19:30:00	–4.594	153.068	52	6.4	Area of New Ireland, Papua New Guinea	100.51	74.21
125	21.12	22:28:08	–14.325	167.260	205	6.2	Vanuatu Islands	93.45	70.69
Total number of registered earthquakes with *MPSP*≥6.0 for 2012								114	81
Total number of earthquakes with *MPSP*≥6.0, which participated in the summary processing for 2012								94	60

Most of the epicenters of earthquakes registered by Mirny and Novolazarevskaya stations are in the southern hemisphere, in the regions of the Pacific seismic belt /5/, a significant number – in the territory of Indonesia, Vanuatu, New Zealand, South America, South Africa, the Scotia Sea, the South Shetland Islands and the South Sandwich Islands and also the Australian-Antarctic Rise, African-Antarctic, Atlantic and the South Pacific oceanic ridges (Fig. 7.2). During processing of the records of earthquakes at the stations, the coordinates of the epicenters were not determined, so for mapping (Fig. 7.2) these data were adopted from the Seismological Bulletin /4/ and the Electronic Catalogue EDR of the USA Geological Survey NEIC /6/. The analogues in the indicated sources /4, 6/ were not found for all seismic events from the station bulletins of Mirny and Novolazarevskaya stations, so the epicenters of only 1546 earthquakes were mapped with 298 events registered by both stations, 1075 – only by Novolazarevskaya station and 173 – only by Mirny station.

Figs. 7.3 and 7.4 show a three-component digital record at Novolazarevskaya station of two earthquakes that had occurred in Antarctica in 2012.

According to data /6/, three earthquakes occurred in Antarctica in 2012: on 1 June at 05:07:01 on the Saunders shore (φ=77.08°S, λ=148.86°W) with m_b=5.8, on 3 August at 06:06:09 on the coast of the Victoria Land (McMurdo Bay in the Ross Sea) (φ=76.31°S, λ=164.07°E) with m_b=5.1 and on 21 August at 09:26:02 in the continental part of Antarctica (φ=84.42°S, λ=41.47°E) with m_b=4.4. Novolazarevskaya station has recorded all three events (Figs. 7.3 and 7.4) and the registration capabilities of Mirny station have allowed it to register only the strongest earthquake on 1 June.

The strongest earthquake on 1 June with m_b=5.8 was preceded by two preliminary foreshocks on 13 January with m_b=4.7 and 4.8, and on 1 June in 15 hours, the aftershock followed with m_b=4.4 /6/. These weak events were not registered by Novolazarevskaya and Mirny stations.

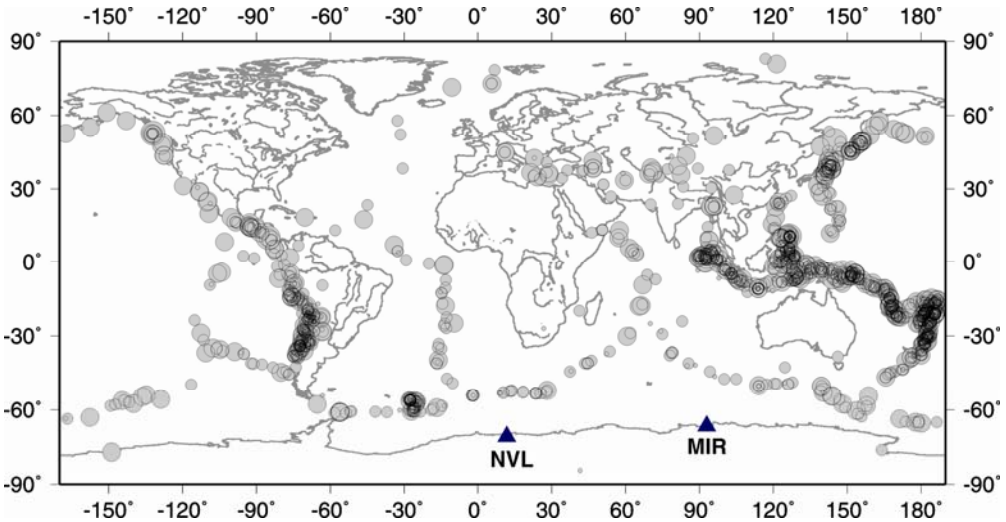

а

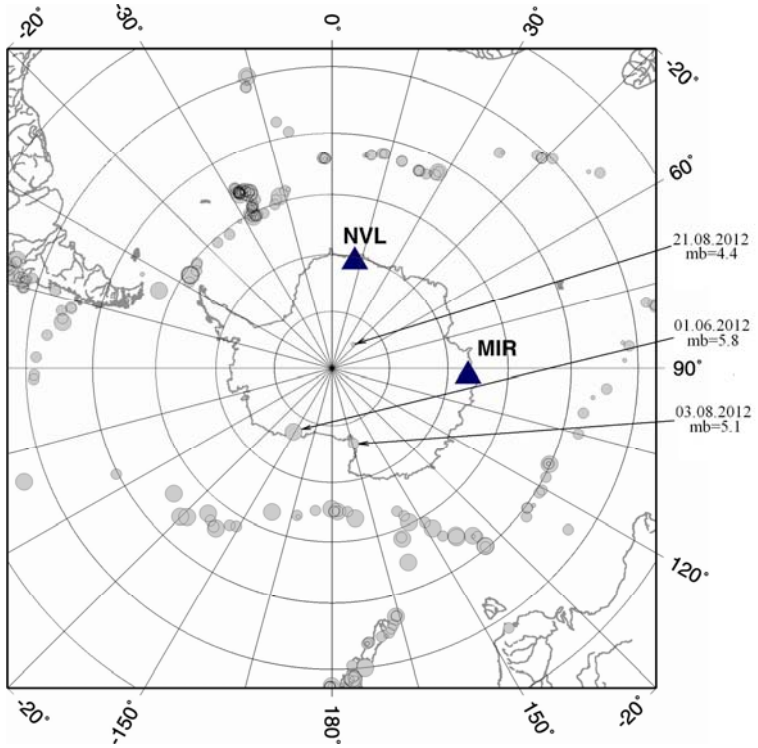

б

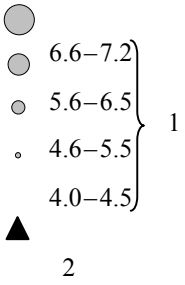

Fig.7.2. (a, b). Maps of the epicenters of earthquakes registered by Mirny and Novolazarevskaya stations in 2012 at the Earth (a) and in the area of the seismic belt of Antarctica /5/ (b) from data in /4, 6/:
1 – magnitude *MPSP* (m_b); 2 – seismic station. Arrows show the epicenters of earthquakes in Antarctica registered by Novolazarevskaya and Mirny stations.

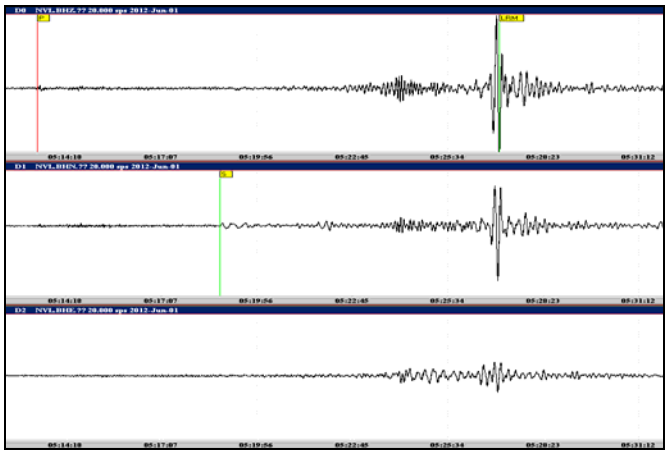

Fig. 7.3. Three-component non-filtered record at Novolazarevskaya station (Δ=31.5°) of the earthquake on 01.06.2012 at 05:07:01 on the Saunders shore, Antarctica, with m_b=5.8 /6/.

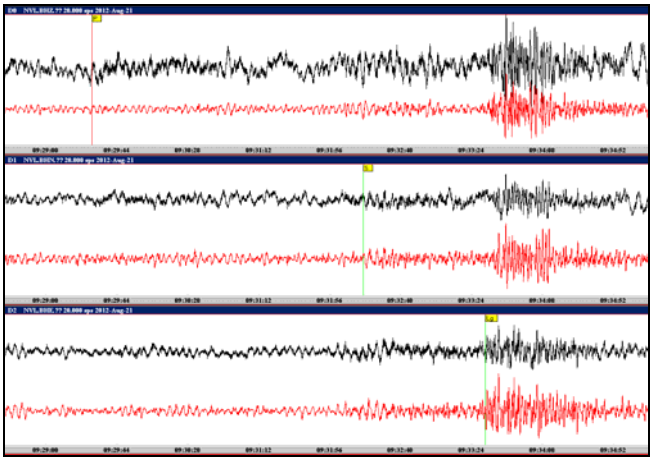

Fig.. 7.4. Three-component record at Novolazarevskaya station (Δ=14.6°) of the earthquake on 21.08.2012 at 09:26:02 in the continental part of Antarctica with m_b=4.4 /6/. Upper (black) curves – non-filtered record, bottom (red) curves – record is filtered in the band of 0.2–1.4 *Hz*.

All observation materials (seismograms and CD) and the results of processing the data (station logs, reports and databases) obtained at Mirny and Novolazarevskaya stations are stored in the archive of the GS RAS and are provided on request to a wide range of users. The authors express their gratitude to the staff of GS RAS V.F. Babkina and O.P. Kamenskaya for the help in preparation of the materials for the article.

References:

1. Report of the GS RAS for 2012 on the R&D topic "Continuous seismological, geophysical and geodynamic monitoring at the global, federal and regional levels, improvement and development of its methods and means" (Head – corresponding member of RAS A.A. Malovichko). V. 2. – Obninsk: Archives of GS RAH,, 2013. – 144 c.

2. O.Ye. Starovoit, I.P. Gabsatarova., D.Yu. Mekhryushev, A.V. Korotin, S.A. Krasilov, V.V. Galushko, Yu.N. Kolomiyets, S.G. Poigina, O.P. Kamenskaya. Study, development and creation in the Russian Federation of the system of seismic and geodynamic observations for continuous national and global seismic monitoring. Report under Agreement 01.700.12.0094 of 01.10.2004. – Obninsk: Archives of GS RAH, 2004. – p. 77.

3. Instruction about the order of making and processing observations at seismic stations of the USSR uniform system of seismic observations. M., Nauka, 1982. – 273 p.

4. Seismological Bulletin (published every 10 days) for 2012 / Editor-in-Chief O.Ye. Starovoit. – Obninsk GS RAS, 2012–2013.

5. Gutenberg B. and Rikhter Ch. The Earth's seismicity. – M.: Foreign literature, 1948. – 160 p.

6. Machine-readable EDR. – NEIC, 2012-2013. – On CD.

8. MAIN RAE EVENTS IN THE THIRD QUARTER OF 2013

01.07 – 30.09	Preparation for the next 59th RAE.
06 – 07.07	Sessions of the Steering Group of the Antarctic DROMLAN air network in Seoul.
07 – 10.07	In Seoul, the 25th Jubilee session of COMNAP was held. From the Russian Antarctic Expedition, V.V. Lukin, V.L. Martyanov, V.V. Pomelov and A.N. Skorodumov took part. The Czech Antarctic Program has joined the COMNAP. The Antarctic Program of the Republic of Belarus' was given the status of the interim observer.
26 – 27.07	First trials of the R/V "Akademik Tryoshnikov" were carried out at the OOO "Admiralteiskiye Verfi" in the framework of the guarantee repair from the series of the performance trials in the Gulf of Finland.
28 – 29.07	In Minsk, sessions of the Extended Interagency Commission of the Republic of Belarus' on the issues of activities in the Antarctic were held. The RAE representatives V.V. Lukin and V.L. Martyanov attended. A joint working group on the cooperation in the Antarctic of Belarus' and Russia was established.
07 – 11.08	At Novolazarevskaya station, the next, 6th traverse from the beginning of wintering to the barrier base was made for the delivery of diesel fuel, aviation kerosene and other cargos.
12 – 18. 08	In the Gulf of Finland, the second stage of performance trials of the R/V "Akademik Tryoshnikov" were carried out in the framework of the guarantee repair.
03 – 07.09	Head of the Indian Bharati station and the mechanic-driver of this station arrived to Progress station for medical aid. The necessary aid was rendered to both persons and the recommendation was given about the urgent departure for treatment at the stationary hospital.
05 – 07, 17 – 13.09	At Novolazarevskaya station, the next sledge-tractor traverses to the barrier base were made.
16.09	Work on preparation of the airfield at Novolazarevskaya station was started. The airfield complex was reactivated. Work on cleaning the runway from the snow layer one meter and a half thick began.